

ISTANBUL TECHNICAL UNIVERSITY ★ GRADUATE SCHOOL OF SCIENCE
ENGINEERING AND TECHNOLOGY

**DETERMINATION OF IN-PLANE SHEAR CHARACTERISTICS OF RC
VOIDED SLABS BY EXPERIMENTAL AND ANALYTICAL METHODS**



M.Sc. THESIS

Ali ATTARIYAN

Department of Civil Engineering

Structural Engineering Programme

DECEMBER 2019

ISTANBUL TECHNICAL UNIVERSITY ★ GRADUATE SCHOOL OF SCIENCE
ENGINEERING AND TECHNOLOGY

**DETERMINATION OF IN-PLANE SHEAR CHARACTERISTICS OF RC
VOIDED SLABS BY EXPERIMENTAL AND ANALYTICAL METHODS**

M.Sc. THESIS

**Ali ATTARIYAN
(501171001)**

Department of Civil Engineering

Structural Engineering Programme

Thesis Advisor: Assoc. Prof. Dr. Beyza TAŞKIN

DECEMBER 2019

İSTANBUL TEKNİK ÜNİVERSİTESİ ★ FEN BİLİMLERİ ENSTİTÜSÜ

**BOŞLUKLU DÖŞEMELERİN DÜZLEM İÇİ KAYMA ÖZELİKLERİNİN
DENEYSEL VE ANALİTİK YÖNTEMLERLE BELİRLENMESİ**

YÜKSEK LİSANS TEZİ

**Ali ATTARIYAN
(501171001)**

İnşaat Mühendisliği Anabilim Dalı

Yapı Mühendisliği Programı

Tez Danışmanı: Doç. Dr. Beyza TAŞKIN

ARALIK 2019

Ali ATTARIYAN, a **M.Sc.** student of **ITU Graduate School of SCIENCE ENNGINEERING AND TECHNOLOGY** student ID **501171001** successfully defended the **thesis/dissertation** entitled “**DETERMINATION OF IN-PLANE SHEAR CHARACTERISTICS OF RC VOIDED SLABS BY EXPERIMENTAL AND ANALYTICAL METHODS**”, which he prepared after fulfilling the requirements specified in the associated legislations, the jury whose signatures are below.

Thesis Advisor : **Assoc. Prof. Dr. Beyza TAŞKIN**
Istanbul Technical University

Jury Members : **Prof. Dr. Ercan YÜKSEL**
Istanbul Technical University

Prof. Dr. Bilge DORAN
Istanbul Yıldız University

Date of Submission : 15 November 2019

Date of Defense : 12 December 2019



To my parents, brothers and everyone who I love,





FOREWORD

I would like to express my deep gratitude towards my advisor, Assoc. Prof. Dr. Beyza Tşkın, who gave me a lot of confidence in myself and knowledge about the subject from the beginning of this thesis to the last days. I am extremely pleased that this thesis is written under the teaching supervision of her and without her encouragement, supports and infinite patience this thesis would not have been done. It was an honor for me to know Assoc. Prof. Dr. Beyza Tşkın in my academic years to improving myself by learning her experinces, and I sincerely appreciate it. I wish to learn from her in my future academic life.

I also would like to express a huge and warm thanks to Prof. Dr. Ercan Yüksel who gave me motivation and courage to complete this investigation successfully. I am so honored for knowing him and learning from his knowledge and experiences in the civil engineering laboratory and this project could not have been completed without him.

I want to thank dear Dr. Kerem Peker of being great and undeniable help for doing this experiment and he had a great role in simulating the model in Abaqus software.

I appreciate the ABS Construction company especially Gizem Şahin that had a deep effect on occurrence of this project.

PHD students, dear Ergun Binbir and Arastoo Khajehdehi, without your help and support during this investigation, completing this thesis would be very difficult. I was so proud to be with you.

Dear my father and mother, I offer my best respects and regards to you that endured my absence during these years and support me in every aspects to see my development in my life and I wish that I could compensate your affection, and also I thank my brothers Mohammad reza and Amir for their supports.

Finally I want to thank all the people who helped me to complete this thesis.

December 2019

Ali ATTARIYAN
(Civil Engineer)

TABLE OF CONTENTS

FOREWORD	ix
TABLE OF CONTENTS	xi
ABBREVIATIONS	xiii
LIST OF TABLES	xv
LIST OF FIGURES	xvii
BOŞLUKLU DÖŞEMELERİN KAYMA ÖZELİKLERİNİN DENEYSEL VE ANALİTİK YÖNTEMLERLE BELİRLENMESİ	xxiii
1. INTRODUCTION	1
1.1 Purpose of Thesis	1
1.2 Historical development	2
1.3 Literature Review	6
2. THE GENERAL THEORIES	15
2.1 Introduction	15
2.2 Diaphragm Behavior	15
2.3 Stress components	17
2.4 Strain components and displacement	18
2.5 Plate Theory	20
2.5.1 Membrane plate.....	20
2.5.2 Thin plates.....	21
2.5.2.1 Basic Equations.....	21
2.5.3 Thick Plates.....	24
2.5.3.1 Basic Equations.....	25
2.6 Shear Stress	26
2.6.1 Pure Shear	27
2.6.2 Pure shear in this investigation	28
2.7 Basic Theories	28
2.8 Finite Element Method.....	30
2.9 Abaqus software.....	31
2.9.1 Family	32
2.9.2 Degrees of freedom	32
2.9.3 Number of nodes	32
2.9.4 Formulation and integration.....	33
2.9.5 Materials in Abaqus program.....	33
2.10 Isotropic and orthotropic materials	34
2.11 Cross section properties	35
3. EXPERIMENTAL INVESTIGATION ON VOIDED SLAB	37
3.1 Introduction	37
3.2 Set-up of the investigation.....	37
3.2.1 The measurement system	39
3.3 Analysis step of first sample 1-a	42
3.4 Analysis step of second sample 1-b	46
3.5 The results of the test	49
3.6 Getting samples	63
4. ANALYTICAL INVESTIGATION ON VOIDED SLABS	65
4.1 Introduction	65
4.2 Abaqus/CAE 2019.....	65

4.2.1 Parts of the voided slab.....	66
4.2.2 Materials of the voided slab	67
4.2.3 Assembly of the voided slab.....	69
4.2.4 Step of the voided slab	70
4.2.5 Interaction of the voided slab	70
4.2.6 Boundary condition of the voided slab.....	71
4.2.7 Mesh of the voided slab.....	72
4.3 The results of analysis	73
5. CONCLUSIONS AND RECOMMENDATIONS	79
5.1 Conclusions	79
5.1.1 1-a Voided slab.....	79
5.1.2 1-b Voided slab	79
5.2 Recommendations	80
REFERENCES.....	81



ABBREVIATIONS

$\sigma_x, \sigma_y, \sigma_z$: Normal stress
$\tau_{xy}, \tau_{yz}, \tau_{xz}$: Shear stress
F	: Force
$\epsilon_x, \epsilon_y, \epsilon_z$: Strain
$\gamma_{xy}, \gamma_{yz}, \gamma_{xz}$: Shear angle
u, v, w	: Displacement
κ	: Curvature
E	: Young's modulus
G	: Shear modulus
M_x, M_y, M_z	: Moment
D	: Flexural rigidity
N_x, N_y	: Normal force
V_x, V_y	: Shear force
Q	: Statical moment
I	: Moment of inertia



LIST OF TABLES

	<u>Page</u>
Table 3.1 : The crack sizes of the 1-a voided slab.	50
Table 3.2 : The crack sizes of the 2-a voided slab.	50
Table 3.3 : Summary of the data obtained from the shear stress and shear angle graph.....	62





LIST OF FIGURES

	Page
Figure 1.1 : One-way and two-way slabs.....	1
Figure 1.2 : Cross-sectional of a voided slab.....	2
Figure 1.3 : The first mushroom floor (Coronelli, D. et al. (2016)).	3
Figure 1.4 : The first mushroom floor (Coronelli, D. et al. (2016)).	3
Figure 1.5 : The ancient structures lightened by inserting empty space on the elements (Coronelli, D. et al. (2016)).	4
Figure 1.6 : The ellipse shape.	4
Figure 1.7 : The circular or bubble deck.....	5
Figure 1.8 : The square shape.	5
Figure 1.9 : Strain and stress distributions in a flat plate–voided concrete slab (David A. Fanella et al. (2017)).	6
Figure 1.10 : Critical section for one-way and two-way shear (David A. Fanella et al. (2017))......	7
Figure 1.11 : the minimum overall slab thickness (David A. Fanella et al. (2017))...	8
Figure 1.12 : Hollow spherical and elliptical bubbles (Arati Shetkar and Nagesh Hanche (2015))......	9
Figure 1.13 : The shear failure and bending failure of slabs (Arati Shetkar and Nagesh Hanche (2015))......	9
Figure 1.14 : The parameters of hollow sphere shape (J. H. Chung et al. (2015))...	11
Figure 1.15 : Experimental set-up (Juozas Valivonis et al. (2017)).	13
Figure 2.1 : Flexible diaphragm behavior.....	16
Figure 2.2 : Degrees of freedom in rigid diaphragm.....	16
Figure 2.3 : Rigid diaphragm behavior.	17
Figure 2.4 : The stress components on a three-dimensional body.....	17
Figure 2.5 : The stress components on a two-dimensional body in Cartesian coordinate system.....	18
Figure 2.6 : Strain components on a three-dimensional body in Cartesian coordinate system.....	19
Figure 2.7 : Strain components on a two-dimensional body in Cartesian coordinate system.....	19
Figure 2.8 : Plate in Cartesian coordinate system.....	20
Figure 2.9 : Plate with membrane behavior	20
Figure 2.10 : Kirchhoff plate before and after deformation.....	21
Figure 2.11 : Thin plate element.	22
Figure 2.12 : Stress distribution in plate.	23
Figure 2.13 : In-plane normal forces and bending moments.	23
Figure 2.14 : In-plane shear forces and twisting moments.	24
Figure 2.15 : Mindlin-Reissner plate before and after deformation.	24
Figure 2.16 : Thick plate internal forces.	26
Figure 2.17 : An example of distribution of the shear stress of a beam with rectangular cross section.	26
Figure 2.18 : Transformation of pure shear to normal stresses.....	27
Figure 2.19 : Pure shear in a voided slab.	28
Figure 2.20 : The changed and unchanged form of a voided slab.	29
Figure 2.21 : The area used for obtaining shear force.	29
Figure 2.22 : The shear stress-shear angle graph.....	30

Figure 2.23 : The shear stress-strain graph.	30
Figure 2.24 : Triangular element.....	31
Figure 2.25 : The usual element families in Abaqus software.	32
Figure 2.26 : Abaqus software different elements with vary number of nodes.	33
Figure 2.27 : Cross section of isotropic and orthotropic materials	35
Figure 3.1 : The condition of the bar’s strain gauges of the samples.....	37
Figure 3.2 : The setup of the analysis system.	38
Figure 3.3 : The final situation of the system.....	38
Figure 3.4 : The measurement system (schematically).	40
Figure 3.5 : The strain gauges installed to the bars of the voided slab.	40
Figure 3.6 : The strain gauges on the rods and a transducer.	41
Figure 3.7 : The three transducers on a corner of the voided slab.	41
Figure 3.8 : The other two transducers on another corner of the voided slab.	42
Figure 3.9 : The last and provided condition of the system.	42
Figure 3.10 : The provided 1-a voided slab	43
Figure 3.11 : The first crack of the voided slab.	44
Figure 3.12 : The noticeable cracks of the voided slab.....	44
Figure 3.13 : The failure of the voided slab.	45
Figure 3.14 : The cracks of the bottom of the voided slab.....	45
Figure 3.15 : The 1-b voided slab before the test.....	46
Figure 3.16 : The first crack of the voided slab.	47
Figure 3.17 : Some of the cracks of the voided slab.	47
Figure 3.18 : The failure condition of the voided slab.	48
Figure 3.19 : The last condition of the voided slab.....	48
Figure 3.20 : The bottom cracks of the voided slab.....	49
Figure 3.21 : The Force-displacement graph of the first voided slab.	51
Figure 3.22 : The Force-displacement graph of the second voided slab.....	52
Figure 3.23 : The last version of the Force-Displacement graph of the first voided slab.	53
Figure 3.24 : The last version of the Force-Displacement graph of the second voided slab.	53
Figure 3.25 : The strain-steps of the rods of the first sample.....	54
Figure 3.26 : The strain-steps of the rods of the second sample.	54
Figure 3.27 : The Force-Displacement graph of the upper and downer rods of the first sample.	55
Figure 3.28 : The Force-Displacement graph of the upper and downer rods of the second sample	55
Figure 3.29 : The Force-Displacement graph of the load cells and the rods of the first one.....	56
Figure 3.30 : The Force-Displacement graph of the load cells and the rods of the second one.	56
Figure 3.31 : The strain-step of the first strain gauge installed to the surface of the first sample.	57
Figure 3.32 : The strain-step of the second strain gauge installed to the surface of the second sample.	57
Figure 3.33 : The strain-step of the first strain gauge of the second sample.....	58
Figure 3.34 : The strain-step of the second strain gauge of the second sample.....	58
Figure 3.35 : The graph of the first strain gauge of the bar of the first sample.	59
Figure 3.36 : The graph of the second strain gauge of the bar of the first sample....	59
Figure 3.37 : The graph of the first strain gauge of the bar of the second sample....	60

Figure 3.38 : The graph of the second strain gauge of the bar of the second sample.	60
Figure 3.39 : The shear stress and shear angle graph of the 1-a voided slab.....	61
Figure 3.40 : The shear stress and shear angle graph of the 1-b voided slab.....	61
Figure 3.41 : Shear stress-strain graph.....	63
Figure 3.42 : Shear stress-strain graph.....	63
Figure 3.43 : The taken samples for determining the strength of the concrete.....	64
Figure 3.44 : The observation of the voids places.	64
Figure 4.1 : The general view of the Abaqus/CAE 2019.....	65
Figure 4.2 : The summary of the part section.	66
Figure 4.3 : The properties of the steel.	67
Figure 4.4 : The properties of the concrete.	68
Figure 4.5 : The properties of the concrete.	69
Figure 4.6 : The assembled form of voided slab.....	69
Figure 4.7 : The bars of the voided slab.....	70
Figure 4.8 : The view cut of the voided slab from y axis.	70
Figure 4.9 : The constraint of the voided slab and bars.	71
Figure 4.10 : The boundary condition option.	71
Figure 4.11 : The situation of the voided slab with boundary condition.	72
Figure 4.12 : The last condition of the voided slab before analysis.....	72
Figure 4.13 : The force-displacement graph of the first voided slab.	73
Figure 4.14 : The force-displacement graph of the second voided slab.	73
Figure 4.15 : Comparison of the force-displacement of the results for first sample.	74
Figure 4.16 : Comparison of the force-displacement of the results for second sample.	74
Figure 4.17 : The shear stress graph of the first voided slab.	75
Figure 4.18 : The shear stress graph of the second voided slab.....	75
Figure 4.19 : The simulation of the conventional slab.....	76
Figure 4.20 : The force-displacement of the first conventional slab.	76
Figure 4.21 : The force-displacement of the second conventional slab.....	77



DETERMINATION OF IN-PLANE SHEAR CHARACTERISTICS OF RC VOIDED SLABS BY EXPERIMENTAL AND ANALYTICAL METHODS

SUMMARY

Slabs are the main part of the reinforced concrete structures because of their important role in transmitting the applied loads to columns and provide a flat surface on structures. Designing slabs accurately needs some characteristic satisfactions. For instance, thickness of the slabs should be in a range that avoids extreme deflection, also the span length should be in way that not leads to deformations larger than specific values.

Throughout history, some changes have been made to the design types of slabs to get some advantages. For example, the shape of slabs have been changed by using mushroom slabs. The aim of creating new slab systems was due to the fact that there was a great demand to have larger spans and lighter structures. Another system for slabs that have been developed in the last decades is voided slabs.

Putting some voids within the slabs reduce the self-weight of the structure and gives an opportunity to have larger spans without increasing the thickness of the slab. Moreover, voided slabs decrease the amount of material usage and consequently decrease construction costs. In the other words, if the span length is increased due to the architectural needs, the thickness of the slab should be increased to satisfy the static equilibriums and it would cause the structures to have heavy self-weight, leading to extensive deflection and, it would be more destructive on earthquake. Therefore, the voided slab systems give advantages to have larger spans with the same thickness and less seismic forces due to the less self-weight.

Voided slab system is taken into consideration by many civil engineers to investigate the flexural, shear and its other behavior exposed to different loading conditions. They have attempted to find a useful method to design a voided slab. Also, punching force problem was another subject that has been investigated and it revealed that in the critical areas of the columns, the slab should be constructed as a conventional types.

In this thesis, two voided slabs were tested in Istanbul Technical University (ITU) Structural and Earthquake Engineering Laboratory (STEELab) which were constructed by ABS construction company to investigate the shear behavior of the voided slabs experimentally and analytically subjected to the in-plane shear force. It must be mentioned that the test set-up was designed and implemented for the first time by Prof. Dr. Ercan YÜKSEL. The dimension of the first sample was 178.5 cm 178.5 cm 30 cm and the second one was 201 cm 201 cm 30 cm. Also the space between voids of the first one and second one was 7.5 cm and 15 cm, respectively.

The thesis is consisted of five chapters. At the first chapter, there is some information about the history of the voided slabs and the researches that have been conducted before. After that, the basic theories about the investigation and its test set-up, stress, strain and the relationship between them were studied. Then, in third chapter, the experiment of the voided slabs which had different dimensions and different space between voids were deeply considered and the important graphs such as fore-displacement, shear stress-shear angle and other ones were plotted to get comprehensive information. In the next chapter, the experimented voided slabs were simulated in the Abaqus program, which analyzes the specimens by using the finite

element methods. The simulation was done by considering all the properties of the voided slabs to get the more reliable results to compare the obtained data. In addition, other two conventional slabs with the same dimensions were simulated to compare the voided slab by the conventional slabs. Finally, the conclusion gets from this study was considered in the last chapter. Based on the obtained results, the graphs show that when the shear capacity of the voided slab is around the 1.5 MPa, its behavior can be considered as a rigid diaphragm. Plus, the data obtained from the experimental and analytical studies were almost the same.



BOŞLUKLU DÖŞEMELERİN DÜZLEM İÇİ KAYMA ÖZELİKLERİNİN DENEYSEL VE ANALİTİK YÖNTEMLERLE BELİRLENMESİ

ÖZET

Döşemeler, yapıya uygulanan yüklerin kolonlara aktarılmasındaki önemli rolü ve betonarme üzerinde düz bir yüzey sağlaması nedeniyle betonarme yapıların önemli bir elemanıdır. Düz plak döşeme kullanımı, mimarlar arasında çok popülerlik kazanıyor, çünkü düz plak döşeme sistemi, mimarın kirişsiz yüksek ve tamamen düz tavan konseptini elde etmesini sağlar. Ancak plak döşemelerin doğru bir şekilde tasarlanması, bazı özelliklerin yerine getirilmesine ihtiyaç duyulur. Örneğin, döşemelerin kalınlığı, eğilmeyi önleyen bir aralıkta olmalıdır, ayrıca açıklık uzunluğu belirli değerlerden daha büyük olamaz.

Tarih boyunca bazı avantajlar elde etmek için döşemelerin tasarım tipinde bazı değişiklikler yapıldı. Örneğin, mantar döşemeler kullanılarak döşemelerin şekli değişti. Bu tip döşemelerde, yapının kendi ağırlığını azaltmak için yapılan çabaların sonucuydu. Mantar döşemelerinde, zımbalama probleminden kaçınmak için kolon ve döşeme birleşme bölgelerinde döşemelerin kalınlığı artırıldı, ancak döşemelerin diğer alanları kritik alanlardan daha küçük kalınlığa sahipti.

Döşemeler için yeni sistemler oluşturma amacı, daha geniş açıklıklara ve daha hafif yapılara sahip olmak için büyük bir talep olduğu gerçeğiydi. Geçtiğimiz yıllarda geliştirilen döşemeler için bir başka sistem de boşluklu döşemelerdir. Döşemelerin içinde bazı boşluklar bırakmak, yapının kendi ağırlığını azaltır ve döşemenin kalınlığını arttırmadan daha geniş açıklıklara sahip olma fırsatı verir.

Başka bir deyişle, mimari ihtiyaçlar nedeniyle açıklık uzunluğu artarsa, statik dengeleri karşılamak için döşemenin kalınlığı arttırılmalı ve bu artış beton ve çelik gibi malzemelerin tüketilmesine neden oluyor ki bu artış daha fazla maliyete, yapının ağırlaşmasına, eğilmeye maruz kalmaya ve deprem yükünün daha fazla olmasına neden olacaktır. Bu nedenle, boşluklu döşemeler sistemi, kendi ağırlığının daha az olma nedeniyle aynı kalınlıkta daha büyük açıklıklara ve daha az sismik kuvvetlere sahip olma avantajları sağlar.

Boşluklu döşemelerde bırakılan boşluklar genellikle plastikten yapılır ve şekilleri kare, dairesel ve elips olabilir. Ayrıca her şeklin araştırılabilecek bazı spesifik özellikleride vardır.

Boşluklu döşeme sistemi, farklı yüklemeler sırasında eğilme, kayma ve diğer davranışlarını araştırmak ve boşluklu döşeme tasarlamak için kullanışlı bir yöntem bulmak için birçok inşaat mühendisi tarafından dikkate alınmıştır.

Ayrıca, zımbalama problemi araştırılmış olan başka bir konuydu ve kolonların kritik bölgelerinde, döşemelerin geleneksel döşemelerde olduğu gibi yapılması gerektiğini ortaya koydu.

İnşaat mühendisleri tarafından yapılan araştırmalar, boşluklu döşemelerin maksimum eğilme momentini normal döşemelerinkinden yüzde on daha az olduğunu ortaya koydu. Ancak düzlem içi kesme kuvvetine maruz kalan boşluklu döşemelerin kayma davranışı hakkındaki sınırlı bilgi olması nedeniyle, bu araştırma, boşluklu döşemelerin kayma davranışını belirlemek için yapılmıştır.

ABS inşaat şirketi tarafından farklı özelliklere sahip olan on altı boşluklu döşeme farklı yükleme tipleriyle araştırma yapmak için inşa edildi, ancak bu tezde iki boşluklu döşemenin düzlem içi kesme kuvvetine maruz kalan kayma davranışını deneysel ve analitik araştırmak için ele alınmıştır. Bu iki boşluklu döşemeler, İstanbul Teknik Üniversitesi (İTÜ) Yapı ve Deprem Mühendisliği Laboratuvarında (STEELab) test edilmiştir. Bu deneyin set-upı ilk kez olarak Prof. Dr. Ercan YÜKSEL tarafından tasarlandığı ve uygulandığı belirtilmelidir

İlk döşeme boyutu 178,5 cm 178,5 cm 30 cm, ikincisi ise 201 cm 201 cm 30 cm idi. Ayrıca, birinci ve ikinci döşemelerin boşlukları arasındaki boşluk mesafesi sırasıyla 7.5 ve 15 cm idi. Numunelerin beton ve çelik özellikleri aynı olan, fakat ikincisinin daha büyük olması nedeniyle, donatıların sayısı ikincide daha fazlaydı ancak donatıların alanları eşitti.

Bu tez beş bölümden oluşmaktadır. İlk olarak, boşluklu döşemenin tarih boyunca gelişimi ve daha önce üzerinde yapılmış araştırmalar hakkında bazı detaylı bilgiler verilmiştir.

Ondan sonra numunelerin kurulması ile ilgili ve temel teoriler, gerilme, şekildeğiştirme ve aralarındaki ilişki incelenmiştir. Ayrıca bu bölümde, analiz için sonlu elemanlar yöntemini kullanan Abaqus bilgisayar programı hakkında bazı bilgiler bulunmaktadır.

Daha sonra, üçüncü bölümde, farklı boyutlara ve boşluklar arasında farklı mesafeye sahip olan boşluklu döşemelerin deneyi detaylı bir şekilde ele alınmış ve yük-yer değiştirme, kayma gerilme-kayma açısı, kayma gerilme-şekildeğiştirme ve diğer önemli grafikler kapsamlı bilgi elde etmek için çizilmiştir.

Grafikler, boşluklu döşemelerin kesme kapasitesi 1.5 MPa civarında olduğunda, davranışının rijit bir diyafram olarak değerlendirilebileceğini göstermektedir. Birinci boşluklu döşemede yük kapasitesi 1480 KN ve ikincisinde 1800 KN idi. İlk döşemenin boşlukları birbirine daha yakın olması nedeniyle, ikincisinin sünekliği, birincisinin iki katıydı.

Ayrıca, elastik bölgesinde kayma modülü, ilk numunede ikincisine göre oldukça yüksekti. Betona ve çubuklara yapıştırılan strain gaugelerden elde edilen veriler tamamen güvenilir değildi. Strain gaugelerden bazıları sadece elastik bölgede doğru sonuçlar almıştır.

Bir sonraki bölümde, deneysel kısımdaki boşluklu döşemeler Abaqus programında simüle edilmiş ve numuneleri sonlu elemanlar yöntemleri kullanılarak analiz edilmiştir. Bu simülasyon, elde edilen verileri karşılaştırmak için daha güvenilir sonuçlar elde etmek için boşluklu döşemelerin tüm özellikleri göz önünde bulundurularak yapılmıştır.

Bunun için boşluklu döşemelerin betonunun dayanımını belirlemek için yapılan testler uzun zaman önce olduğundan ve bir betonun dayanımının zamanla doğrudan bir ilişki içinde olduğu gerçeği göz önüne alındığında, altı silindirik numune döşemenin hasar görmediği kısımlarından alınmıştır.

Bu modellemede, boşluklu döşemeler tasarımı için solid eleman düşünölmüş ve donatılar için wire şekli tipi seçilmiştir. Simölasyon için önemli bir karakter, beton hasar davranışınıdır ki bu simölasyonda Popovics beton davranış modeli kullanılmıştır. Meşin boyutun belirlenmesinde başka önemli bir konudur, ki en doğru meş boyutunu elde etmek için bazı meş boyutları incelenmiş ve en doğru sonucu vereni seçilmiştir.

Kesme gerilimi-kesme açısı grafiğı de bu simölasyondan elde edilebilir, ancak Abaqus programı numuneyi sonlu elemanlar yöntemi ile analiz etmesi nedeniyle, çok sayıda eleman vardır ve her bir elemanın kesme gerilimi grafiğı diğerlerinden farklıdır ancak seçilen alanın tüm elemanlarının grafiğı abaqus yazılımından elde edilebilir ancak ortalama değeri elde etmek basit değıl.

Abaqus yazılımının analiz için sonlu elemanlar yöntemi kullandığı için, bazı elemanların kayma gerilimi, deneysel sonuçlardan elde ettiğimiz ortalama değerdan daha fazla olabilir, ancak çoğı elemanın ortalama değerdan deneysel sonuçlara çok benzer.

Sonuç olarak, deneysel ve analitik çalışmalardan elde edilen veriler neredeyse aynıydı. Ek olarak, boşluklu döşemelerin geleneksel döşemeler ile karşılaştırmak için aynı ebattaki diğer iki geleneksel döşeme simüle edildi.

Son olarak, bu çalışmadan çıkan sonuçlar son bölümde ele alınmıştır.

Zimbalama önemi nedeniyle, boşluklu döşemelerin kritik bölgelerdeki kayma davranışını gözlemek için kolonları dikkate alarak boşluklu döşemelerin araştırılması önerilir.

Düşey yükler ve yatay yükler yapılaraya aynı anda uygulandığından, işlenmiş boşluklu döşemelerin momentini ve kayma davranışını gözlemek için aynı anda her iki yük tipine maruz kalan işlenmiş boşluklu döşemelerin dikkate alınması daha gerçekçi olacaktır.



1. INTRODUCTION

Concrete slabs, which are also known as plates, are the important part of every reinforced concrete structures and provide a flat surface. In addition, by accurate designing, they transmit the applied load to the beams and columns. One-way and two-way slabs are the two different type of function that concrete slabs can have. Shortly, if the ratio of the longer length of the slab to the shorter length is shorter than two, then the slab is a two-way slab (Figure 1.1).

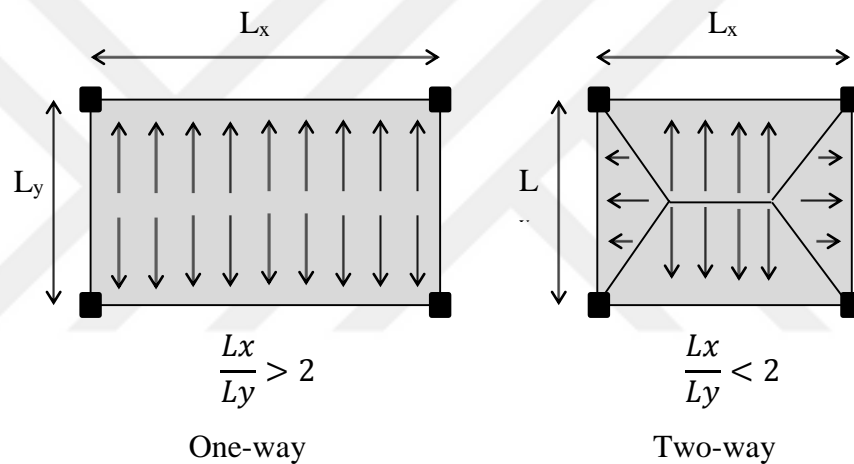


Figure 1.1 : One-way and two-way slabs.

1.1 Purpose of Thesis

Slab is the main element that provide a surface in structures and there has been a great demand for increasing this surface in the last decades. By increasing the span of buildings, slab deflection gets more important and its thickness should be increased to resist the deflection, also the size of beams and columns needs to be increased, which causes structure high self-weight that is destructive for the building specially when earthquakes occur.

Voided slab is a new technic that has attracted the attention of engineers. This type of slab has been investigated in this thesis because of the advantages that are mentioned below:

- Larger spans and areas of structures.
- Optimization the slab thickness and the size of other members like beams and columns.
- Increasing the earthquake resistance due to the reducing self-weight and dead load of structure.
- Materials reduction.

In addition, voided slabs are categorized in bubble deck, u-boot, cobiax, etc. The main purpose of this thesis is determination of shear characteristics of voided slabs subjected to in-plane shear force.

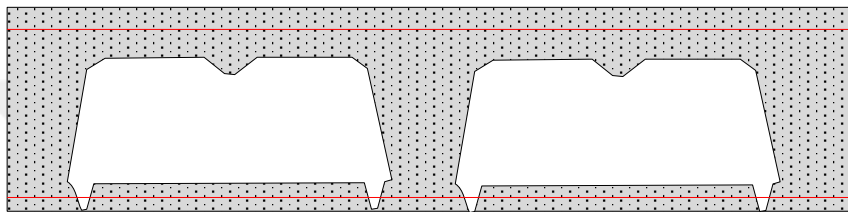


Figure 1.2 : Cross-sectional of a voided slab.

1.2 Historical development

The 1900s was the period of changes in civil engineering, especially the changes in the structures floors. In that era, concrete slabs of buildings were constructed with using beams, so the possibility of reinforced concrete floors without beams became the topic of the studies of Maillart in 1908. Maillart tested several models of concrete buildings without beams, in which the slabs were rested directly on columns. But because of the importance of punching and shear force and the maximum values of stress at the supports, the columns were constructed in widened capital form. Two years after this experimentation, this design was used in the Giesshübel warehouse in Zurich which was soon called mushroom floor because of the columns shape (Figure 1.3).



Figure 1.3 : The first mushroom floor (Coronelli, D. et al. (2016)).

Maillart was not only the one who had this idea but also Turner, independently, was doing some efforts on mushroom columns in the United States in 1905. His system was used in a five-story building in 1906. In that building, the system was reinforced along four axes. As it is obvious in Figure 1.4, the axes were the longitudinal and transversal ones and two diagonal ones.

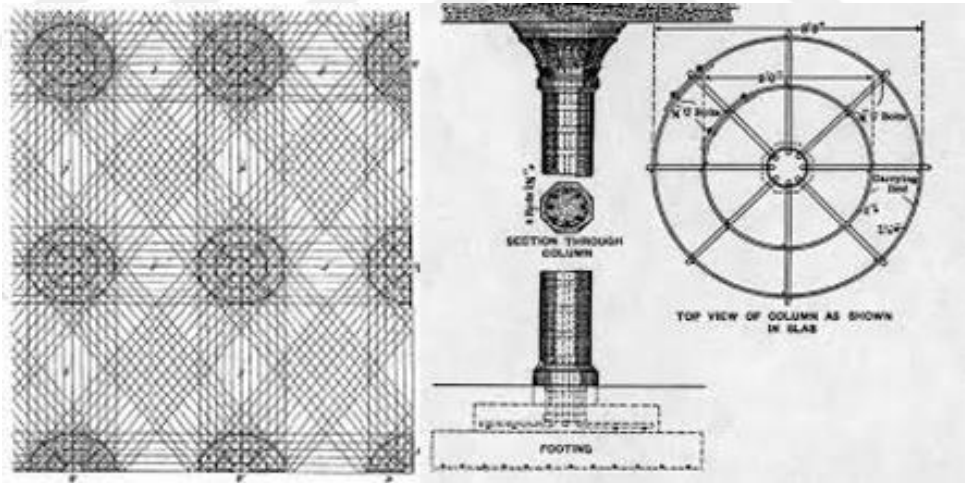


Figure 1.4 : The first mushroom floor (Coronelli, D. et al. (2016)).

In addition, making the structure lighten was important for engineers as well as constructing buildings with large spans. This demand was covered by using some methods, such as using varied materials, since Roman times. After that, creating empty space in some elements was considered and over time, this method of construction was widespread. Figure 1.5 shows the usage of this technique on some well-known structures.

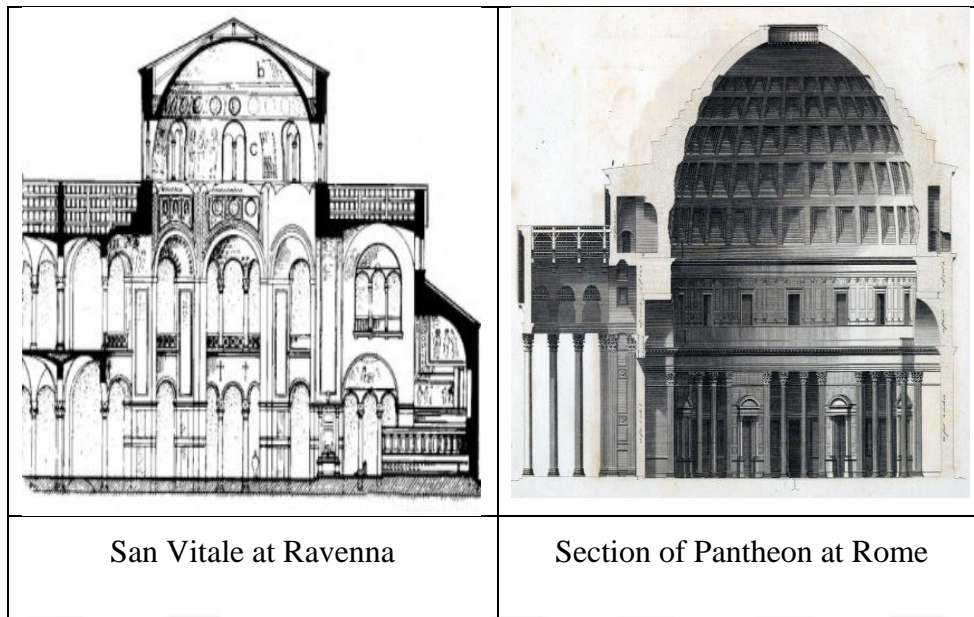


Figure 1.5 : The ancient structures lightened by inserting empty space on the elements (Coronelli, D. et al. (2016)).

After these developments, inserting stationary formworks into the slabs with same thickness was investigated by using advanced knowledge in static behavior of reinforced concrete. Also, inserting voided stationary formworks into the slabs was another idea to make the structure lighten and have larger spans in buildings for the same service loads. By these advances, voided slab was introduced to engineers in an ACI journal.

Nowadays, the usage of structures are developed and changed in comparison with past. Constructing huge shopping malls with parking floors, which needs large spans from an esthetic point of view, and also the needs for more number of story are the few number of reasons that reveal that there is a demand to use voided slab technique in our structures. The different shapes of voids are used in constructing of voided slabs are ellipse (Figure 1.6), circular (Figure 1.7) and square (Figure 1.8).

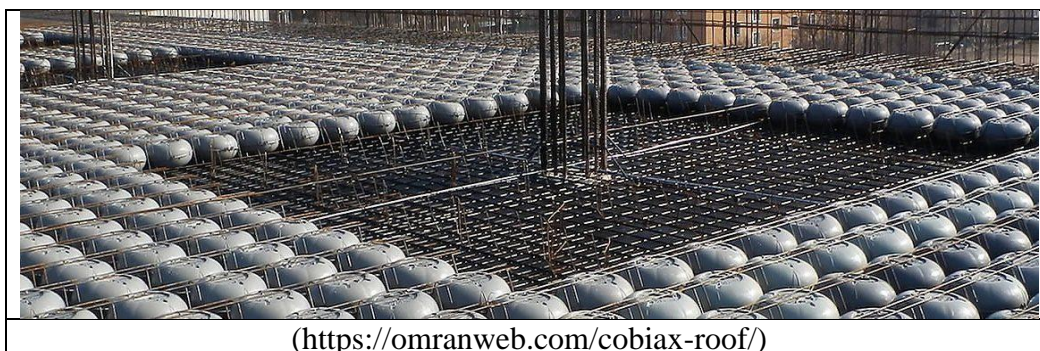


Figure 1.6 : The ellipse shape.



(<http://sakhtemanonline.com/blog/types-of-roof-structures>)



(<http://daryaneng.com/Service.aspx?Id=4>)

Figure 1.7 : The circular or bubble deck



(<http://istaform.ir/en/u-boot-advantages/>)

Figure 1.8 : The square shape.

1.3 Literature Review

David A. Fanella et al. (2017) demonstrated that flat plate-voided concrete slab systems could be designed for strength and serviceability and could satisfy the minimum requirements for vibration control and fire resistance due to the American Concrete Institute (ACI). Strength requirements covering flexural strength and shear strength. Paper shows that for strength requirements all the design conditions in ACI code for any two-way reinforced-concrete slab system should be satisfied exactly for flat plate-voided concrete slabs. It is important to mention that many laboratory flexural tests confirmed that the equivalent stress block is located between the voided forms and the compression edge zone of the slab which is presented in Figure 1.9. Also, it has been revealed that the void-former area in slab is in the range of 70-80%, averagely, which is recommended to be taken as 70% that is used for obtaining self-weight reduction factor.

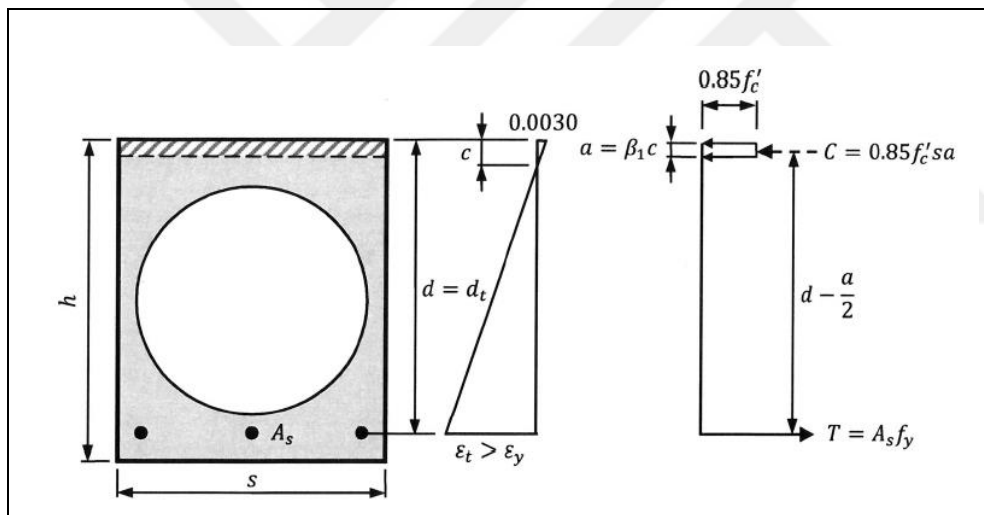


Figure 1.9 : Strain and stress distributions in a flat plate-voided concrete slab (David A. Fanella et al. (2017)).

For shear strength of the plate-voided concrete slabs all the requirements of one-way and two-way shear should be satisfied. For one-way shear, the shear reduction factor for presence of void formers within the slab, which is in the range of 0.5-0.6, is used. The critical sections for satisfying the requirements of one-way shear is located in a distance, d , from the face of the support but it is located in a distance $d/2$ from the face of the columns and $d/2$ from the edge of the solid section of concrete around the columns for checking two-way or punching shear (Figure 1.10).

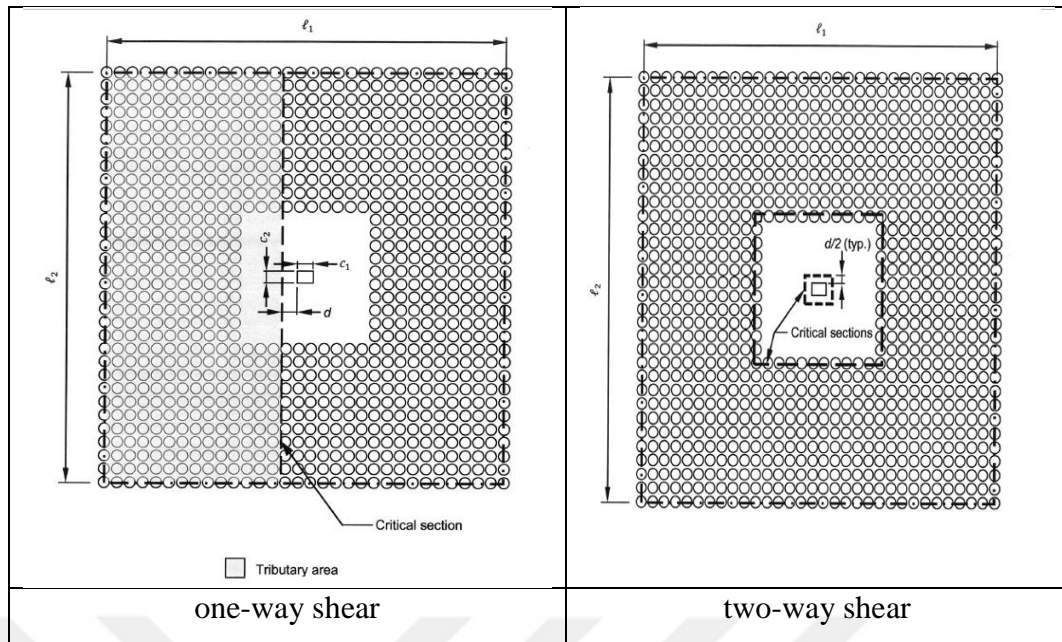


Figure 1.10 : Critical section for one-way and two-way shear (David A. Fanella et al. (2017)).

Deflection which is a part of serviceability requirements that can be satisfied by estimating the slab thickness like two-way slab system, Or by using the deflection value, that should be calculated, to obtain overall slab thickness which the latter is recommended. The other important aspect considered is vibration, which is satisfied by providing an overall slab thickness obtained based on deflection requirements. Figure 1.11 illustrates the minimum overall slab thickness that satisfies acceptance criteria for walking excitation and rhythmic excitations, respectively. Finally, tests for determining the fire resistance on voided concrete slabs showed that the controlling parameter was concrete cover to the reinforcing bars. Also, the voids acted as a thermal isolator. Paper revealed that the weight of the voided concrete slab can be 35% lighter than solid slab. This advantages led to have less dead loads with large spans and less materials which reduced the economic issues. Also, smaller dead loads led to decrease the seismic loads.

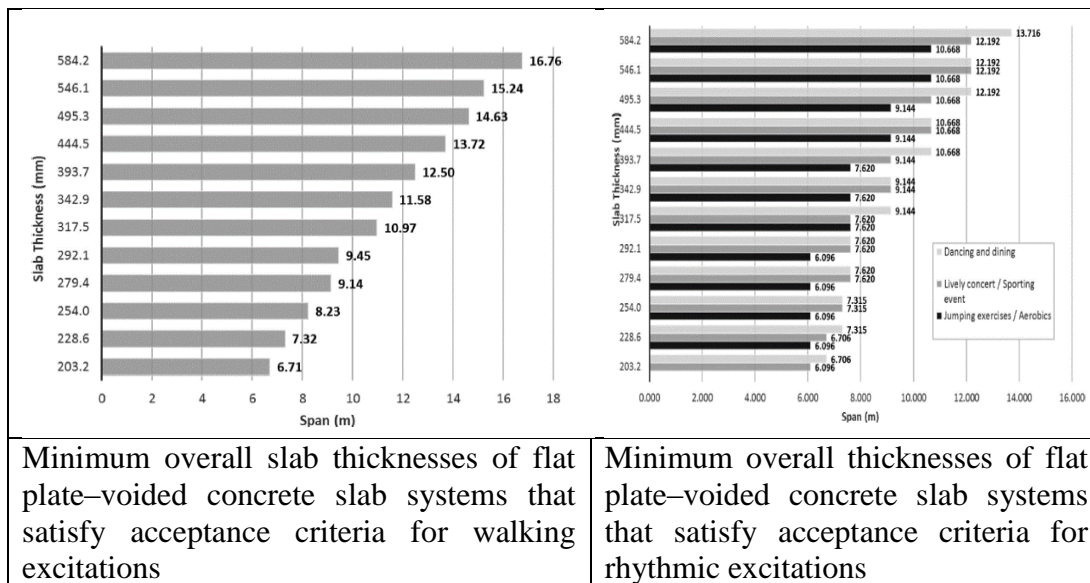


Figure 1.11 : the minimum overall slab thickness (David A. Fanella et al. (2017)).

Kivanc Taskin and kerem peker (2014) compared a two-way, reinforced concrete voided slab with six different bays values with traditional flat plate, ribbed, mushroom concrete slab construction to find design factors and economical applications. Also, this study conducted the modeling of voided slabs using SAP 2000 software due to TS 500 and investigated the economy of different slab systems. There were nine different types of slabs by five different types of loads with sixteen different geometries and continuity of slabs. All the spans were same in length for a significant layout. Loads were applied to the slabs in the normal manner without any lateral loads. For designing voided slabs, moment of inertias for flat and hollow slabs was calculated. It was found out that there was 30 percent or more reduction in the amount of concrete which caused lighter self-weight of the structure with similar load carrying capacity of solid slabs while maintaining the ability to have larger spans. Finally, this study gave some cost comparison of voided slab with other types of slabs with different load applying.

Arati Shetkar and Nagesh Hanche (2015) conducted an experimental study on bubble deck slab system with hollow bubbles. Bubbles were made by high density polypropylene materials which did not react chemically with the concrete or reinforcement bars which can be spherical or ellipsoidal in shape (Figure 1.12). In this study the elliptical balls diameter was 240 mm and height was 180 mm and dependently slab thickness were suitable to the balls. Also, bubbles space from each other was greater than 1/9 bubbles diameter.



Figure 1.12 : Hollow spherical and elliptical bubbles (Arati Shetkar and Nagesh Hanche (2015)).

There were five bubble deck specimens that had the same dimensions and they were simply supported by two steel beams along the short spans. The force was applied in the opposite direction of gravity from the bottom to the top of sample to observe the strain and deformation simply. Figure 1.13 shows the shear failure and bending failure of slabs, respectively. At the end of the test, ultimate loading and deflection of different bubble deck slabs were noticeable.

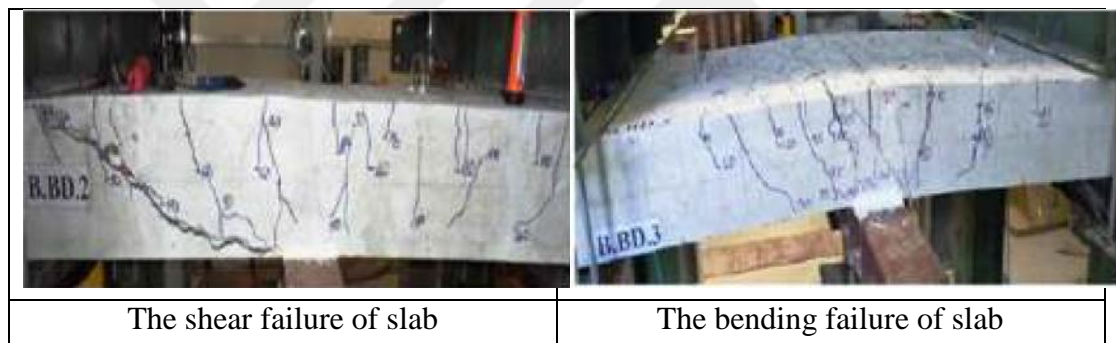


Figure 1.13 : The shear failure and bending failure of slabs (Arati Shetkar and Nagesh Hanche (2015)).

Saifee Bhagat and Dr. K. B. Parikh (2014) studied parametrically reinforced concrete voided and solid flat plate slabs using SAP 2000 software. In this research, 16 slabs with different spans, thicknesses and ball diameters in both direction were studied for each voided and solid slabs in SAP 2000 software. And as a conclusion, the reaction, deflection, moment and reinforcement required for each ones were assessed. This study showed that by using necessary adjustment in certain parameters, a voided slab could be modeled in SAP 2000 software like a solid flat plate slab. It is important to mention that because of the punching shear force criteria, the region around the column was considered as a solid flat slab. Load was adjusted to the center of slabs just as a gravitational load. To confirm the results of voided flat slabs obtaining from SAP 2000 software, reaction, deflection and moment checked numerically and the results were

almost same. While the results for reaction of voided flat slabs were less than that of solid flat slabs, for deflection there were not much difference between them. Also, under the same loading conditions, the maximum moments of voided flat slabs were 7 to 10 percent less than that of solid flat slabs, but the position of maximum moments were the same. Finally, this study revealed that total weight of reinforcement required for voided flat slabs were less than that for solid flat slab, because of the 20 percent decrease of self-weight in voided slab compared with solid flat slab.

M. Bindea et al. (2015) had a numerical research about voided flat slabs and the main concern of this study was to determine the behavior of voided flat slab subjected to shear force. Also, the important variable value was the a/d ratio and steel ratio, but the mechanical characteristics of materials used and the properties of the spherical voids were constant. Computer program for designing the models was Atena 3D and the designing was based on experimental tests on four voided slabs and a normal slab. The experimental test was conducted on four point bending, and the reinforcing percentage and the shear arms were different on slabs. It was clear that for verifying the results, numerical models and experimental models were compared and results was acceptable. The results of the analysis revealed that the voided slabs with the rate of less than 0.5% longitudinal reinforcement did not fail under the shear force and there was not remarkable differences between the results of voided slabs and solid slab comparison but, as this value increased, shear force capability of voided flat slabs decreased in comparison with solid slabs with the same increased rate. When this reinforcing percentage value was between 0.5%-0.8% ranges, failure in voided flat slabs occurred through inclined cracking which was the shear force indication, while the failure in solid flat plate occurred in normal cracks from bending with the almost same maximum shear force. In the same a/d ratios for slabs with spherical voids percentage of 0.52% shear force was the failure factor, but the slabs with spherical voids percentage of 0.31% failed at bending moment and all the solid flat slabs collapsed at bending moment. Finally, it was concluded that the conservative shear force bearing capacity of voided flat slabs could be considered as a 60% of shear force bearing capacity of solid flat slabs.

J. H. Chung et al. (2015) conducted an analytical study on the impact of hollow shapes on bi-axial hollow slabs. In this paper, various biaxial hollow slabs with different shapes of hollow spheres have been studied by simulating in LUSAS, which is a finite

element method software, to determine the parameters of voided slabs, also to find out the excellent hollow sphere shapes. Considering the parameters of hollow sphere shape have been determined the three characteristics, which are the type of the shapes, corner radius of hollow spheres and the hole diameter of hollow spheres (Figure 1.14).

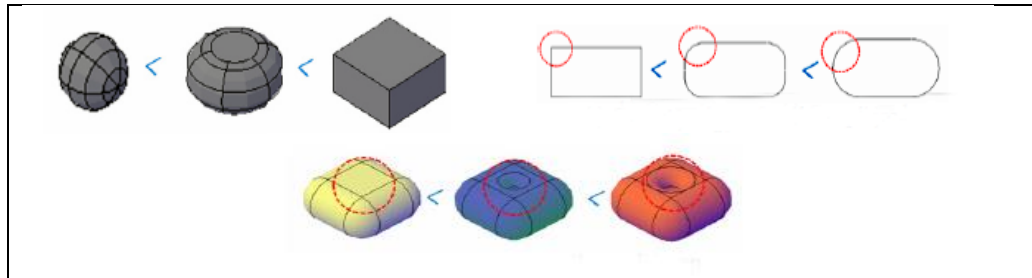


Figure 1.14 : The parameters of hollow sphere shape (J. H. Chung et al. (2015)).

Because of simplicity, these parameters were considered on two-dimensional model and as a result, the deflection and crack pattern were compared on each different parameters and reported on separate graphs. After that, by using nonlinear Finite Element Methods a target structure system with three-dimensional model was constituted in LUSAS software and the size of hollow spheres was chosen based on the height of compressive stress block in the slab, and 8 types of hollow sphere shape were considered. As a result, it was admitted that sphere shapes with a radius more than 50 mm was an optimal choice in 250 mm thick hollow slab, and the hole diameter of hollow spheres had a reverse relationship with deflection.

Jerry Paul Varghese and Manju George (2018) investigated parametrically on the seismic response of voided and solid slab systems. In this study, square and rectangular solid and voided slabs with 28 cm thickness which were subjected to uniform load and seismic force were analyzed in ANSYS 16.0 software to compare the seismic response, deflection response and structural capacities of voided and solid slab systems in terms of equivalent stress and directional deformation. As a conclusion, it was admitted that voided and solid slabs had a similar pattern in the percentage variance of deformation and stress, also it was noticed that there was not a considerable different deflection behavior of voided and solid slab under seismic force and the load carrying capacity of slabs when they were adjusted to similar uniform loads.

Joo-Hong Chung et al. (2017) investigated punching shear force design method of voided slabs. Studies showed that the presence of punching shear crack was at the void zone in first layer near the column. To investigate the reason of this occurrence, the

ratio of control perimeter (b_0) to effective depth of slab (d) in voided slabs was considered and it was verified that they were related to each other. At the end, a design method with predictable punching shear strength of voided slab was suggested.

Joo-Hong Chung et al. (2015) had another study about one-way shear strength in voided slabs, so a finite-element analysis was conducted on three voided slabs and one conventional solid slab with different void shape parameters and materials to investigate the effects of variables on the shear behavior of voided slabs. The considered void shapes were doughnut and round box void shapes, and it was believed that the ratio of void with (b_v) to slab height (H) had effects on shear strength of voided slabs. It was shown that a lower cross-sectional of voided slab, (because of the presence of voids), is the reason of lower shear strength on voided slab compared with solid slab. The crack propagation revealed that in solid type the shear crack angle was 45° , but in voided slabs with doughnut void shapes shear crack angle were 21° and 23° , which exposed that the material did not influence the shear crack angle. Also, the shear crack angle on round box voided slab was 35° that showed the void-shaper has an effect on shear crack angle. The initial shear cracking load and ultimate shear load of the voided slabs was 40.8%-43% and 60%-78% that of solid slab, respectively. Ultimate shear strength of voided slabs was 60%-81% that of solid slab. After these results, the research focused on finite element analysis of voided slab with doughnut void shapers by using LUSAS program and the results of this simulation was similar to the test results.

Juozas Valivonis et al. (2017) investigated the loss of punching capacity due to the smaller cross-sectional of voided slab and compared the results of experimental and theoretical study. In this study, the most concern was on the slab-column connection areas, based on the fact that the maximum shear strength on that point caused shear punching failure. On experimental research, six voided slabs with shear reinforcement were considered and loading was applied by a hydraulic jack (Figure 1.15).



Figure 1.15 : Experimental set-up (Juozas Valivonis et al. (2017)).

The difference between the specimens was the extent of plastic on the column-slab connection zone and as a result of experimental test, the shear failure was similar on all the specimens, but the punching shear capacity of voided slabs with solid cross shapes and shear reinforcement in the slab-column junction area was 18% greater than the voided slabs with void formers along the entire area which revealed that there should be shear reinforcements on the punching failure zone.

Mehmet Gezer (2018) carried out experimental and analytical research on concrete voided slabs. First of all, he expressed the plate theory and investigated the equilibrium equations of voided slabs as an orthotropic material and found stiffness, area, volume and correction coefficients. After that, it was shown that the compression bearing capacity was same in the voided and solid slabs when the compressive stress block was higher than the flange thickness of slab. Then, some void formers were studied parametrically to determine the optimal void formers. Also, he conducted a project in SAP 2000 software by using voided slabs and observed the results. Finally, two voided slabs were provided and were analyzed to compare the results.



2. THE GENERAL THEORIES

2.1 Introduction

In this chapter, general theories about diaphragm behavior, stress-strain relationships, finite element method and Abaqus software have been given. Also, the basic information about the investigated voided slabs and the test set-up are considered.

2.2 Diaphragm Behavior

The definition and function of the lateral forces resisting systems of buildings are usually composed of two parts. The vertical elements and horizontal elements (or approximately horizontal). The horizontal elements transfer the horizontal forces, such as earthquake and wind, to the vertical elements, and the vertical elements also transfer these forces to the foundations and to the ground. The transmitter horizontal elements are called diaphragm, and in conventional buildings, diaphragms include floors and ceilings. In such buildings, the diaphragms carry the gravity load at the same time. Also in industrial buildings, horizontal braces are responsible for transferring the horizontal forces to the vertical elements and therefore are considered as diaphragms. It is obvious that in concrete buildings, slab endures the most part of the structure's load and it should distribute the lateral load to the vertical elements by considering the stiffness ratio. This distribution is related to the diaphragm behavior that can be divided to flexible, rigid and semi-rigid.

In flexible diaphragm, the in-plane stiffness is very low and it faced with significant flexural deformation. Also in this type of diaphragm, the distribution of seismic loads, in each frame, is proportional to the seismic weight (dead weight and percentage of live weight) of that frame (Figure 2.1).

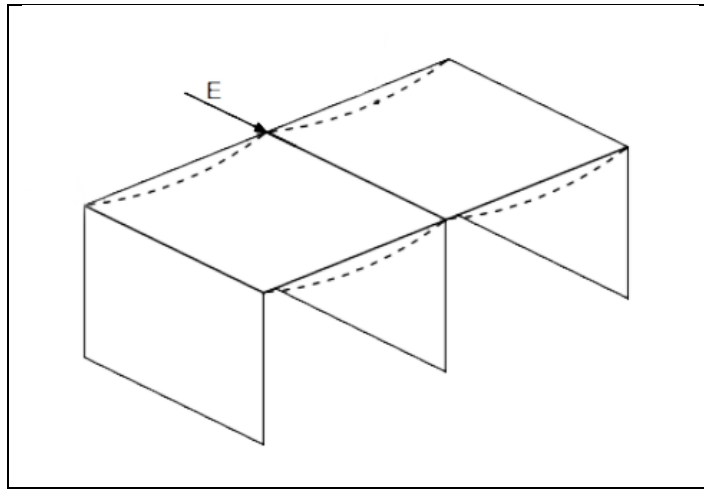


Figure 2.1 : Flexible diaphragm behavior.

On the contrary, the in-plane stiffness of rigid diaphragm is very high and the flexural deformations influenced by seismic loads are negligible. In other words, the diaphragm stiffness is so high that by connecting the elements to the diaphragm, the in-plane diaphragm degrees of freedom is limited to 3 degrees (2 degrees horizontal and 1 torsional), which is shown in Figure 2.2. Therefore, the seismic force will be applied as a concentrated load in the center of mass of floor. Concentrating seismic forces will reduce computations (narrowing the hardness matrix) and will reduce the calculations during analysis (Figure 2.3).

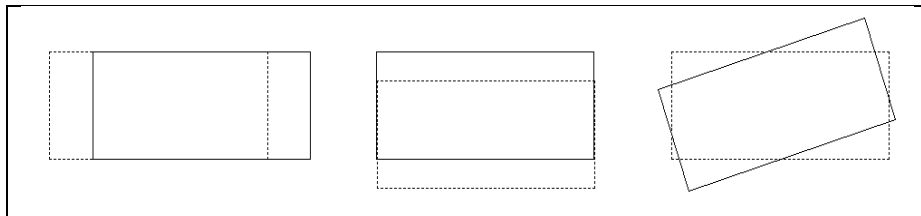


Figure 2.2 : Degrees of freedom in rigid diaphragm.

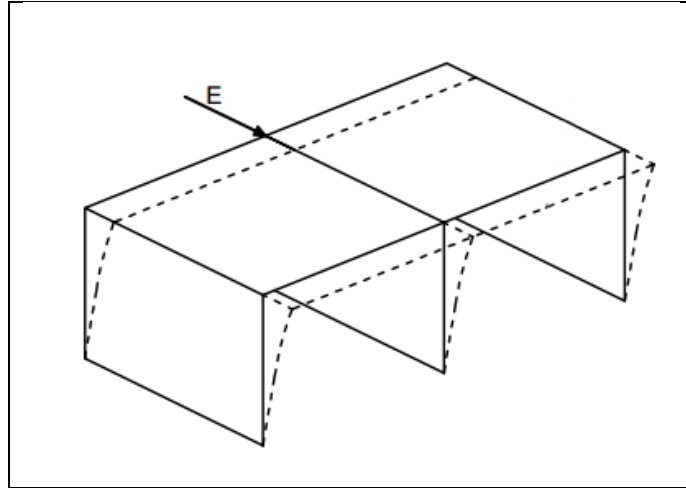


Figure 2.3 : Rigid diaphragm behavior.

Semi-rigid diaphragm, behave like both of the behaviors mentioned above.

2.3 Stress components

External forces that apply to a body, produce internal forces that called stress, and it is measured in units of force per unit area (N/m^2). Stresses can be divided to normal stress and shear stress. Normal stress is resulted from the force vector component perpendicular to the cross section, but shear stress is resulted from the force vector component parallel to the cross section. Figure 2.4 and 2.5 depict the stress components on a three-dimensional and two-dimensional body in Cartesian coordinate system, respectively and Equation (2.1) shows the relationship of stress equation:

$$\sigma = \tau = \frac{F}{A} \quad (2.1)$$

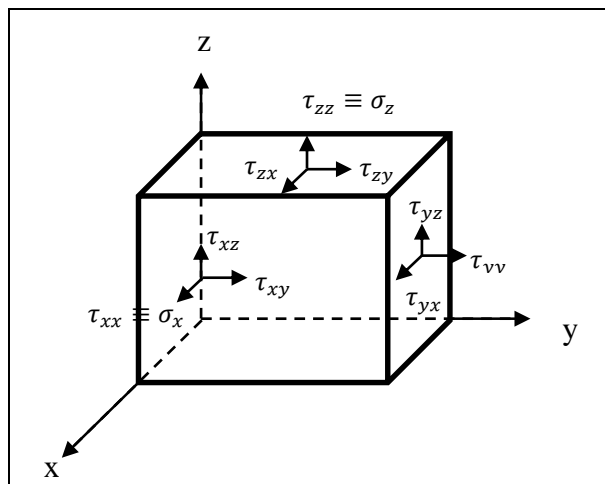


Figure 2.4 : The stress components on a three-dimensional body.

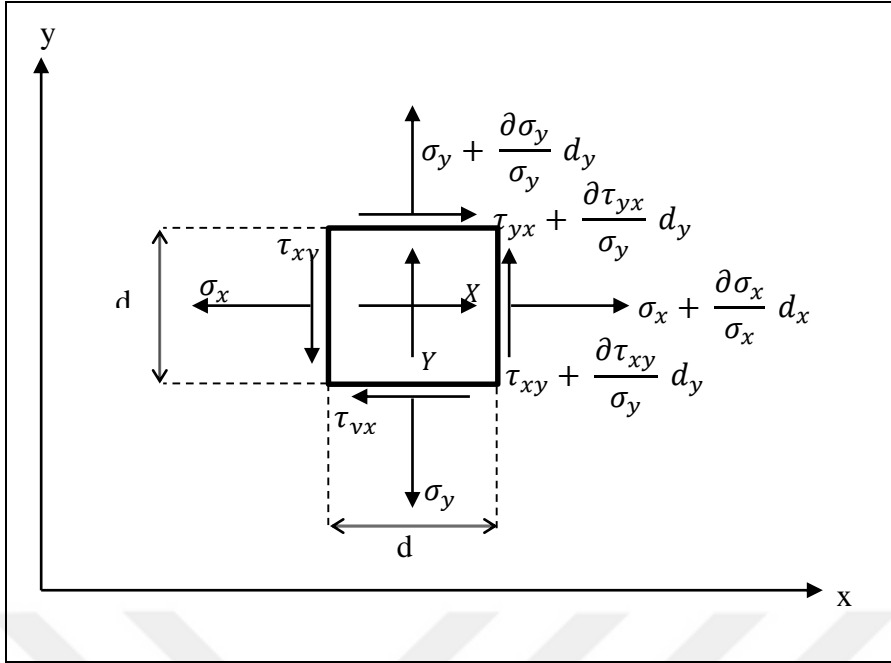


Figure 2.5: The stress components on a two-dimensional body in Cartesian coordinate system.

Where, σ represents the normal stress, and τ shows the shear stress. F is the applied force and A is the cross sectional area.

2.4 Strain components and displacement

External forces that apply to a body cause deformation, and the changes of body length depend on the stiffness of the body. Therefore the strain can be defined as the ratio of the deformation length on the original length. Assume a body like Figure 2.6.a and consider a small arbitrary portion (Figure 2.6.b) with Δx , Δy and Δz dimensions to find out the strain components. After applying forces, as it is illustrated in Figure 2.6.c, the dimension of the deformed portion will be:

$$(1+\varepsilon_x)\Delta x \quad (1+\varepsilon_y)\Delta y \quad (1+\varepsilon_z)\Delta z \quad (2.2)$$

And the changed angles of the deformed portion can be calculated as:

$$\frac{\pi}{2} - \gamma_{xy} \quad \frac{\pi}{2} - \gamma_{yz} \quad \frac{\pi}{2} - \gamma_{zx} \quad (2.3)$$

The components of displacements are u , v and w which are represent the displacements in x , y and z directions, respectively. By considering definitions of strain and displacement, Equation (2.4) can be found simply:

$$\varepsilon_x = \frac{\partial u}{\partial x} \quad \varepsilon_y = \frac{\partial v}{\partial y} \quad \varepsilon_z = \frac{\partial w}{\partial z} \quad (2.4)$$

Also, the shear strains are obtained as Equation (2.5)

$$\gamma_{xy} = \frac{\partial v}{\partial x} + \frac{\partial u}{\partial y} \quad \gamma_{yz} = \frac{\partial w}{\partial y} + \frac{\partial v}{\partial z} \quad \gamma_{zx} = \frac{\partial w}{\partial x} + \frac{\partial u}{\partial z} \quad (2.5)$$

Where, ϵ represents the direct strain, and γ corresponds to shear strain.

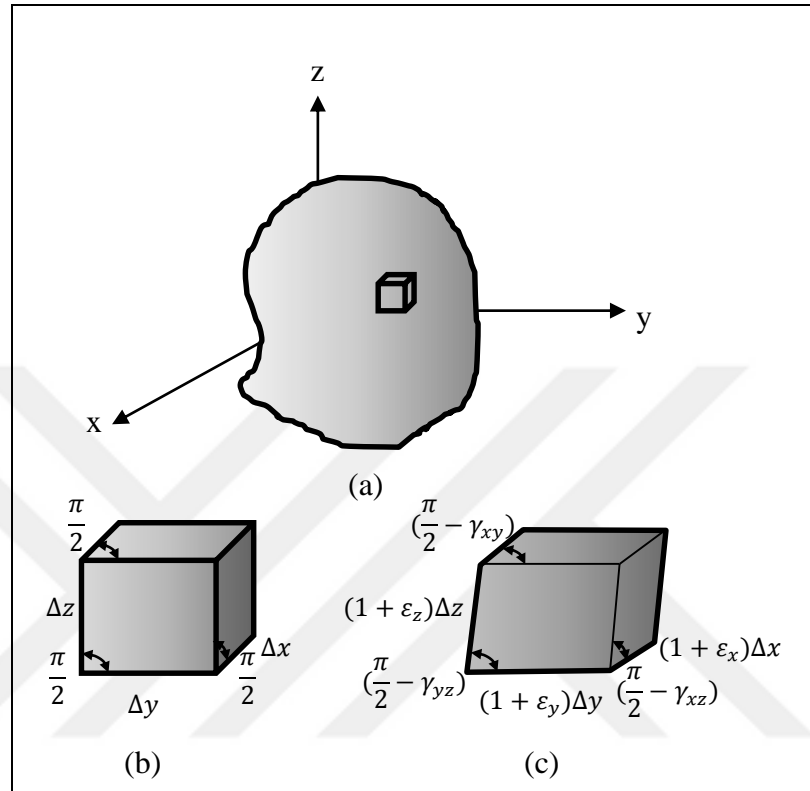


Figure 2.6 : Strain components on a three-dimensional body in Cartesian coordinate system.

In addition, strains on an undeformed and deformed small two-dimensional portion are shown in Figure 2.7.

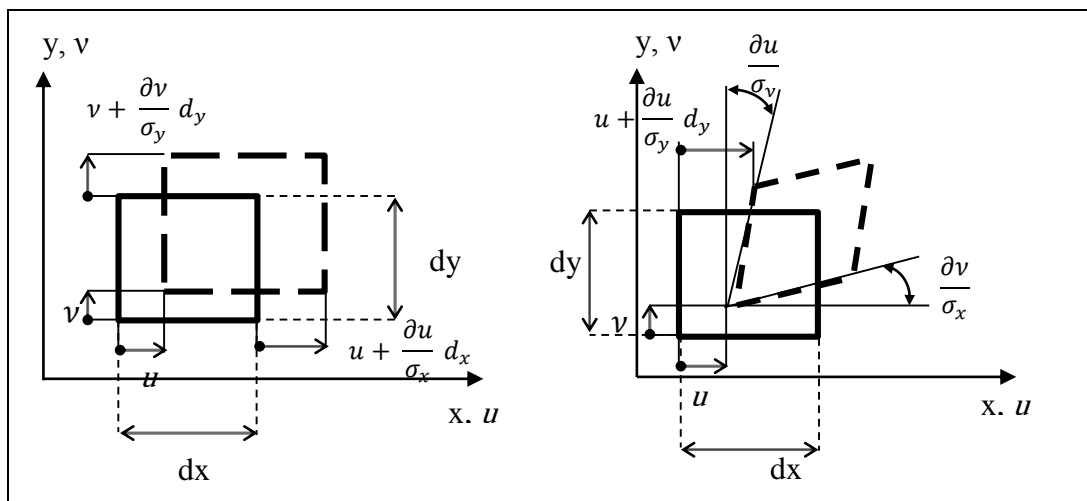


Figure 2.7 : Strain components on a two-dimensional body in Cartesian coordinate system.

2.5 Plate Theory

In structural engineering, plate is defined as a three-dimensional body, which the thickness is smaller in comparison to the other two dimensions, (Figure 2.8). The stresses and deformations of plates, which subjected to loading (which purpose of the thesis is to determine them), depend largely on the thickness than of two other dimensions. The advantage of plate theory is simplifying the three-dimensional problem to two-dimensional one.

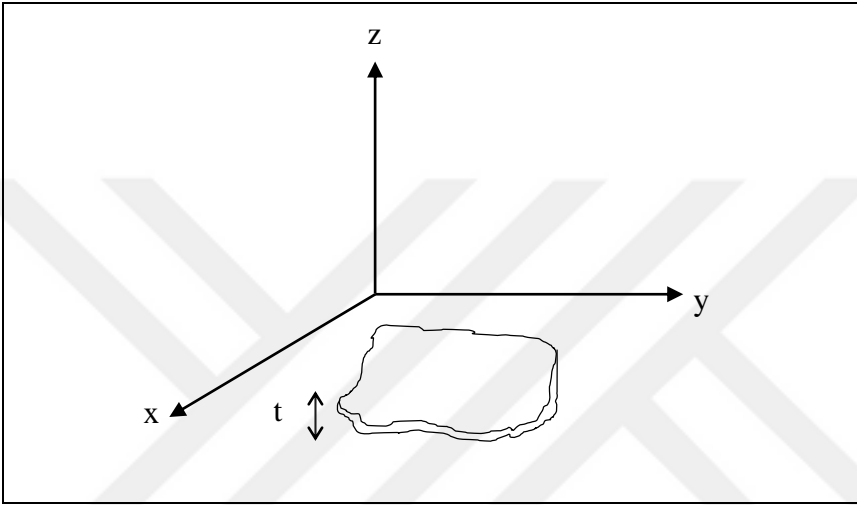


Figure 2.8 : Plate in Cartesian coordinate system.

Plate depends on thickness can behave in different ways which are considered briefly as follows.

2.5.1 Membrane plate

Plate with membrane behavior has very thin thickness and just axial forces (membrane forces) are considered, thus moments are negligible. For simulating a model, membrane behavior are used for shear wall and some slabs (Figure 2.9).

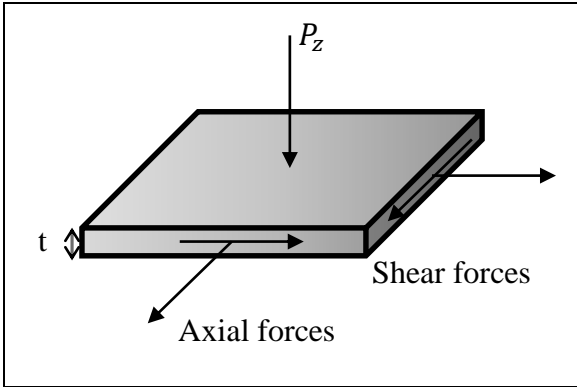


Figure 2.9 : Plate with membrane behavior

2.5.2 Thin plates

If the ratio of the thickness (t) to the width (b) of a plate is less than 0.1, then the plate is called thin plate. Also, thin plates follow the classical theory (Kirchhoff) which has three assumptions as follows (Figure 2.10):

1. The straight lines perpendicular to the mid-surface of plate, remain perpendicular after deformation.
2. The normal stress in thickness direction σ_z is ignored. And this is the reason of converting the three-dimensional problems to the two-dimensional problems.
3. The straight lines perpendicular to the mid-surface of plate do not change in length after deformation, (thickness of plate remains constant).

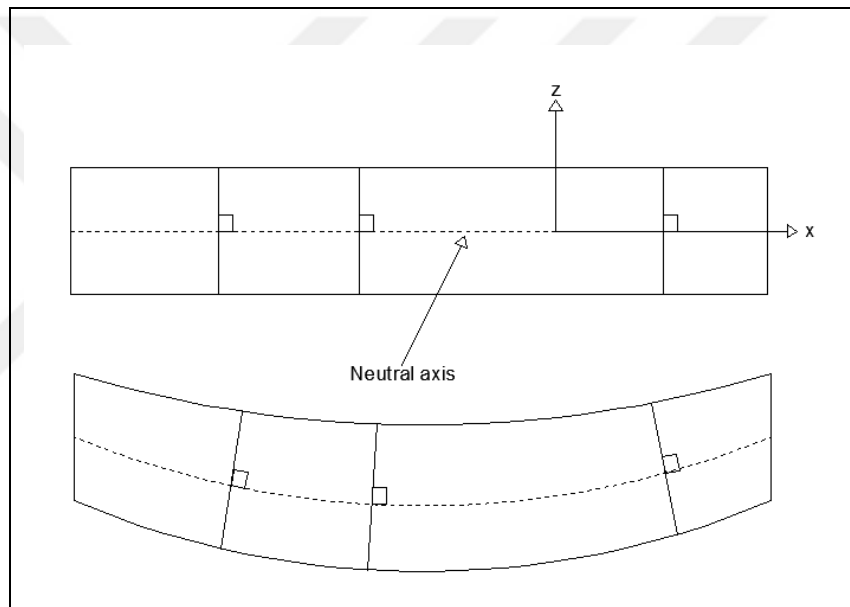


Figure 2.10 : Kirchhoff plate before and after deformation.

2.5.2.1 Basic Equations

Basic relationships for thin plates can be easily obtained by assuming a plate located in x , y and z coordinates with u , w and v displacements of any points. Let y be a constant value and mid-surface of plate be located on x - z coordinates (Figure 2.11). Thus, as it is shown in Equation (2.6), the displacements of x and z across the thickness can be obtained in terms of w , which is deflection of plate in z direction.

$$u = -z \frac{\partial w}{\partial x} \qquad v = -z \frac{\partial w}{\partial y} \qquad (2.6)$$

Also, by using equations in Equation (2.4) and (2.5), strain and deflection can be related to each other as shown in Equation (2.7).

$$\begin{aligned}\varepsilon_x &= \frac{\partial u}{\partial x} = -z \frac{\partial^2 w}{\partial x^2} = z \kappa_x & \varepsilon_y &= \frac{\partial v}{\partial y} = -z \frac{\partial^2 w}{\partial y^2} = z \kappa_y \\ \gamma_{xy} &= \frac{\partial v}{\partial x} + \frac{\partial u}{\partial y} = -2z \frac{\partial^2 w}{\partial x \partial y} = z \kappa_{xy}\end{aligned}\quad (2.7)$$

$$\begin{Bmatrix} \varepsilon_x \\ \varepsilon_y \\ \gamma_{xy} \end{Bmatrix} = -z \begin{bmatrix} \frac{\partial^2}{\partial x^2} \\ \frac{\partial^2}{\partial y^2} \\ \frac{\partial^2}{\partial x \partial y} \end{bmatrix} w$$

Where, κ represents the curvature along respective directions.

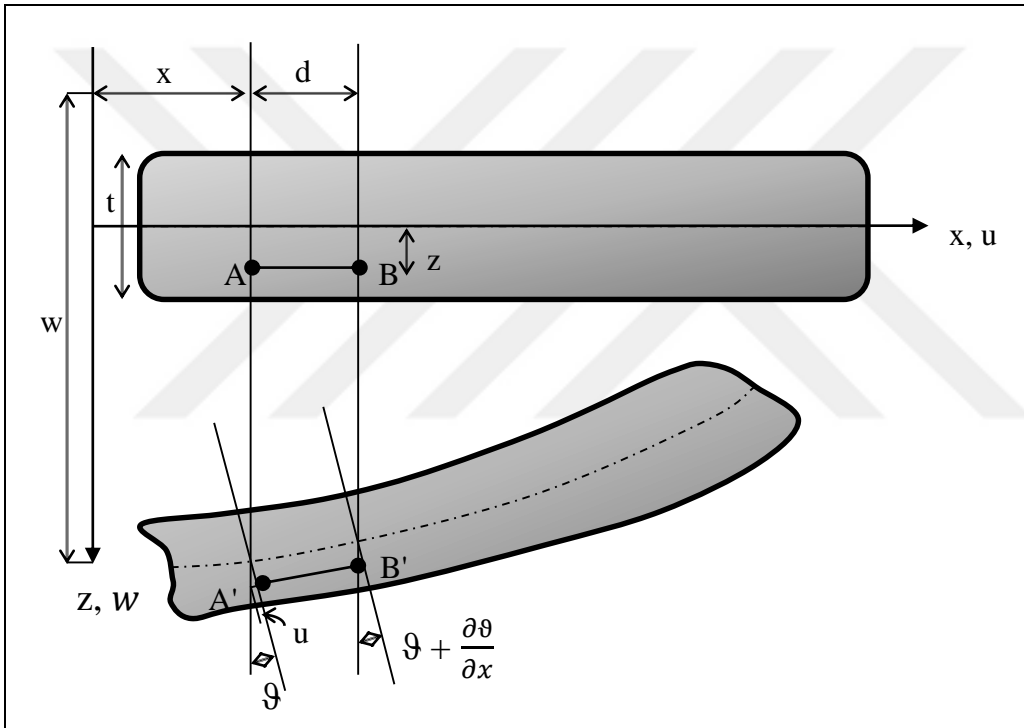


Figure 2.11 : Thin plate element.

In addition, by using Hooke's law stress and strain relationships can be calculated as Equation (2.8)

$$\begin{aligned}\sigma_x &= \frac{E}{1-\nu^2} (\varepsilon_x + \nu \varepsilon_y) & \sigma_y &= \frac{E}{1-\nu^2} (\varepsilon_y + \nu \varepsilon_x) \\ \tau_{xy} &= \tau_{yx} = G \gamma_{xy} = \frac{E}{2(1+\nu)} \gamma_{xy}\end{aligned}\quad (2.8)$$

$$\sigma = \frac{E}{(1-\nu^2)} \begin{bmatrix} 1 & \nu & 0 \\ \nu & 1 & 0 \\ 0 & 0 & \frac{1-\nu}{2} \end{bmatrix} \varepsilon \quad \sigma = [D] \varepsilon$$

Where, E and G are Young's modulus and shear modulus, respectively and ν is the Poisson ratio.

Moreover, Equation (2.9) shows the stress and displacement relationships by considering mentioned equations.

$$\sigma_x = -\frac{Ez}{1-\nu^2} \left(\frac{\partial^2 w}{\partial x^2} + \nu \frac{\partial^2 w}{\partial y^2} \right) \quad \sigma_y = -\frac{Ez}{1-\nu^2} \left(\frac{\partial^2 w}{\partial y^2} + \nu \frac{\partial^2 w}{\partial x^2} \right) \quad (2.9)$$

$$\tau_{xy} = \tau_{yx} = \frac{Ez}{1+\nu} \left(\frac{\partial^2 w}{\partial xy} \right)$$

The summary of stress distributions are illustrated in Figure 2.12, which shows the stress distribution. Also, in-plane normal forces and bending moments are shown in Figure 2.13.

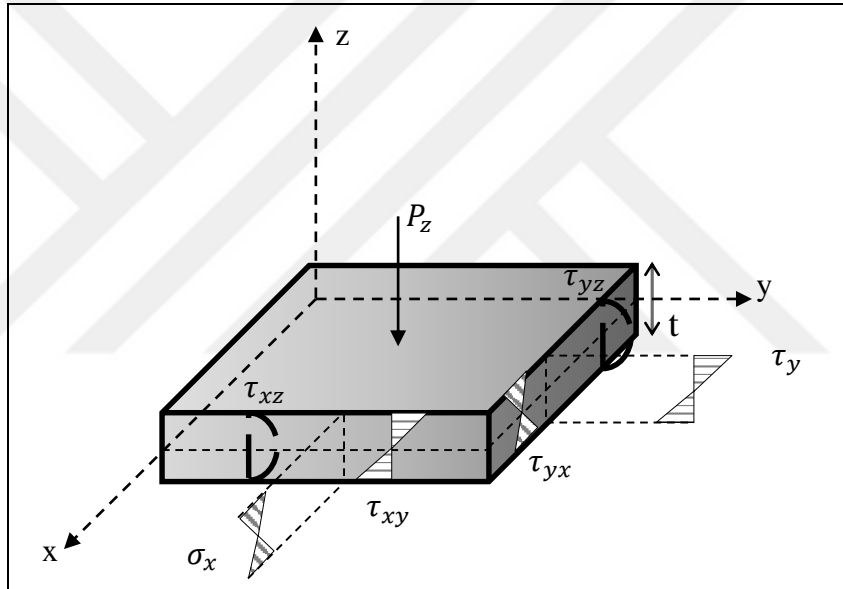


Figure 2.12 : Stress distribution in plate.

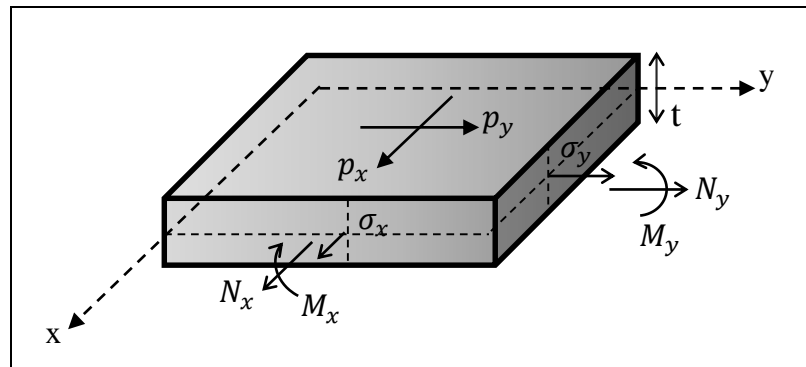


Figure 2.13 : In-plane normal forces and bending moments.

In addition, the in-plane shear forces and twisting moments can be considered as are described in Figure 2.14.

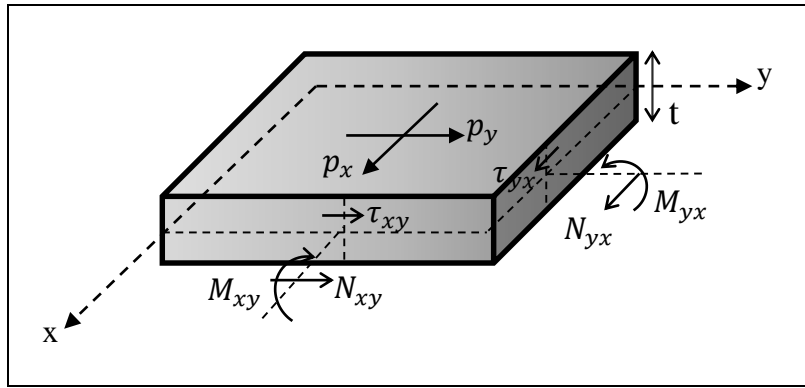


Figure 2.14 : In-plane shear forces and twisting moments.

Finally, force equilibriums in x and y-directions are calculated by considering P_x and P_y as follow:

$$\frac{\partial N_x}{\partial x} + \frac{\partial N_{yx}}{\partial y} + p_x = 0 \quad \frac{\partial N_y}{\partial y} + \frac{\partial N_{xy}}{\partial x} + p_y = 0 \quad (2.10)$$

2.5.3 Thick Plates

Kirchhoff theory is not a general principle for all of the plates, and it is not accurate for thick plates, which the thickness to width ratio is greater than 0.1, because the Kirchhoff theory is correct just for plates with small deformation. But for analyzing thick plates, the Mindlin-Reissner plate theory, which include the effect of transverse shear deformation, can be applied. In Mindlin-Reissner plate theory the straight lines normal to the mid-surface of plate before deformation are not essentially remain normal to it after deformation (Figure 2.15).

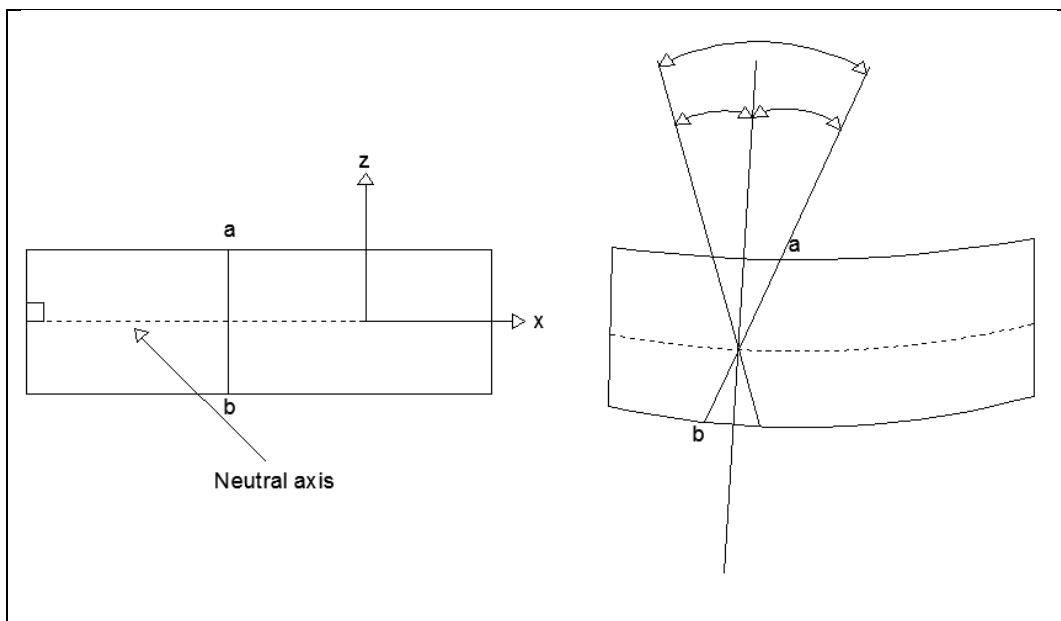


Figure 2.15 : Mindlin-Reissner plate before and after deformation.

2.5.3.1 Basic Equations

In case of thick plate, by taking the Mindlin-Reissner theory into consideration (Figure 2.15), u and v are found as follows:

$$u(x, y, z) = z\theta_x(x, y) \quad v(x, y, z) = -z\theta_y(x, y) \quad w(x, y, z) = w(x, y) \quad (2.11)$$

Also, the transverse strains can be obtained as:

$$\gamma_{xz} = \theta_x + \frac{\partial w}{\partial x} \quad \gamma_{yz} = -\theta_y + \frac{\partial w}{\partial y} \quad (2.12)$$

For small displacements, we can write Equation (2.13) to find displacement and strains relationships:

$$\begin{aligned} \varepsilon_x &= \frac{\partial u}{\partial x} = -z \frac{\partial \theta_x}{\partial x} & \varepsilon_y &= \frac{\partial v}{\partial y} = -z \frac{\partial \theta_y}{\partial y} \\ \gamma_{xy} &= \frac{\partial v}{\partial x} + \frac{\partial u}{\partial y} = -z \left(\frac{\partial \theta_x}{\partial y} + \frac{\partial \theta_y}{\partial x} \right) \\ \gamma_{xz} &= \frac{\partial u}{\partial z} + \frac{\partial w}{\partial x} = \frac{\partial w}{\partial x} - \theta_x \\ \gamma_{yz} &= \frac{\partial v}{\partial z} + \frac{\partial w}{\partial y} = \frac{\partial w}{\partial y} - \theta_y \end{aligned} \quad (2.13)$$

Further, the Equation (2.14) shows the stress relationship with strain and displacements:

$$\begin{aligned} \sigma_x &= \frac{E}{1-\nu^2} (\varepsilon_x + \nu \varepsilon_y) & \sigma_y &= \frac{E}{1-\nu^2} (\varepsilon_y + \nu \varepsilon_x) \\ \tau_{xy} &= G \gamma_{xy} & \tau_{xz} &= G \gamma_{xz} & \tau_{yz} &= G \gamma_{yz} \\ \sigma_x &= -\frac{Ez}{1-\nu^2} \left(\frac{\partial \theta_x}{\partial x} + \nu \frac{\partial \theta_y}{\partial y} \right) & \sigma_y &= -\frac{Ez}{1-\nu^2} \left(\frac{\partial \theta_y}{\partial y} + \nu \frac{\partial \theta_x}{\partial x} \right) \\ \tau_{xy} &= -Gz \left(\frac{\partial \theta_x}{\partial y} + \frac{\partial \theta_y}{\partial x} \right) & \tau_{xz} &= G \left(\frac{\partial w}{\partial x} - \theta_x \right) & \tau_{yz} &= G \left(\frac{\partial w}{\partial y} - \theta_y \right) \end{aligned} \quad (2.14)$$

In summary, the internal forces are shown in Figure 2.16, which represents a thick plate subjected to external forces:

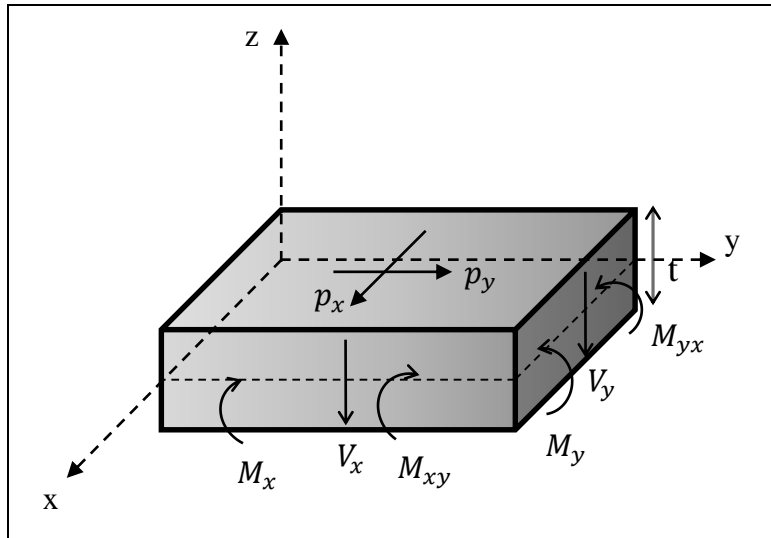


Figure 2.16 : Thick plate internal forces.

2.6 Shear Stress

Shear stress, as mentioned, is resulted from the force vector component parallel to the cross section of material and it can be obtained by Equation (2.15) for beams.

$$\tau = \frac{VQ}{It} \quad (2.15)$$

Where, V is total shear force applied to the beam, Q is statical moment of area, I is moment of inertia and t is the thickness of the material.

For instance, Figure 2.17 represents the distribution of the shear stress of a beam with rectangular cross section of width b and height h subjected to a shear force V . By using Equation (2.15), shear stress can be obtained as Equation (2.16).

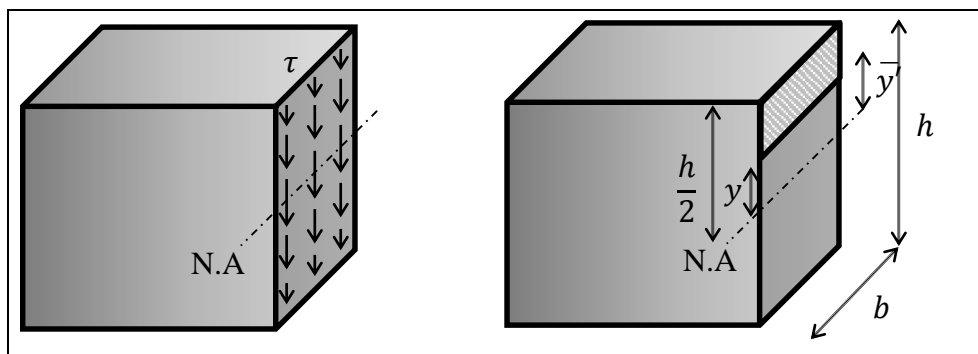


Figure 2.17 : An example of distribution of the shear stress of a beam with rectangular cross section.

$$Q = \bar{y}' A = \left(y + \frac{1}{2} \left(\frac{h}{2} - y \right) \right) \times \left(\left(\frac{h}{2} - y \right) b \right) = \frac{1}{2} \left(\frac{h^2}{4} - y^2 \right) b$$

$$I = \frac{bh^3}{12} \quad t=b \quad \tau = \frac{VQ}{It} = \frac{V \times \frac{1}{2} \left(\frac{h^2}{4} - y^2 \right) b}{\frac{bh^3}{12} \times b} = \frac{6V}{bh^3} \left(\frac{h^2}{4} - y^2 \right) \quad (2.16)$$

2.6.1 Pure Shear

Pure shear is an action of shear on an object which there is no normal stresses or bending. Figure 2.18 shows a state of pure shear that can be transformed into an equivalent system of normal stresses. In this case, normal stresses are equal to zero, so by considering the Equation (2.17) the principle stresses can be obtained as $\sigma_{1or2} = \tau_{xy}$. Also, the condition of principle planes is calculated by Equation (2.18). The angle of principle planes are $\theta_1 = 45^\circ$ and $\theta_2 = 135^\circ$. For determining the tension and compression planes, $\theta_1 = 45^\circ$ is substituted in Equation (2.19) and as a result, $\sigma_1 = \tau_{xy}$ so the normal tension stress is applied to AB plane.

$$\sigma_{1or2} = \frac{\sigma_x + \sigma_y}{2} \pm \sqrt{\left(\frac{\sigma_x - \sigma_y}{2}\right)^2 + \tau_{xy}^2} \quad (2.17)$$

$$\tan 2\theta = \frac{2\tau_{xy}}{\sigma_x - \sigma_y} \quad (2.18)$$

$$\sigma_x' = \frac{\sigma_x + \sigma_y}{2} - \frac{\sigma_x - \sigma_y}{2} \cos 2\theta + \tau_{xy} \sin 2\theta \quad (2.19)$$

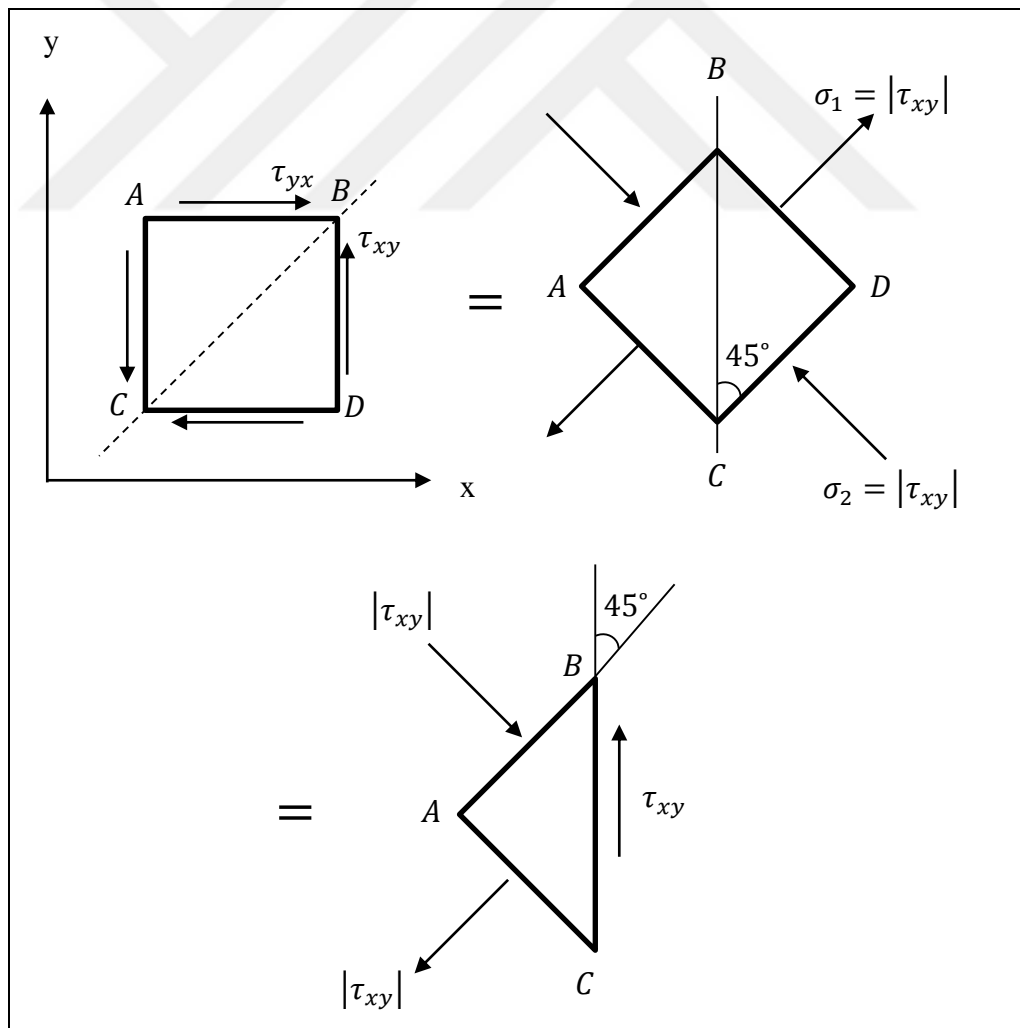


Figure 2.18 : Transformation of pure shear to normal stresses.

2.6.2 Pure shear in this investigation

The purpose of this thesis is researching the behavior of voided slabs subjected to a pure shear force. So, the mentioned principles can be used to determine a set-up to investigate this test. Figure 2.19 shows the applied forces to a plate which can be considered as a voided slab. But in reality, subjecting the shear force in the form of two components can be complicated, so applying the resultant vector is considered as a basic theory of a set-up.

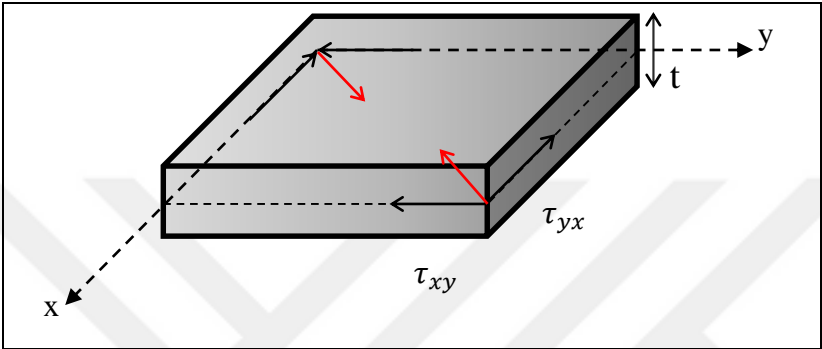


Figure 2.19 : Pure shear in a voided slab.

2.7 Basic Theories

In this investigation, the effects of shear force on diaphragm behavior of a voided slab is considered. Figure 2.20 shows a voided slab before and after applying a load, schematically. According to the direction of the loading (P), the slab is squeezed due to the compression in the same direction of the loading and it is shrank due to the tension in the other direction, which are shown in the Figure by v and h, respectively. Shear force can be easily calculated by Equation (2.20). The area used in this equation is the diagonal area which the resultant force vector is tangent to. As it is obvious in Figure 2.21, areas of the voids should be eliminated to obtain the pure area. The strains in each direction are obtained by dividing the squeezing or the shrinking values of the corners to the unchanged diagonal size of the slab. The summation of the two strains shows the shear angle (Equation 2.21).

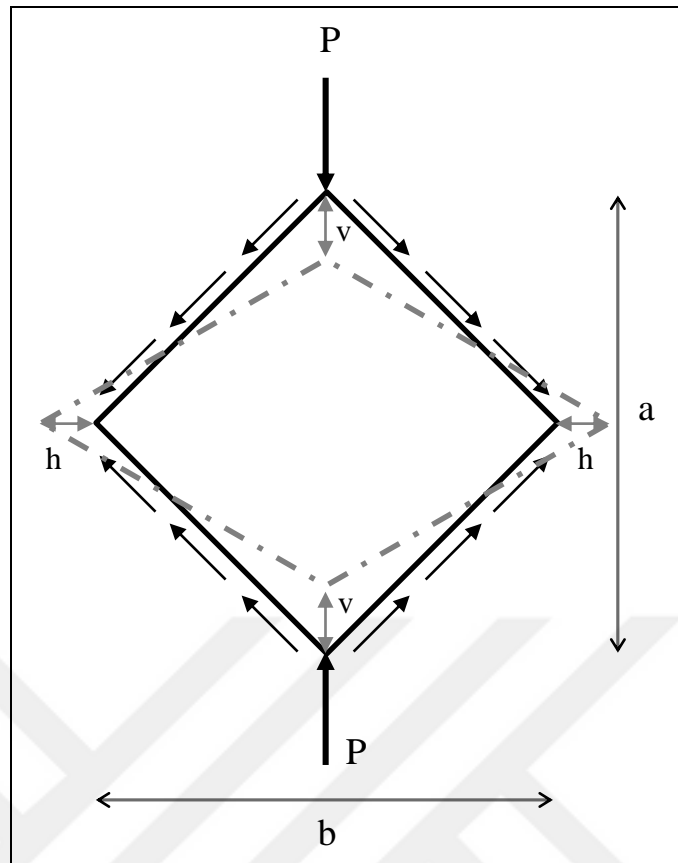


Figure 2.20 : The changed and unchanged form of a voided slab.

$$\tau = \frac{P}{A} \quad A = A_{total} - A_{void} \quad (2.20)$$

$$\varepsilon_v = \frac{\Delta v}{a} \quad \varepsilon_h = \frac{\Delta h}{b} \quad \gamma = \varepsilon_h + \varepsilon_v \quad (2.21)$$

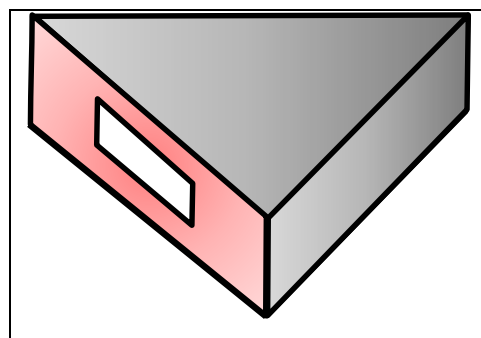


Figure 2.21 : The area used for obtaining shear force.

The graph of the shear stress-shear angle can be drawn as Figure 2.22 after obtaining the corresponding values. The elastic shear stress is 0.7 of the maximum shear stress approximately and the ratio of the elastic shear stress and elastic shear angle is the shear modulus of the voided slab (Equation 2.22).

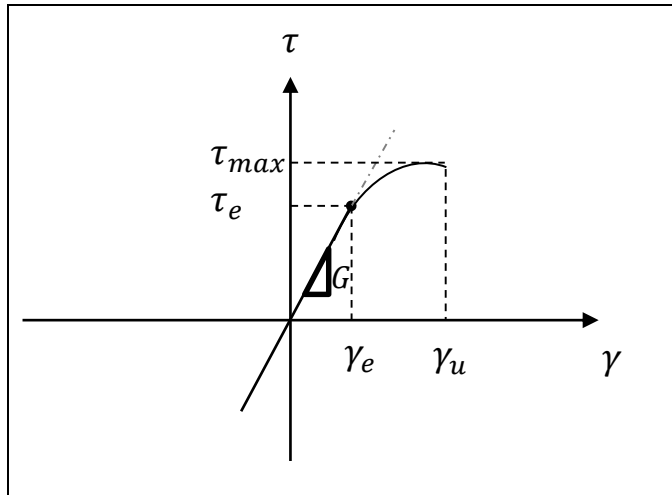


Figure 2.22 : The shear stress-shear angle graph.

$$\tau_e \cong 0.7 \tau_{max} \qquad G = \frac{\tau_e}{\gamma_e} \qquad (2.22)$$

In addition, another graph which can be drawn by using the obtaining parameters is shear stress-strains graph. As it is obvious in Figure 2.23, this graph shows the relationship between shear stress and strain in both directions. The positive part of the graph shows the tension and the negative part shows the compression in voided slab.

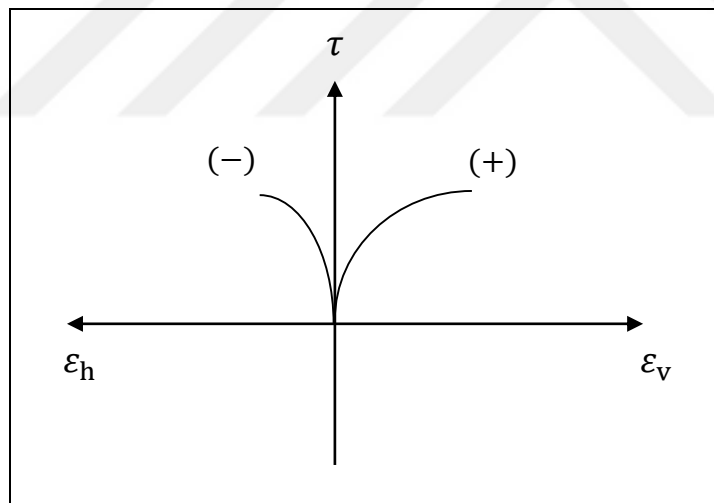


Figure 2.23 : The shear stress-strain graph.

2.8 Finite Element Method

Finite element method is a very powerful numerical technic to simulate any physical phenomenon, especially used for structural analysis, by using digital computer. Voided slabs which are considered as plates are simulated by using this method to investigate the different behavior of them. The main advantage of this method over other mathematical methods is that it can solve any irregular geometries routinely. The one well-known way of this method is to divide a structure into an equivalent system of

large number of smaller and simple units which represent the original structure. In this way, which is named going from part to whole, the mathematical operation for solving the problem of the structure is applied to each smaller unit separately, and the general solution is obtained by combining the solution of each participant. In this method, smaller elements, which can be one, two or three dimensional, are considered interconnected at joints that are called nodes and the displacements of these nodes will be the basic unknown parameters of the problem. The triangle in Figure 2.24 is the popular two-dimensional element that can be used in dividing any two-dimensional structure to hundreds or thousands of these triangles.

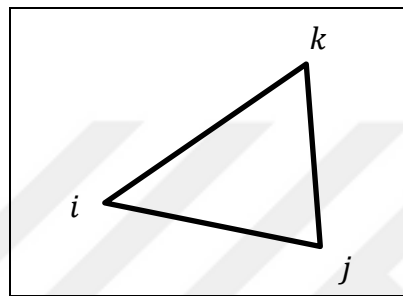


Figure 2.24 : Triangular element.

There are two main ways to solve stress-strain problems in this method. In differential method, solution for equilibrium of an elastic body can be reduced to a differential equation, but in energy method, solution for equilibrium of an elastic body can be reduced to an extremum problem of an integral equation.

2.9 Abaqus software

The provided voided slabs are simulated in Abaqus computer program which can analyze the wide range of systems by using finite elements and rigid bodies that are the fundamental component of Abaqus software. The shape of rigid bodies does not change when they move through space, but finite elements are deformable. The main difference between rigid bodies and finite elements is the number of degrees of freedom, where the rigid bodies have 6 degrees of freedom, but the finite elements have many. Voided slab which is considered as a plate is simulated by using finite element method to investigate the shear behavior of it. This method is a very powerful numerical technique to simulate any physical phenomenon, especially used for structural analysis, by using digital computer. The main advantage of this method over other mathematical methods is that it can solve any irregular geometries routinely. The one well-known way of this method is to divide a structure into an equivalent system of

large number of smaller and simply unites which represents the original structure. In this way, which is named going from part to whole, the mathematical operation for solving the problem of the structure is applied to each smaller unite separately, and the general solution is obtained by combining the solution of each participants. In this method, smaller elements, which can be one, two or three dimensional, are considered interconnected at joints that are called nodes and the displacements of these nodes will be the basic unknown parameters of the problem and plates are considered as four node elements.

2.9.1 Family

Elements with different shapes and geometries are existed in Abaqus program used in a stress analysis which are shown in Figure 2.25.

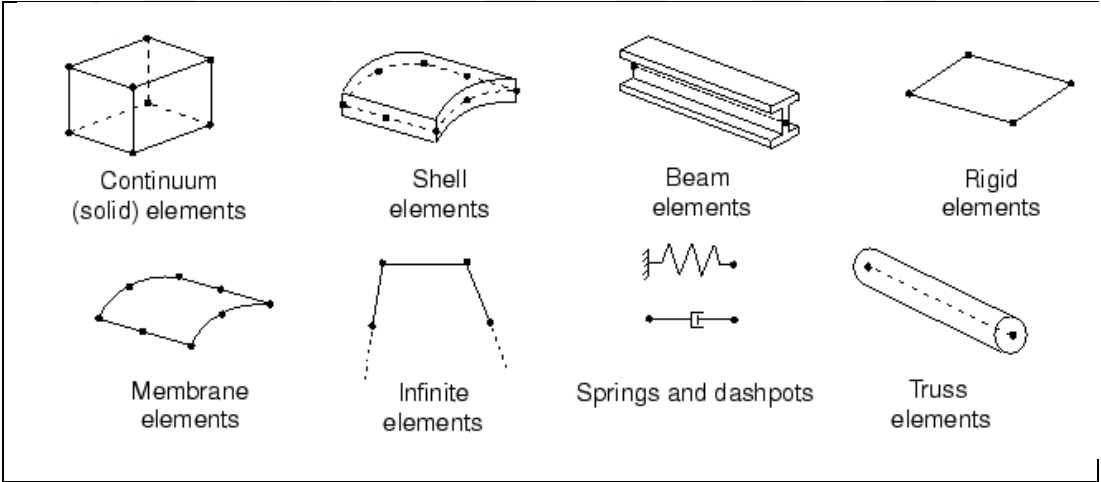


Figure 2.25 : The usual element families in Abaqus software.

2.9.2 Degrees of freedom

The number of independent displacements that each node of an element can have is called degrees of freedom. In shell elements, these displacements are translation and rotational degrees of freedom. Also, many degrees of freedom are used for any simulation in Abaqus software.

2.9.3 Number of nodes

As mentioned above, in finite element method, nodes are main components to investigate. Also, the degrees of freedom are related to nodal displacements, and interpolating from the nodal displacements is used for finding the displacements of

any point of an element. Figure 2.26 shows three type of different elements with vary number of nodes which is used in Abaqus program.

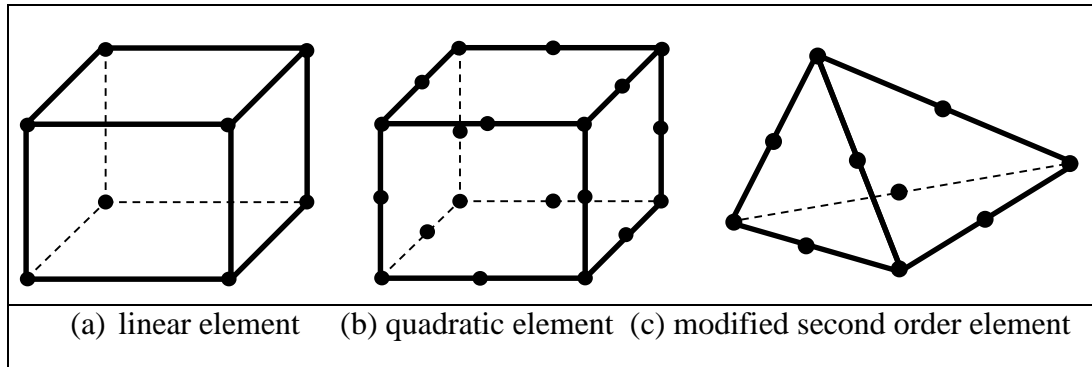


Figure 2.26 : Abaqus software different elements with vary number of nodes.

2.9.4 Formulation and integration

Formulation is the mathematical expression used to determine the element's behavior. In Abaqus software, the elements in a family which have different types of behavior are formulated in different types. Numerical techniques are used to integrate ...

Voided slab is considered as a shell element, because in shell element the thickness is expressively smaller than other dimension, which is explained formerly in plate theory. Thus, for simulating voided slab in Abaqus program, considering five aspect, shell element should be chosen. Shell element, in Abaqus software, can be considered as a general-purpose, thin-only and thick-only. Because the shell element is a three-dimensional element, it has 6 degree of freedom. The properties of shell element is related to its section property such as thickness and material properties. The stiffness of shell element can be calculated by using numerical integration through the shell thickness, which is used for both linear and nonlinear materials, or by considering the cross section before the analysis, that is just for linear materials, and in this method there is no need for integrating any quantities over the element cross-section. Further explanation about simulation is mentioned in forth chapter.

2.9.5 Materials in Abaqus program

For simulating a voided slab, there is a need to consider the properties of the materials of a voided slab which is consist of steel and concrete. Assignment of the properties of steel is much easier than concrete. For modeling the steel material, density, Young's module, Poisson's ratio, yield stress and plastic strain will be sufficient. It is important to be mentioned that the plastic strain starts from zero and reach a peak at ultimate

strain. In other words, the assigning strain is obtained from subtraction of the plastic strain and elastic strain of the steel. But for simulating concrete material, there are plenty models and ways. For general and elastic properties of the concrete the density, Young's module and Poisson's ratio is enough, but because the nonlinear behavior of a voided slab is considered in this investigation, the parameter of damage of the concrete should be assigned too. Concrete damage plasticity is a one option in Abaqus software to define the damage parameter of the concrete. For compressive behavior of concrete, the Popovics model is used which is considered by Equation (2.23).

$$\sigma_{ci} = \left(\frac{\varepsilon_{ci}}{\varepsilon_c}\right) f'_c \frac{n}{n-1 + \left(\frac{\varepsilon_{ci}}{\varepsilon_c}\right)^{nk}} \quad k = \begin{cases} 1 & 0 < \varepsilon_{ci} < \varepsilon_c \\ 0.67 + \frac{f'_c}{62} & \varepsilon_{ci} > \varepsilon_c \end{cases} \quad n = 0.8 + \frac{f'_c}{17} \quad (2.23)$$

Where σ_{ci} is the stress of the concrete in each strain (ε_{ci}). f'_c is the compressive strength of a concrete and ε_c is the ultimate strain of a concrete.

Tension behavior models of the concrete has no significant differences in their results, so the tensile strength of the concrete is considered as 10% of compressive strength conventionally ($\sigma_{ct} = 0.1\sigma_{cu}$). And when the tension stress is 0.01 of the ultimate tension strength, the corresponding strain is taken as 10 times of the strain, in which stress was equal to ultimate tensile strength.

Another parameter which is used for compression and tension behavior of the concrete damage plasticity is the damage parameter which is ranging from zero to one.

2.10 Isotropic and orthotropic materials

Materials which have the identical values of a property in all the components of the material and have the same behavior in all the directions are called isotropic materials. Steel and glass are the obvious examples for isotropic materials. These materials follow the Hooke's law in analysis. But voided slab, because of the existence of voids in a slab, do not show the same behavior in all directions and some considerations should be done to analyze this type of material by basic equations. This type of material is called orthotropic material and voided slab is an example for this material.

2.11 Cross section properties

It is obvious that orthotropic material has different cross section properties in compared with isotropic material. Thus, some important cross-sectional properties of both type of materials are considered in Figure 2.27 and Equation (2.24).

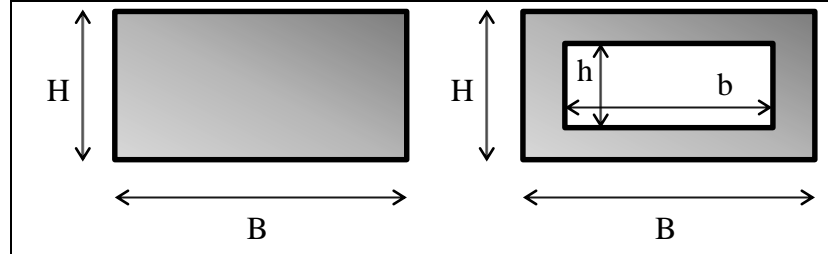


Figure 2.27 : Cross section of isotropic and orthotropic materials

$$\begin{aligned}
 A_{slab} &= BH & A_{voided slab} &= BH - bh \\
 I_{slab} &= \frac{BH^3}{12} & I_{voided slab} &= \frac{BH^3}{12} - \frac{bh^3}{12} \\
 S_{slab} &= \frac{BH^2}{6} & S_{voided slab} &= \frac{B}{6H} (H^3 - h^3)
 \end{aligned}
 \tag{2.24}$$

Also, these equations can be considered per one meter dimension by dividing the equations to by B. By obtaining the ratio of orthotropic and isotropic materials, the correction factor value can be calculated for any kind of sample.



3. EXPERIMENTAL INVESTIGATION ON VOIDED SLAB

3.1 Introduction

Two voided slabs were provided by ABS Company to investigate the diaphragm behavior. The both slabs were reinforced concrete with same material properties and one varied value was the dimension of the slabs which were 1-a with 178.5 cm × 178.5 cm dimension, and 1-b with 201 cm × 201 cm dimension. Another varied value was the space between voids that in second one, the space between voids were designed two times of that in the first one. Before concreting the voided slabs, two strain gauges were installed perpendicularly to the bars of the samples (Figure 3.1).

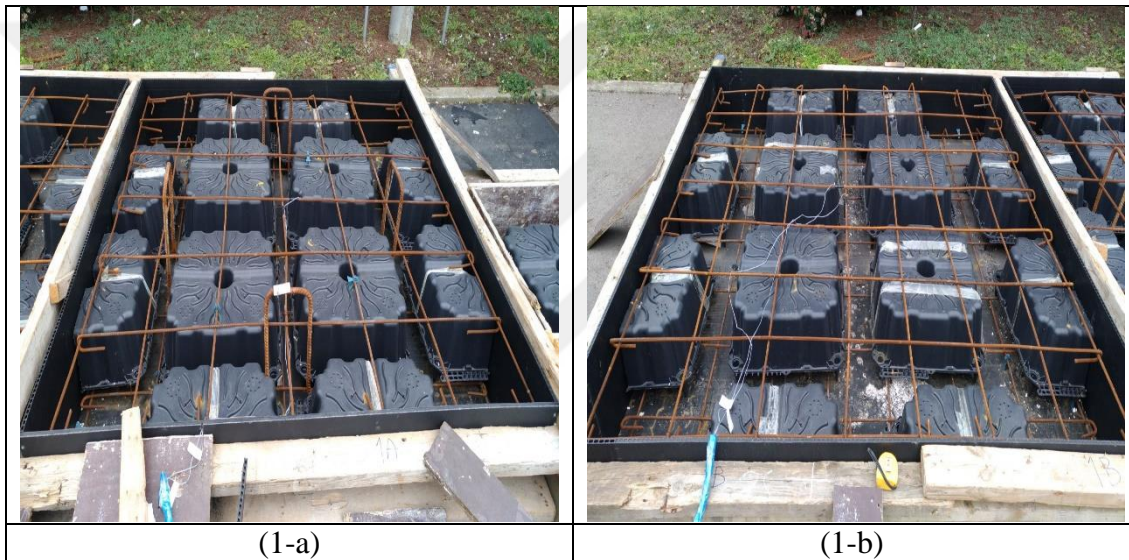


Figure 3.1 : The condition of the bar's strain gauges of the samples.

3.2 Set-up of the investigation

For doing the analysis on the voided slabs, there was a need for a set-up to keep the voided slabs and measured the shear force to observe the shear strength of the structure by subjecting displacement. Also, this set-up should be in a form to make pure shear force to the system. Thus, some elements were provided to analyze this system. All the elements were composed of steel with six holes to be maintained together by six rods. First element was installed to a corner of the edge of the voided slab (Figure 3.2 A1). In the opposite direction of the voided slab, the second element (Figure 3.2 B2) was fitted like the first element. Both elements had triangular plate on the bottom to hold the voided slab. In the backside of this element, there should be a hydraulic jack

to make displacement to the system and for holding this hydraulic jack the third element which was a rectangular plate (Figure 3.2 B3) was mounted in the back. Finally, because this hydraulic jack could not measure the applied load in each step, there was a need for a load cell, which should be fixed at the opposite point. Because each load cell's capacity was 100 ton, there should be three of them and again for holding these load cells the last element (Figure 3.2 B3) was installed.

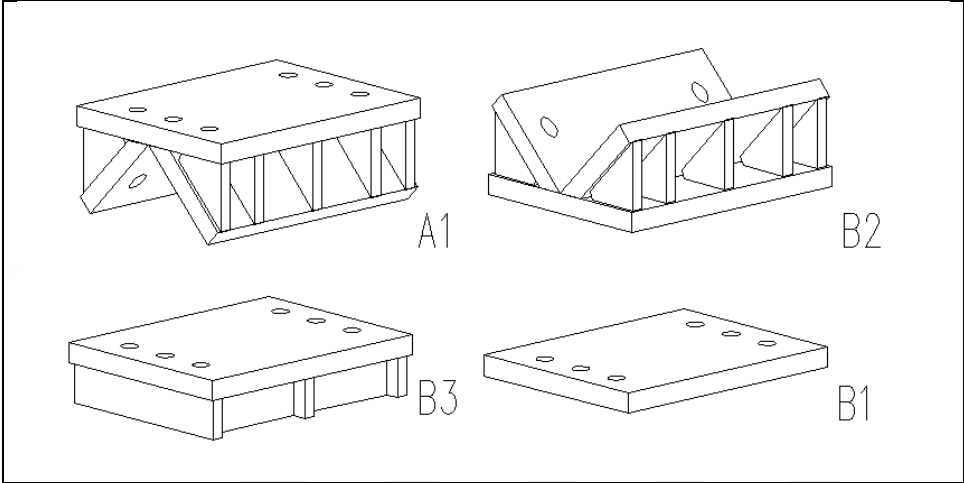


Figure 3.2 : The setup of the analysis system.

For connecting the supports to the slab, concreting the joint areas of slab and supports was required. Also, as mentioned above, six holes on each plates were designed to use six rods to keep this system together, but in this system four rods were sufficient, which two rods were at the top of the system and the other ones were at the bottom. For decreasing the friction, plates which were covered by a layer of grease were put on the bottom of the supports. Finally, the system was fastened from each side by nuts on each bar and fastening system by nuts should make equal force on each bar. The last condition of the system is shown schematically in the Figure 3.3.

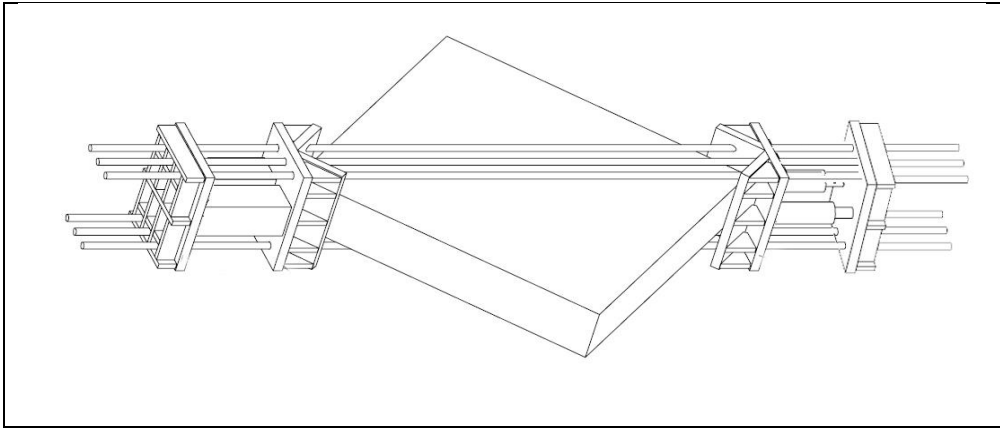


Figure 3.3 : The final situation of the system.

3.2.1 The measurement system

It was essential to have some measurement instruments in this investigation to obtain the changed values during the test. As mentioned before, the force that should be obtained as a result of the applied displacement could not be found by an available hydraulic jack, so, because of the limited capacity of the available load cells, three of them were used in this experiment. Before concreting the voided slab, two strain gauges were installed to the top bars of the slab, in the same direction of the bars, perpendicular to each other to measure the strains on the bars as shown schematically in Figure 3.4-1. As it is obvious from the loading condition, the edges of the slab which are on the supports are going to be in the compression situation and the other ages are going to be in tension condition, so after concreting the slab, a strain gauge was installed to the surface of the upside of the slab in the direction of the loading, and the other one was installed perpendicularly to it to measure the strains of the concrete. The two other strain gauges were installed like the upside ones to the downside to compare the strains in the two surface of the slab during the experiment (Figure 3.4-2). The last strain gauges that were installed at the each rods of the setup to compare the obtained load values from the load cells and these strain gauges. The four strain gauges are shown in the Figure 3.4 which the number 3 show the upper rod's strain gauges and the number 4 are for the downside rod's strain gauges. Another measurement device that was used in this system was the transducer to obtain the displacement of the certain point of the voided slab. Six transducers were needed to this experiment to obtain the required displacements. So, firstly four points were determined at the each corner and after that four rods were embedded at the each points. Also, some flat bars were joined to the mentioned rods to connecting the points and keeping the transducers to move easily and to obtain the displacements. It is obvious that during the loading, these four embedded rods are going to move as voided slab moves and the transducers which are connecting to the rods will obtain the values of displacements. The transducers were arranged in a form as showing in Figure 3.4-5.

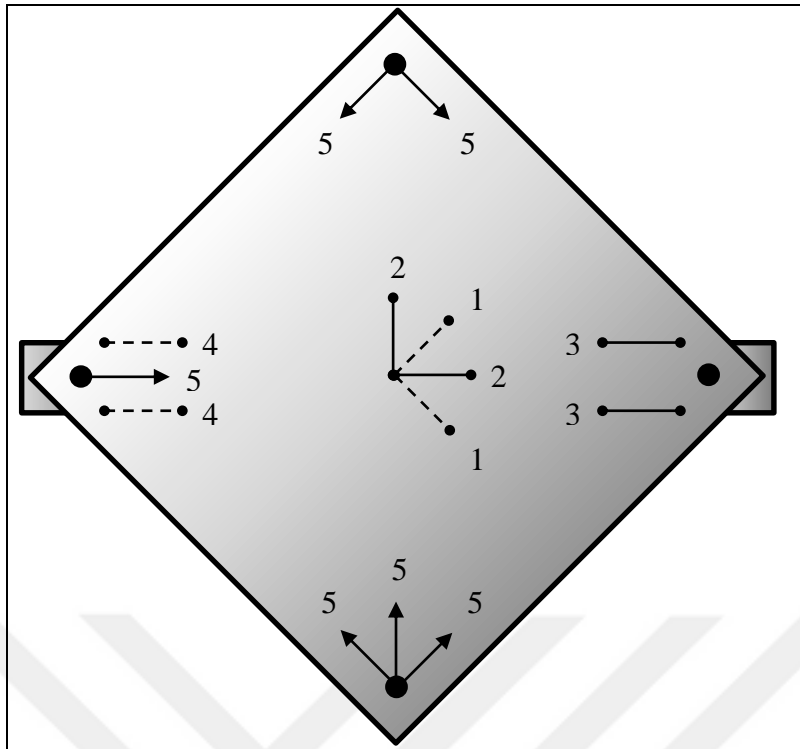


Figure 3.4 : The measurement system (schematically).

The following Figures show the experimental condition of the measurement system:

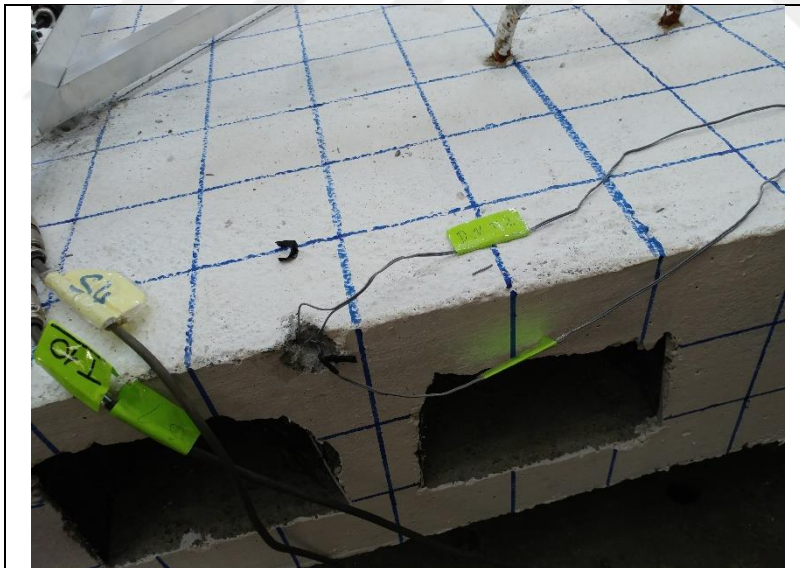


Figure 3.5 : The strain gauges installed to the bars of the voided slab.

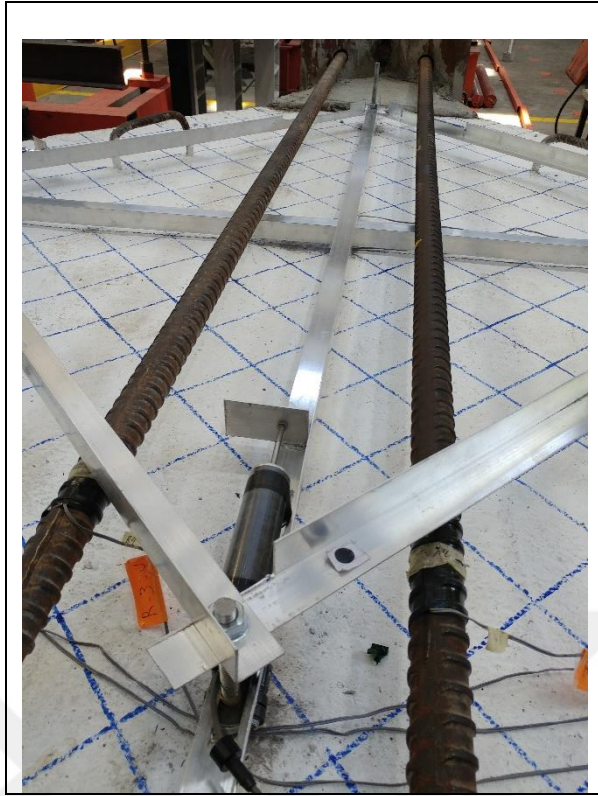


Figure 3.6 : The strain gauges on the rods and a transducer.

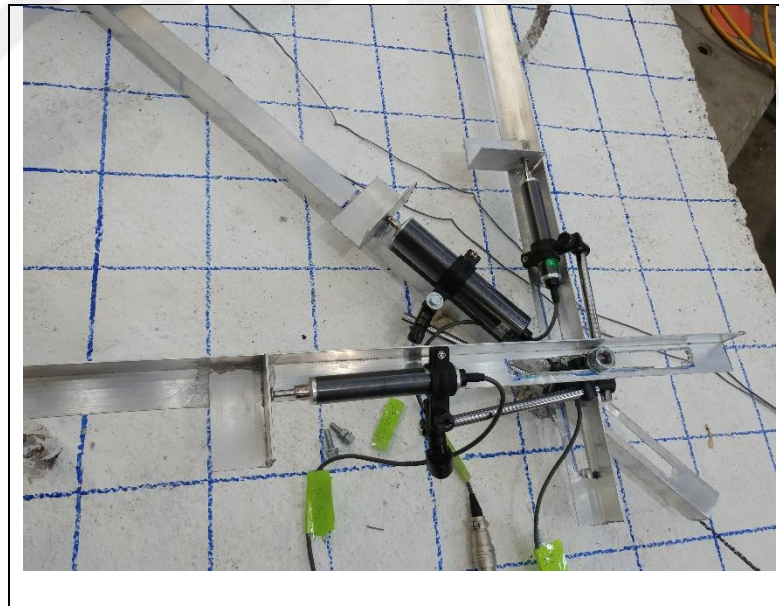


Figure 3.7 : The three transducers on a corner of the voided slab.



Figure 3.8 : The other two transducers on another corner of the voided slab.



Figure 3.9 : The last and provided condition of the system.

3.3 Analysis step of first sample 1-a

The voided slab named 1-a was the first sample which was experimented. The designed dimensions of this slab was $178.5 \text{ cm} \times 178.5 \text{ cm}$ and the space between the voids was 7.5 cm . In this voided slab the positions of the rods, which were embedded to obtain the displacements by transducers, were in the 49.5 cm from the corners. It is obvious that when the system was fastened by the nuts of the rods, the amount of load was subjected to the system so, as mentioned before, the applied load that was carried by each rod should be equal to each other before the beginning of the experiment. Also, the sum of the loads of the up side rods were equal to the down side's to transfer the same amount of load to the both surface. In addition, the total value of this load could

be compared and controlled by the values which were obtained from the rod's strain gauge and the load cells. The provided form of the first voided slab before the test is shown in Figure 3.10.

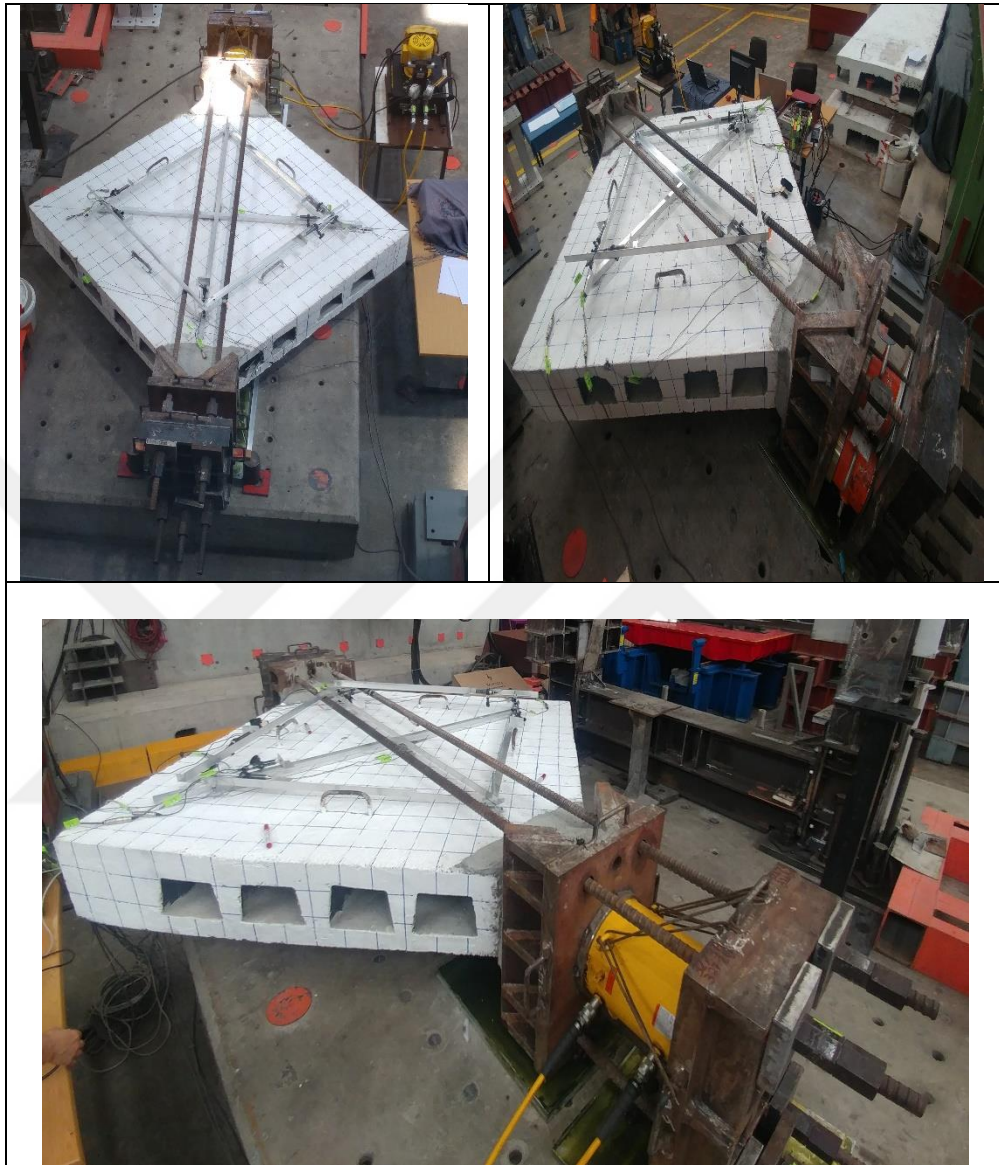


Figure 3.10 : The provided 1-a voided slab

At the beginning of the experiment, the loading was in the elastic behavior of the system. So, the steady amount of load, around 400 KN, was subjected to the voided slab and after observing the graphs, the system was unloaded.

At the next step, the loading was continued until occurring the first crack on the voided slab. So, the loading was increased gradually and at the 795.763 KN the noticeable crack arose which can be seen in the Figure 3.11 and it is obvious that the bars of the voided slab were in the yield condition.



Figure 3.11 : The first crack of the voided slab.

The loading operation was continued after observing the crack size. After a modest increase in the amount of loading, in each step of loading the other new cracks were monitored and also the size of the prior cracks were increased. Figure 3.12 shows a general view of the noticeable cracks and the condition of the voided slab under a significant amount of load.



Figure 3.12 : The noticeable cracks of the voided slab.

This loading process was repeated and finally the subjected load reached its peak and the failure of the voided slab happened abruptly. The highest point of the loading was 1480 KN then it reduced to 1466 KN and after that the subjected load on the system decreased sharply to the 213 KN. After that, the applied load was increased few times and as more load was subjected, the failure was increased. Lastly, the test was stopped at the 65 KN of load (Figure 3.13).



Figure 3.13 : The failure of the voided slab.

Figure 3.14 shows the bottom of the first voided slab at the last point.



Figure 3.14 : The cracks of the bottom of the voided slab.

3.4 Analysis step of second sample 1-b

The second investigation was on 1-b voided slab which was larger than first one in dimension and also in this voided slab, the space between voids was greater than the first ones. The dimension was 201 cm × 201 cm and the space between the voids was 15 cm. The position of the rods, which were embedded in this voided slab, was 53 cm from each corner. This voided slab became ready just like the first one and again the subjected load in each rods of the set-up of the system was almost equal to each other. Figure 3.15 shows the last condition of the second voided slab before the test.



Figure 3.15 : The 1-b voided slab before the test.

The steps of this test were like the first voided slab. The first level was started by applying a load which was in the elastic behavior of the voided slab. In this test, because of the larger dimension compared with first one, 500 KN was applied to the system and then unloaded. This step was repeated few times to observe the elastic behavior of the voided slab.

After first step, the loading was continued until emerging the first crack on the voided slab. In 993 KN the first crack was observed which had a tiny size. The displacement of a transducer in the same direction of the loading in this step was 0.53 mm. (Figure 3.16).

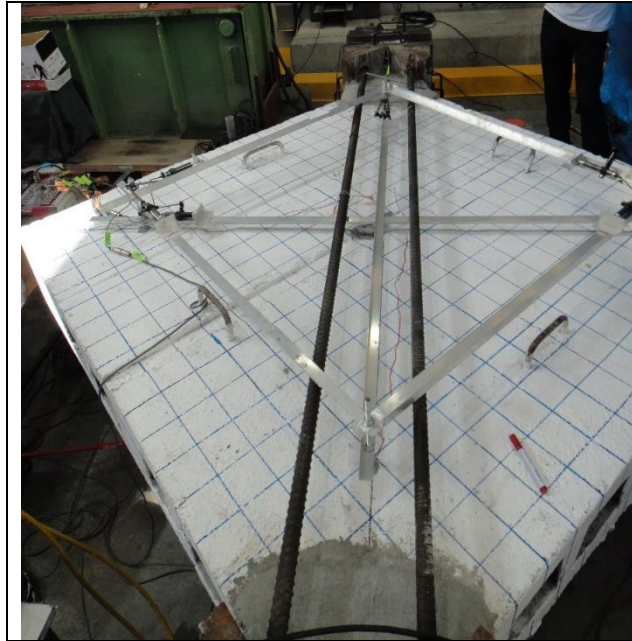


Figure 3.16 : The first crack of the voided slab.

In the next steps, as the loading process was continued, the plenty number of cracks showed up with different dimensions and the prior ones changed significantly in compared with the previous levels. Figure 3.17 shows the almost all the showed up cracks in the remarkable amount of a loading.

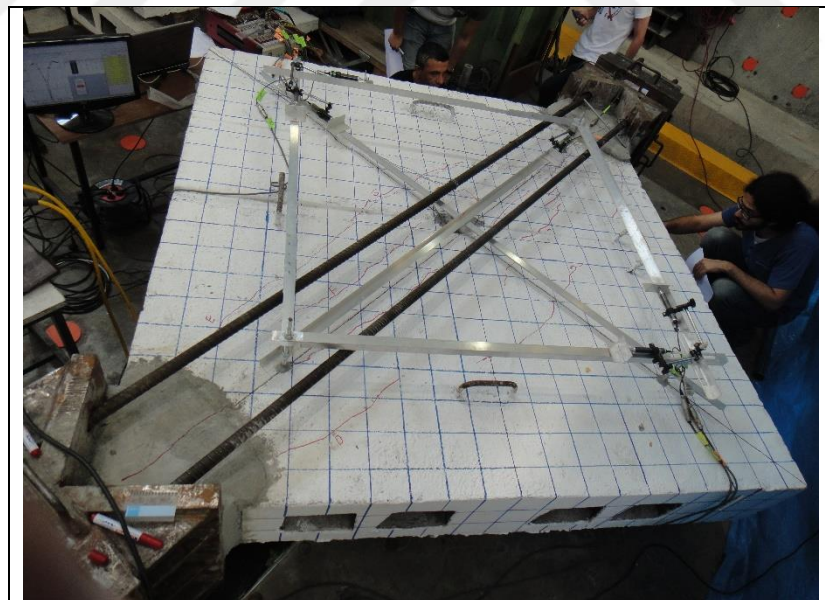


Figure 3.17 : Some of the cracks of the voided slab.

Finally, when the loading reached to 1807 KN, the operation was maintained to observe the showed up cracks and in that moment, the voided slab fractured abruptly. In this amount of a force, the displacement was 3.36 mm but, because of maintaining the loading to note the cracks, the force decreased to 1642 KN and displacement

increased to 5.21 mm and in this point the failure happened. Also, after fracture, the force and displacement changed to 723KN and 6.55 mm, respectively. So Figure 3.18 shows the failure level of the system with significant changes in size of the cracks.

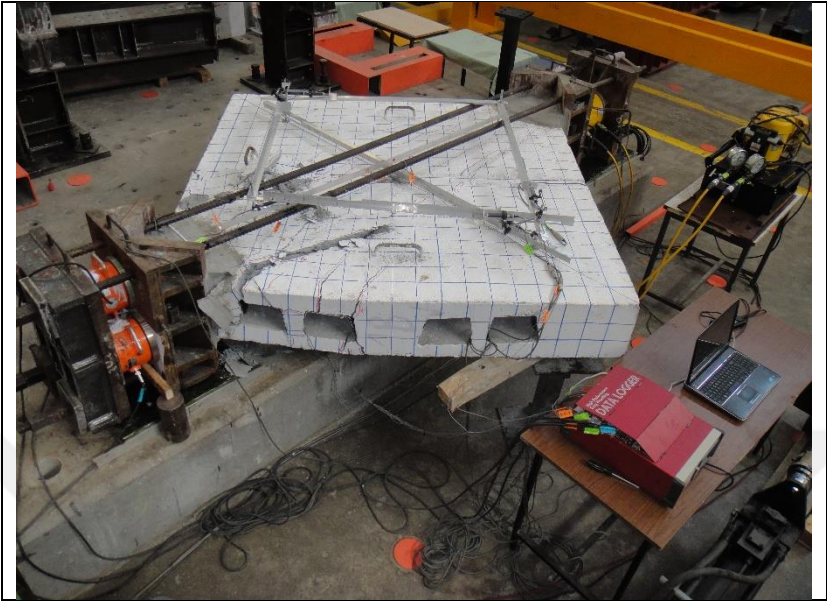


Figure 3.18 : The failure condition of the voided slab.

As it was done in the first voided slab, the loading was continued few more steps to observe the final condition of it. Because the rods of the set-up buckled due to the subjected load and it hit to the transducers, the data of them could not be reliable, so the test was stopped. The last point can be observed obviously in Figure 3.19.

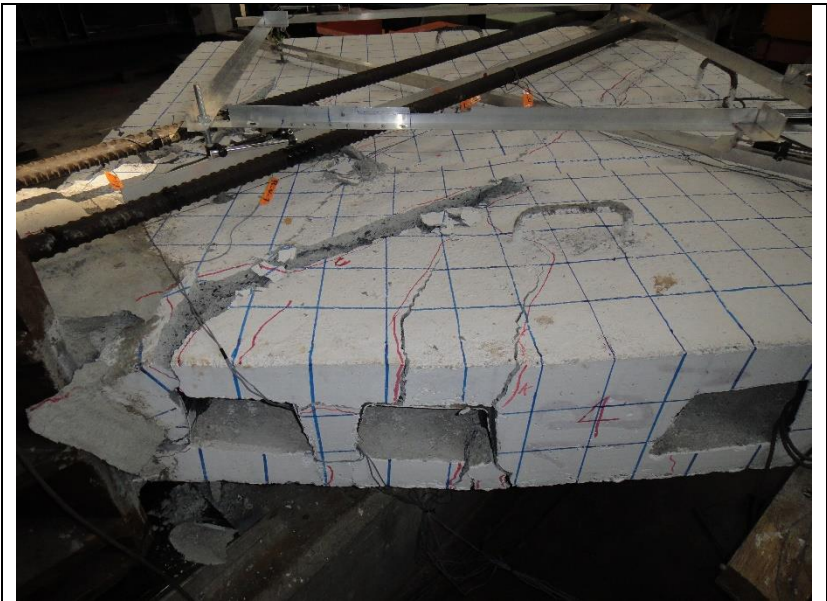


Figure 3.19 : The last condition of the voided slab.

Figure 3.20 shows the bottom condition of the second sample and its crack patterns.



Figure 3.20 : The bottom cracks of the voided slab.

3.5 The results of the test

In this section, some important information of the results of the voided slabs are gathered to observe and investigate the analysis. Firstly, the following tables (Table 3.1 and Table 3.2) show the crack sizes of the voided slabs as they were observed. First column shows the forces in KN unit and the second one shows the displacement of the voided slab in the same direction of the force applied which is in mm unit. The other columns are the crack names and their sizes in mm unit. It is obvious that as loading was continued, the new cracks were observed and in each steps the size of the some previous cracks was increased. At the last step of the first one, during the crack

observing the failure was happened so the sizes could not be measured but the data of failure level for the second voided slab are available.

Table 3.1 : The crack sizes of the 1-a voided slab.

		A	B	C	D	E	F	G	H	I	J
KN	mm										
795	0.2	0.4									
1067	0.47	0.8	0.15	0.2							
1131	0.56	0.9	0.15	0.35	0.25						
1216	0.63	0.95	0.2	0.55	0.45	0.15					
1310	0.7	0.95	0.25	0.7	0.45	0.2	0.1	0.1	0.08	0.1	
1369	0.76	1	0.3	0.85	0.5	0.2	0.15	0.15	0.08	0.1	0.1
1480	0.84										
1467	0.86										

Table 3.2 : The crack sizes of the 2-a voided slab.

		A	B	C	D	E	F	G	H	I	J	K
KN	mm											
993	0.53	0.1										
1143	0.67	0.3										
1549	1.19	0.8	0.2	0.2	0.1	0.1	0.2	0.15	0.08			
1837	1.74	1	0.7	0.7	0.2	0.6	0.45	1.1	0.1	0.5	0.1	0.15
1807	3.36	1.3										
1642	5.21	5.5	failed	2.4	0.2	2.2	0.6	3.5	0.6	0.9	0.25	4.5

Figure 3.21 and 3.22 show the force-displacement graph of the first and second voided slabs, respectively in total displacement and the displacement of the ultimate force. As it is obvious from the first sample's graph, the ultimate force that the slab could resist was 1480 KN which caused 0.84 mm and after that the failure was happened and force and displacement became to 213 KN and 11.8 mm, respectively. The last steps of this graph shows some more load applying which in the last point the load was 87 KN and the displacement was 26 mm.

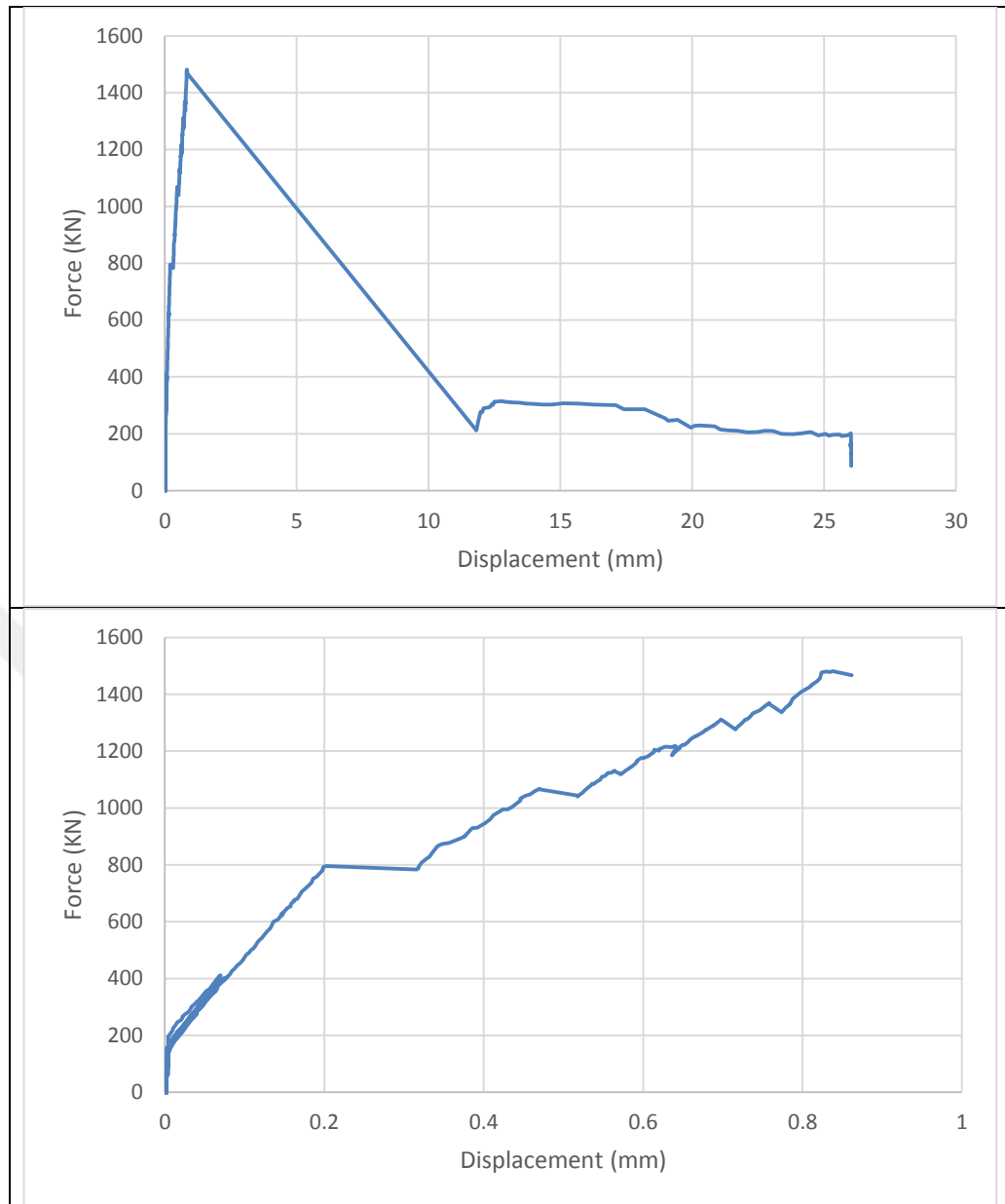


Figure 3.21 : The Force-displacement graph of the first voided slab.

The second sample's graph shows that 1837 kN was the peak point of the force with 1.74 mm of displacement but the failure was happened in 1642 kN of force and 5.21 mm of displacement. After that, force and displacement became to 720 kN and 14.3 mm, respectively. For the last steps of the experiment, the loading was continued and at the final point the force became to 183 kN and displacement was 21.4 mm.

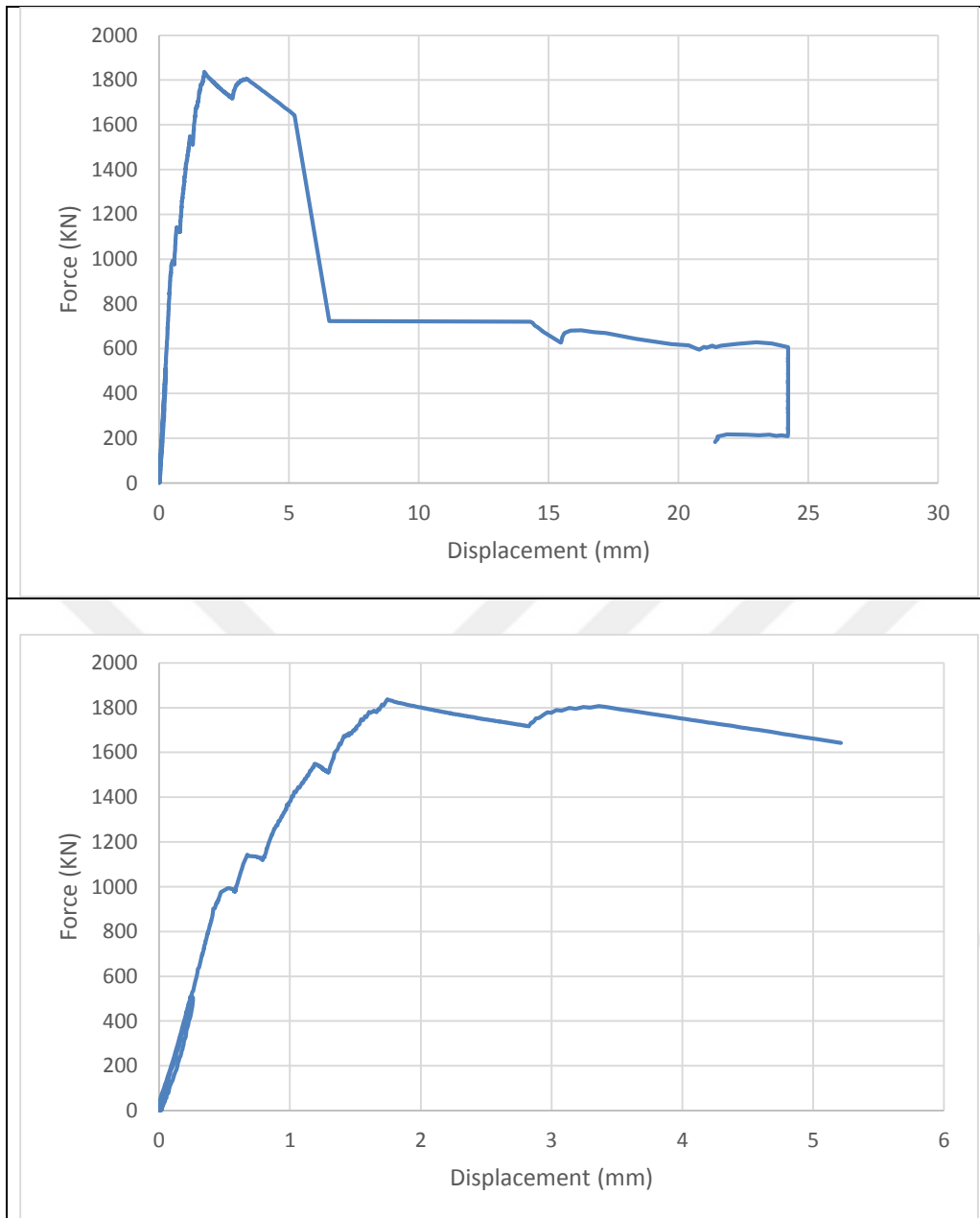


Figure 3.22 : The Force-displacement graph of the second voided slab.

As it is obvious from the previous Figures, at the beginning of the test the slope of the graphs are extremely high which was caused by the fraction. And, for observing the elastic behavior of the voided slabs, some amount of force was loaded and unloaded at first. So, to making the graphs to get started from the zero and continue with a same slope, they are excelled in the next graphs. Also, there is a fact that during the tests, the loading were paused to make notes and observe the changes in the samples so in a specific force the displacement did not stop and it increased in value. But for getting the valid results from the computer software the graphs should be corrected because of the fact that the program analysis the samples continuously without any pausing.

Figure 3.23 and 3.24 show the corrected form of the force-displacement graphs of the first and second voided slabs, respectively.

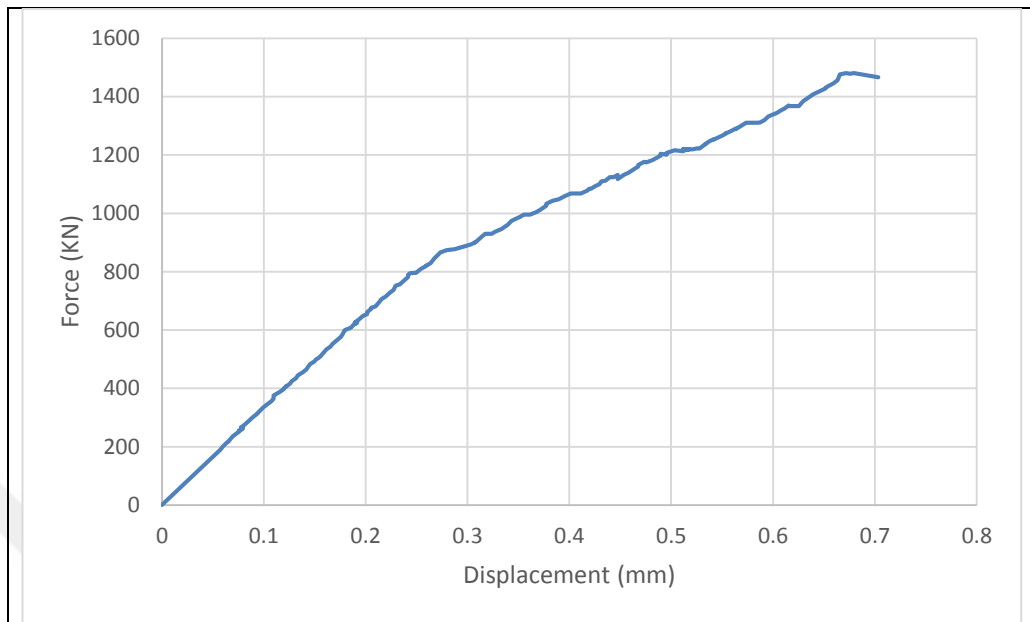


Figure 3.23 : The last version of the Force-Displacement graph of the first voided slab.

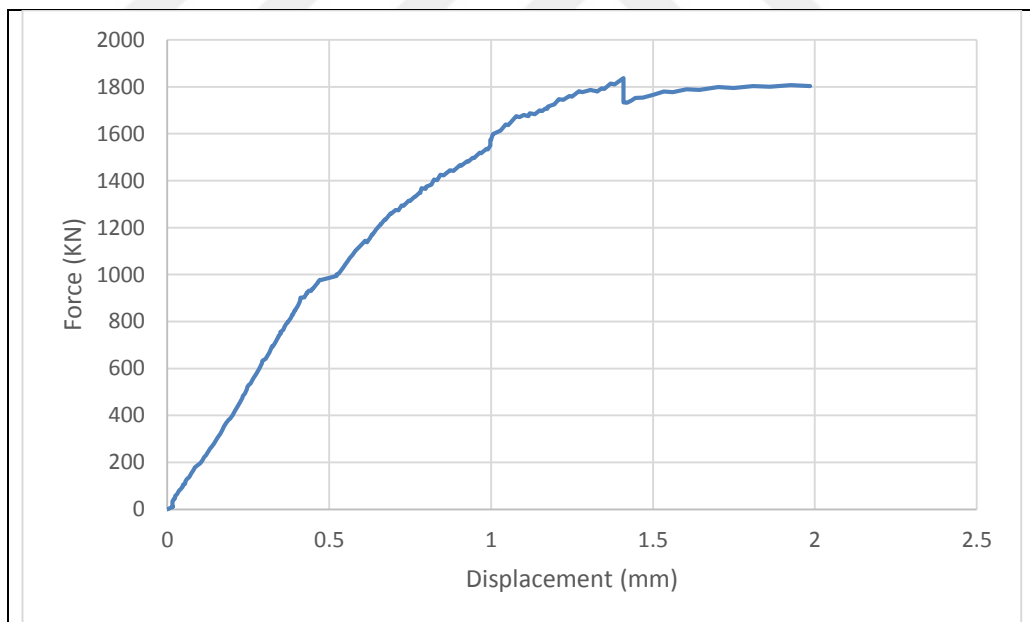


Figure 3.24 : The last version of the Force-Displacement graph of the second voided slab.

The strain gauges which were installed to the rods of the set-up are considered in Figure 3.25 and 3.26 for the two voided slabs. The blue graphs are the average value of the upper two rods strain and the red ones show the average value of the downer two rods strain. The y axis is the strain value and the x axis is the step numbers. It

shows that the load transforming was equal at the both surface of the voided slabs which caused the almost same values of strain in the rods of the set-up.

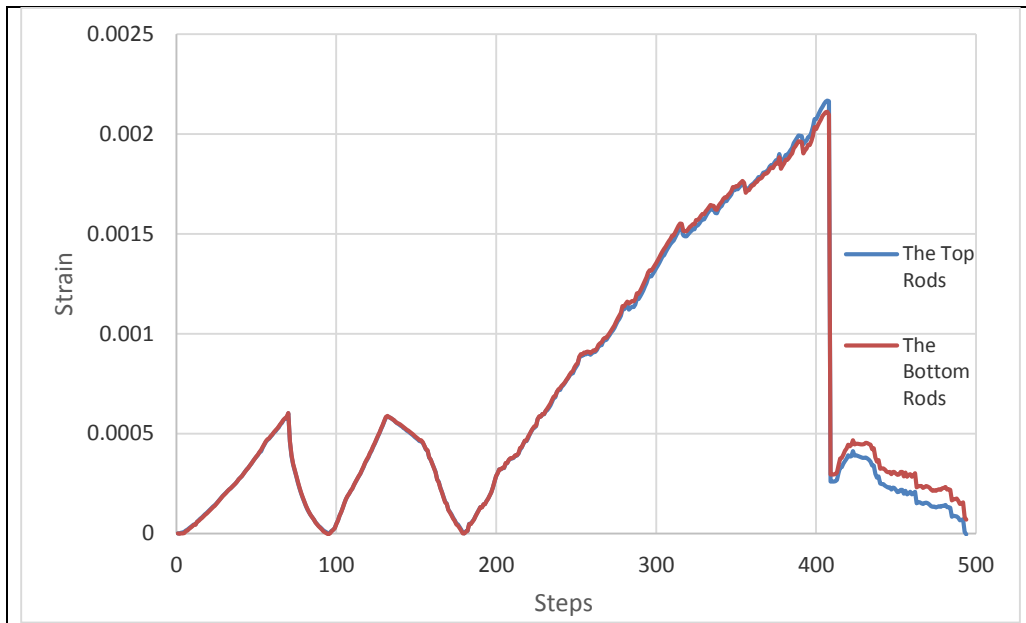


Figure 3.25 : The strain-steps of the rods of the first sample.

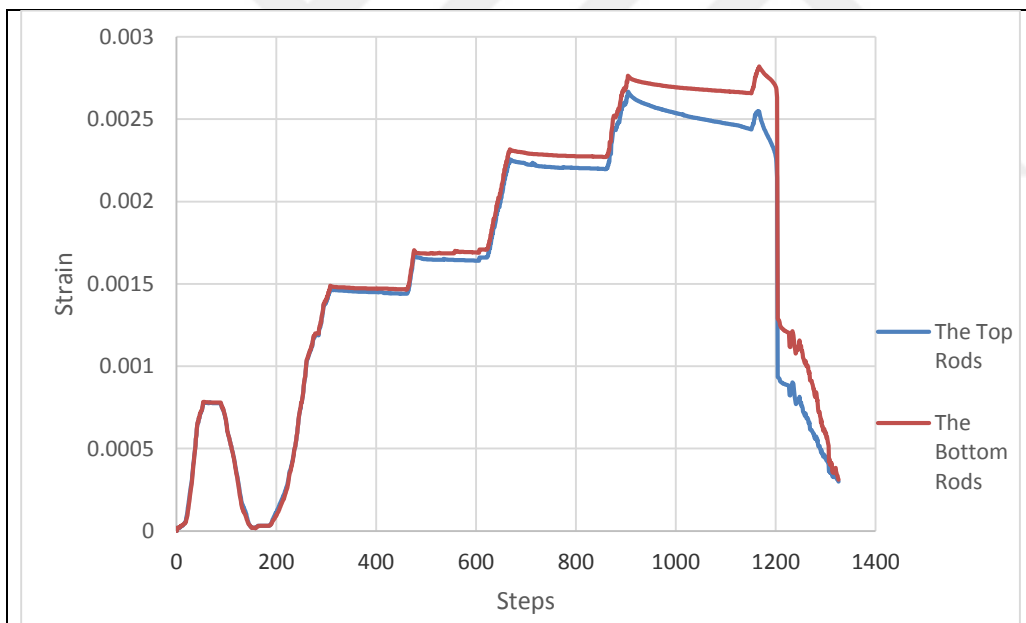


Figure 3.26 : The strain-steps of the rods of the second sample.

In addition, the force of the rods was calculated by using the strains during the tests to control the ratio of the obtaining rods forces of the upper and downer surfaces which was almost 1 for the both voided slabs (Equation 3.1). And the ratio of the obtaining rods forces and the forces obtained from the load cells was observed to check the validity of the forces values and it was nearly 1 too for both of them. The flowing two graphs, which are for the first and second voided slabs, (Figure 3.27 and 3.28) show

the sum of the obtaining upper rods forces (blue ones) and downer ones (red ones) and the displacement in the direction of the loading.

$$\sigma = E \times \varepsilon \quad F = \sigma \times A \quad (3.1)$$

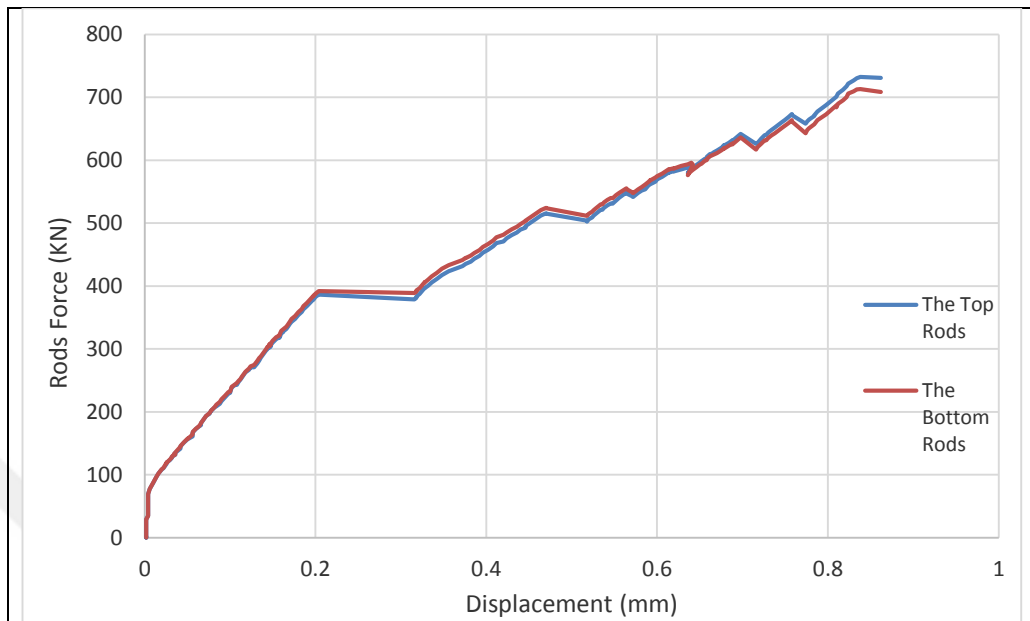


Figure 3.27 : The Force-Displacement graph of the upper and downer rods of the first sample.

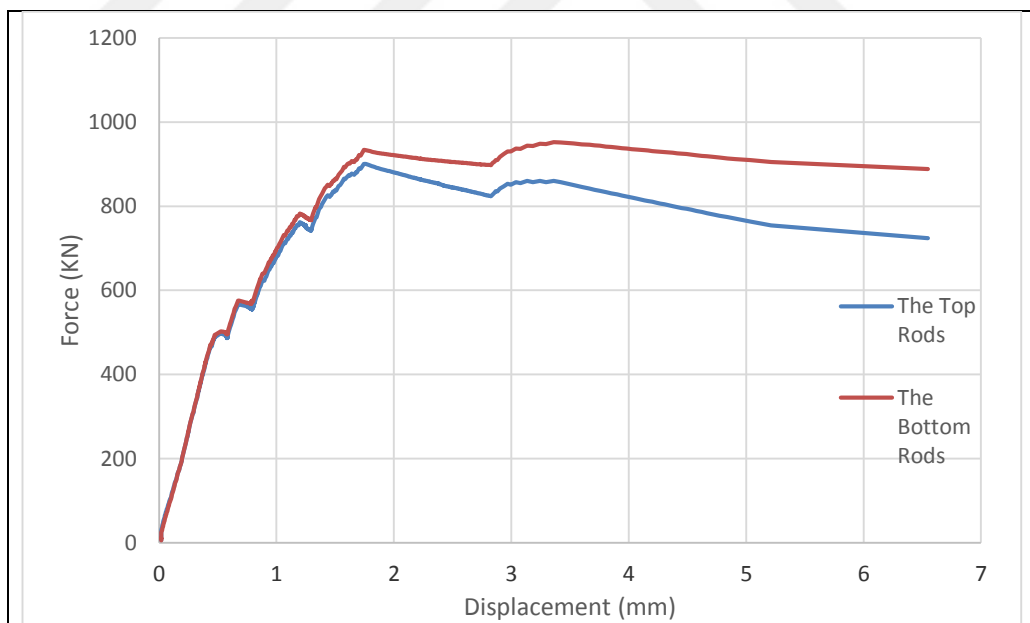


Figure 3.28 : The Force-Displacement graph of the upper and downer rods of the second sample

Also, the total value of the force obtained from rods and load cells are compared in Figure 3.29 and 3.30, where the blue graphs represent the force obtaining by the load cells and the red ones show the calculated rods forces. The previous and this graph show that the load transforming from the upper and downer surface of the voided slabs

was equal to each other and the force values are reliable because of the same value obtaining from load cells and the rods.

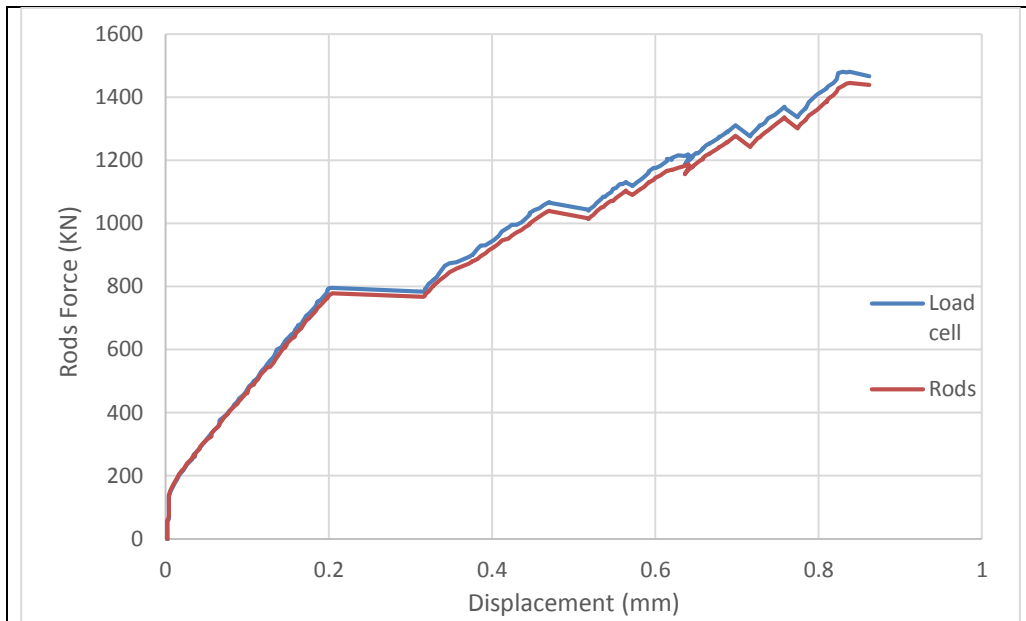


Figure 3.29 : The Force-Displacement graph of the load cells and the rods of the first one.

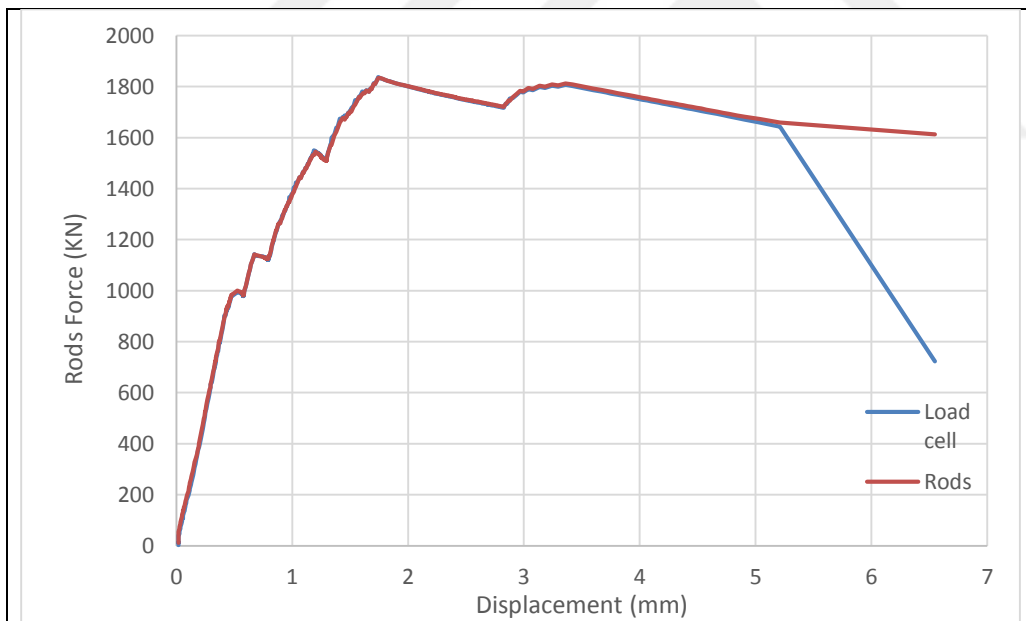


Figure 3.30 : The Force-Displacement graph of the load cells and the rods of the second one.

As mentioned before, two strain gauges were installed to the upper surface of the both voided slabs perpendicular to each other. And in second sample the other two strain gauges were installed to the downer surface of the voided slab. Figure 3.31, which is for the first sample, shows the strain and the step numbers graph which is for the strain gauge in the same direction with loading that was under compression and Figure 3.32

is for the strain gauge perpendicular to the first one which was under tension for the same sample. In the first graph the ultimate value of the strain was 3.52×10^{-3} which also is the ultimate strain of the concrete but for the second one this value was 1.57×10^{-4} which was for the step 408 and after that the strain gauge did not get any data.

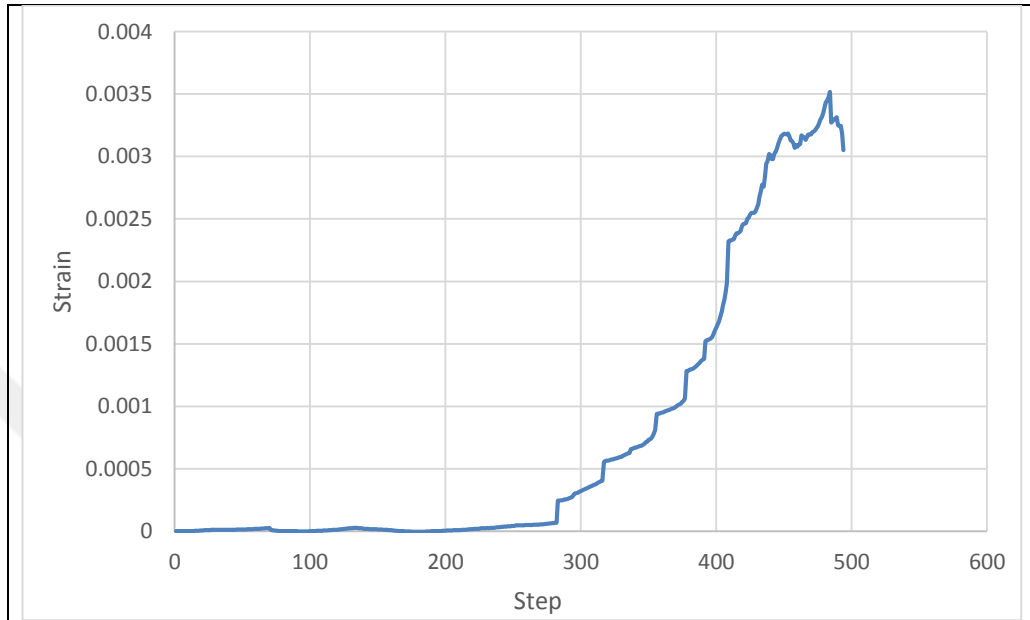


Figure 3.31 : The strain-step of the first strain gauge installed to the surface of the first sample.

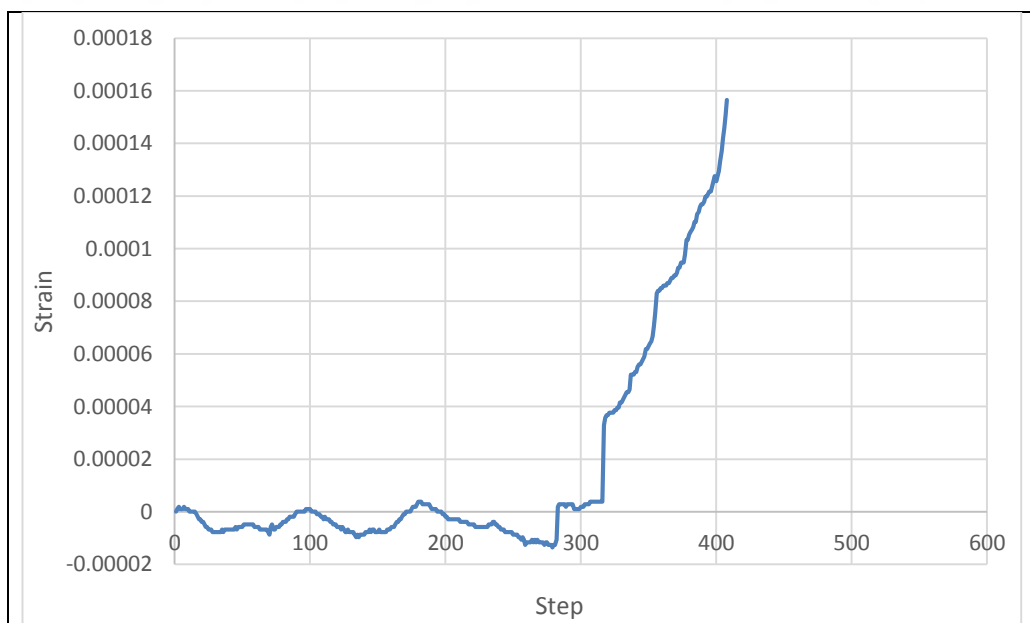


Figure 3.32 : The strain-step of the second strain gauge installed to the surface of the second sample.

Similarly, in Figure 3.26, which is the strain and step graph of the second sample, the blue graph is for the strain gauge of the upper surface of the second voided slab in the

same direction with loading that was under compression and red one shows the strain gauge of the downer surface of the sample with the same direction. The upper and downer strain gauges perpendicular to the first ones which was under tension are illustrated in Figure 3.33 for the same voided slab. The pattern of the first graph of the strain gauges is almost same but in some points there are some difference in strain values. For instance, the ultimate strain for the upper surface is 6.35×10^{-4} but for the downer surface this value is 8.32×10^{-4} . In Figure 3.34 the pattern of the graph is much different from each other and in some points the strains values are different in compression and tension.

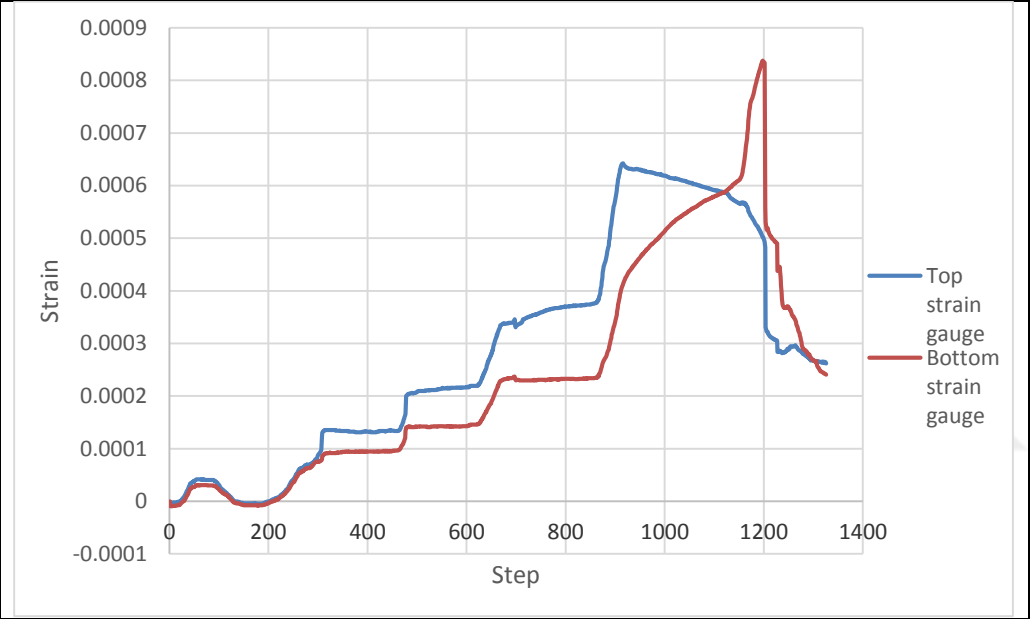


Figure 3.33 : The strain-step of the first strain gauge of the second sample.

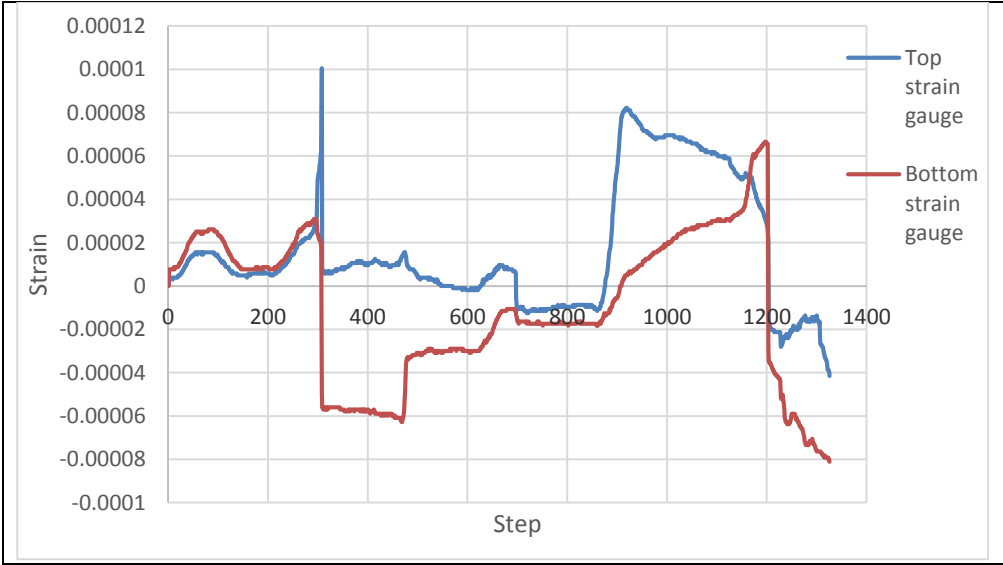


Figure 3.34 : The strain-step of the second strain gauge of the second sample

The elastic behavior of the voided slab is noticeable in these graphs for the both samples which the strain values changed from zero to a specific value and again became to zero during the loading and unloading.

Before concreting the voided slab, two strain gauges were installed to the upper bars of the voided slabs perpendicular to each other. Figure 3.35 and 3.36 show the behavior of these strain gauges for the first sample which the y axis is the strain and the x axis represents the step numbers. In the first graph it can be noticed that the value of the strain at yield stress was about 0.002 and the force was 795 KN at that moment.

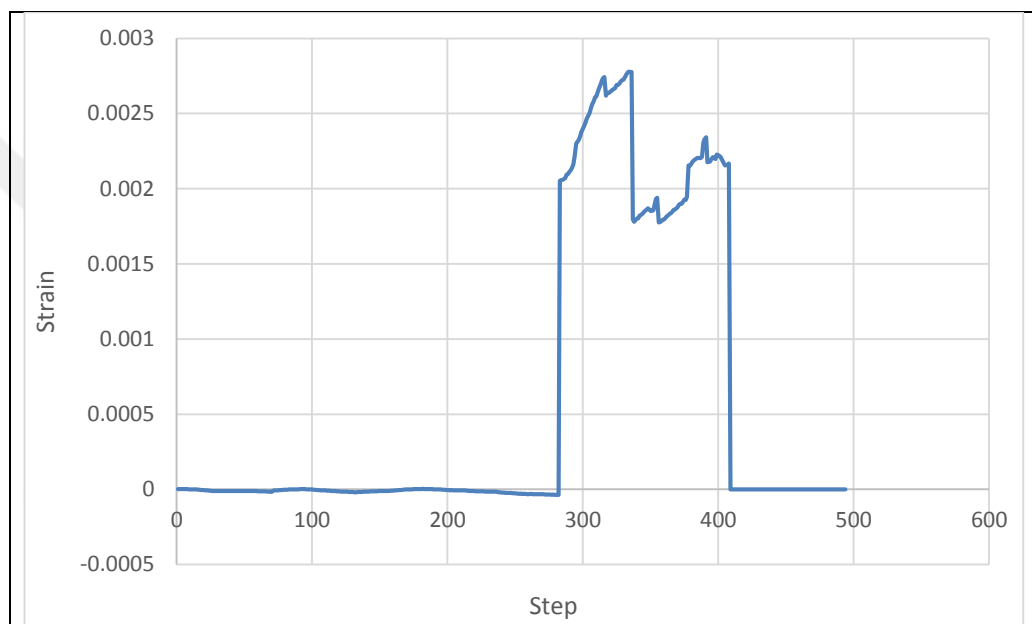


Figure 3.35 : The graph of the first strain gauge of the bar of the first sample.

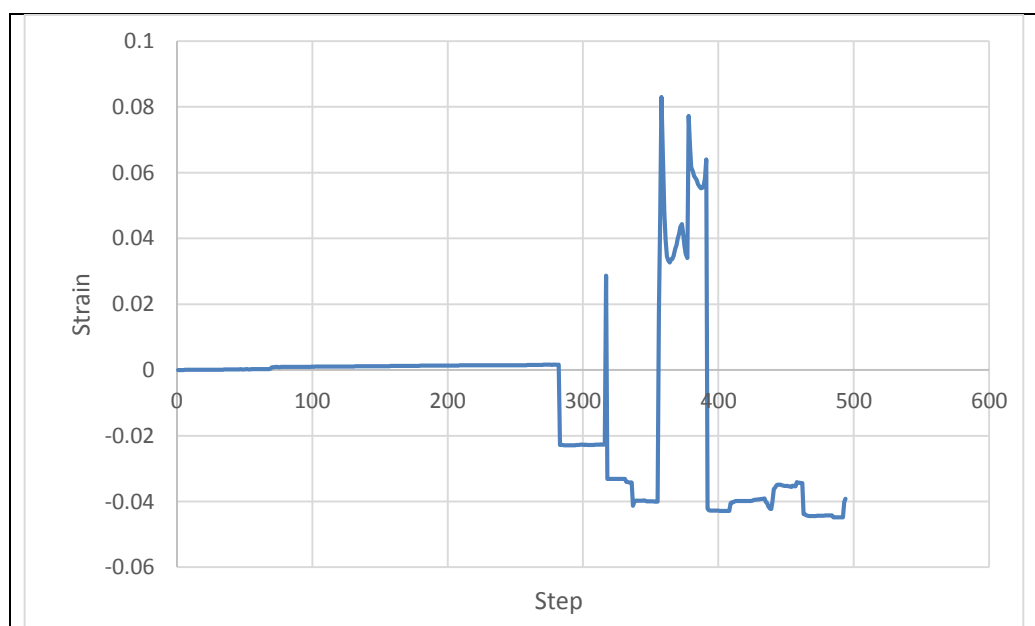


Figure 3.36 : The graph of the second strain gauge of the bar of the first sample.

This type of graph also can be drawn for second voided slab with the same axis characteristics. Figure 3.37 and 3.38 show the same graph for the second test which are for the strain gauges of the bars embedded within the voided slab. The value of the strain for the bar at its yield stress was 0.002 when the force was 1740.5 KN which can be noticed in Figure 3.30 but the next graph shows that the strain of the perpendicular bar reached to 0.002 just after failure happening.

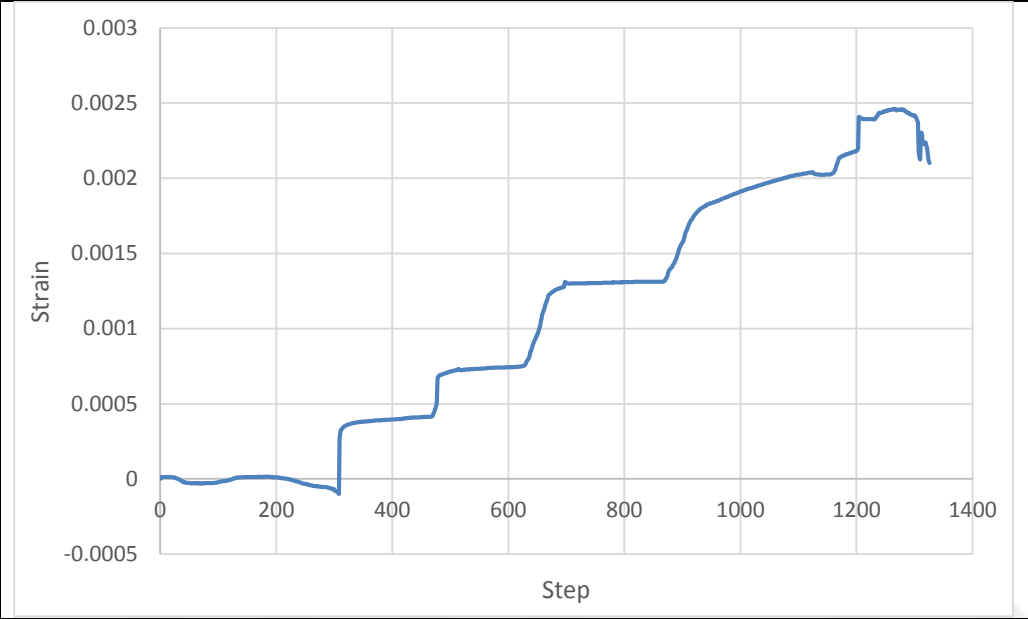


Figure 3.37 : The graph of the first strain gauge of the bar of the second sample.

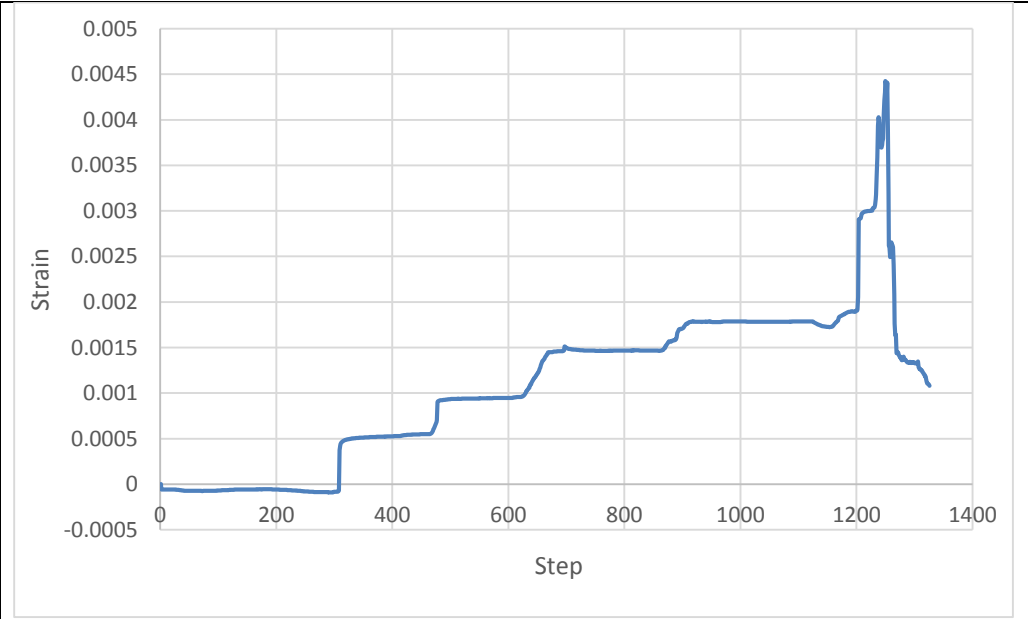


Figure 3.38 : The graph of the second strain gauge of the bar of the second sample.

Another important graph which can be obtained from the data of the investigation is shear stress and shear angle. As mentioned in chapter two, the influenced area can be

easily calculated for the voided slabs and the shear stress is obtained by dividing the force to the influenced area. By using Equation (3.2) the area and shear force can be found for the two voided slabs, where B and H are the length and height of the voided slabs and b and h are the length and height of the voids, respectively. Figure 3.39 and 3.40 show the shear stress and shear angle graph from the data obtained from the investigation for the first and second voided slabs, respectively. The y axis is the shear stress and x axis represents shear angle.

$$A = (B \times \sqrt{2} \times H) - (2 \times b \times h) \quad \tau = \frac{F}{A} \quad (3.2)$$

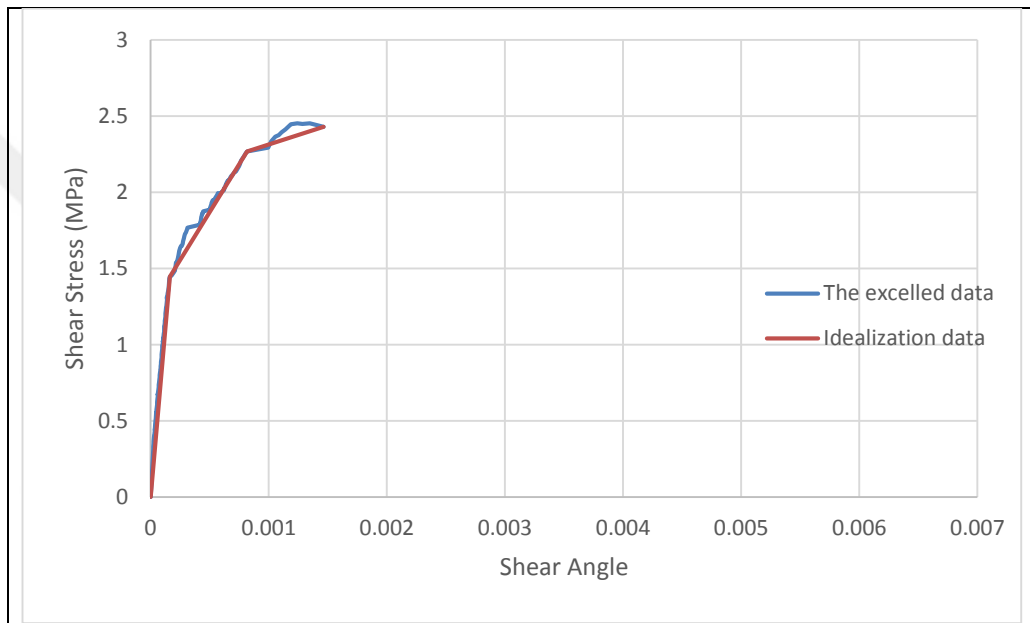


Figure 3.39 : The shear stress and shear angle graph of the 1-a voided slab.

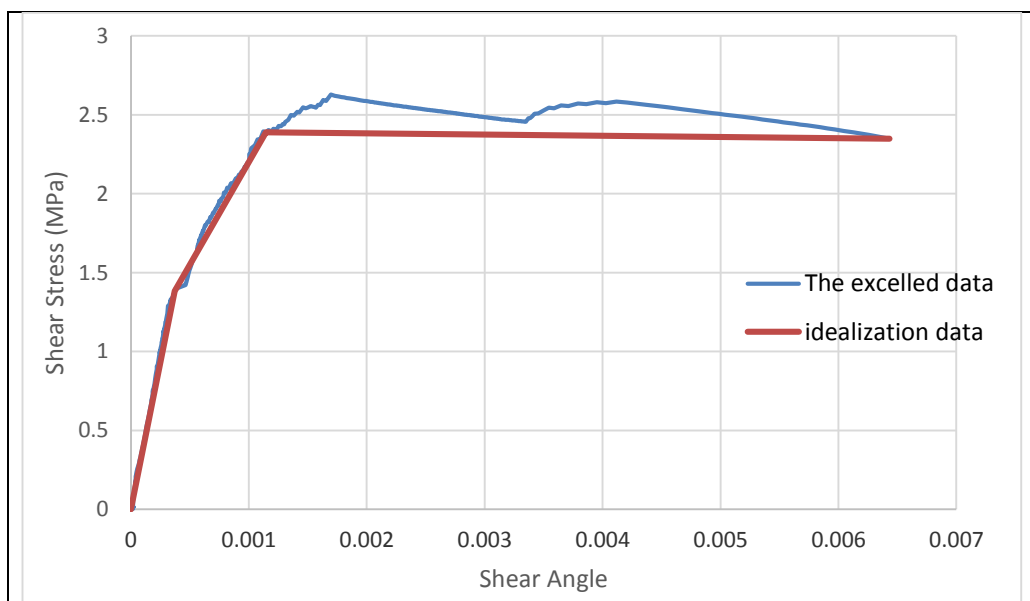


Figure 3.40 : The shear stress and shear angle graph of the 1-b voided slab.

As it is obvious in previous Figures, the elastic shear stress was about 1.5 Mpa in the both samples. After that, the shear modules changed and the shear stress became to almost 2 Mpa. Finally, the ultimate shear stress was about 2.5 Mpa. The other information gathered from the Figures are in Table 3.3.

Table 3.3 : Summary of the data obtained from the shear stress and shear angle graph.

The samples	Shear stress τ (MPa)	Shear angle γ	Shear modulus G (MPa)	Shear stress ratio τ/τ_1	Shear angle ratio γ/γ_1	ductility $\frac{\gamma_u}{\gamma_e}$
1-a voided slab	1.45	1.63×10^{-4}	8.88×10^3	1	1	8.99
	2.27	8.16×10^{-4}	2.78×10^3 (effective)	1.57	5	
	2.43	1.46×10^{-3}	1.66×10^3	1.68	8.99	
1-b voided slab	1.38	3.71×10^{-4}	3.73×10^3	1	1	17.35
	2.39	1.14×10^{-3}	2.09×10^3 (effective)	1.73	3.09	
	2.35	6.43×10^{-3}	3.65×10^2	1.7	17.35	

The obtained shear stress can be used to draw another graph with shear angle which can be easily obtained by summation of the horizontal strain and vertical strain (compression and tension). In Figure 3.41 and 3.42, which refer to the first and second sample, respectively, the y axis shows the shear stress and the positive parts of the x axis represent the strain of the tension direction of the voided slab (red ones) and the negative parts show the strain value of the strain gauges which were installed to the surface of the voided slabs with the same direction of the loading (blue ones).

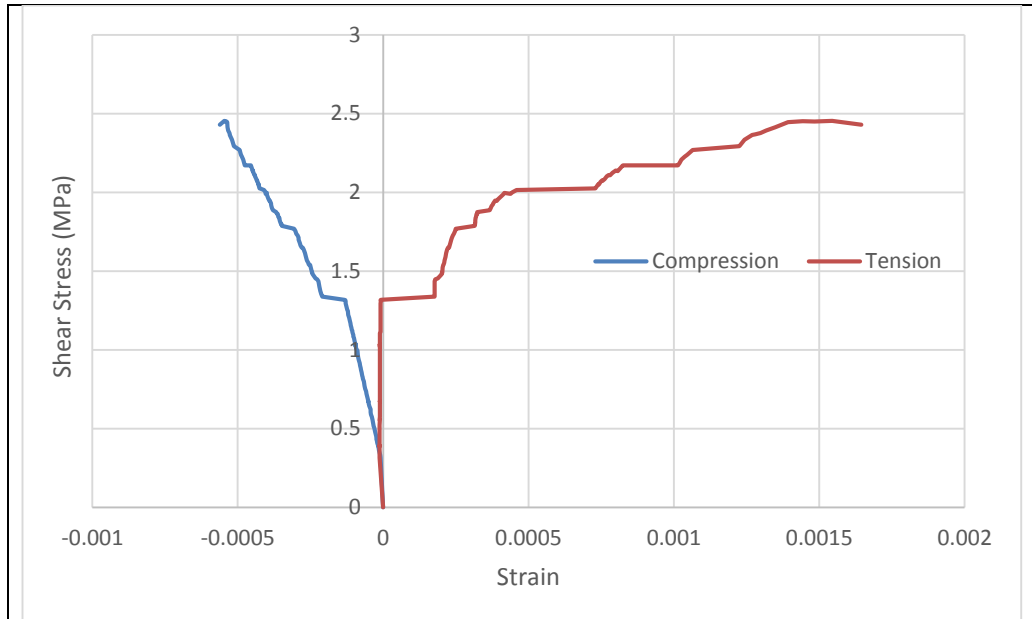


Figure 3.41 : Shear stress-strain graph.

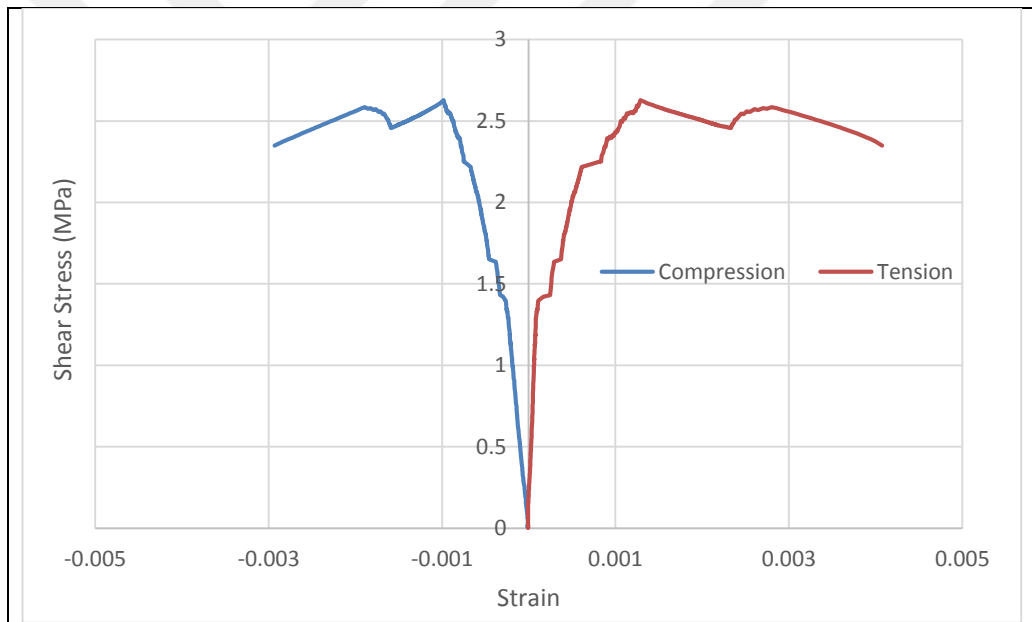


Figure 3.42 : Shear stress-strain graph.

3.6 Getting samples

Because the tests for determining the strength of the concrete of the voided slab was for a long time ago, and by considering the fact that the strength of a concrete has a direct relationship with time, six cylindrical samples were gotten from the suitable parts of the voided slab which are shown in Figure 3.43.



Figure 3.43 : The taken samples for determining the strength of the concrete.

It is obvious that the concreting the voided slab contained some faults, such as varied values in length, width, height of the slab, sinking and rotation of the voids, thus it was tried to destruct the surface of the first voided slab to observe the exact location of the voids and the accurate measures of the varied values (Figure 3.44).



Figure 3.44 : The observation of the voids places.

4. ANALYTICAL INVESTIGATION ON VOIDED SLABS

4.1 Introduction

The investigation on the two voided slabs was done and the simulation of them in Abaqus/CAE 2019 is considered in this chapter. As mentioned in chapter two, Abaqus is a finite element program which can be used to simulate investigated voided slabs.

4.2 Abaqus/CAE 2019

Abaqus/CAE 2019 is used in this simulation. This program uses the finite element method to model and analyze the elements in different aspects. It is possible to model the voided slabs in this program and analyze them to compare the results of experimental and simulated models. The units, which are used to model voided slabs, are N m Kg. Figure 4.1 shows the general view of this program.

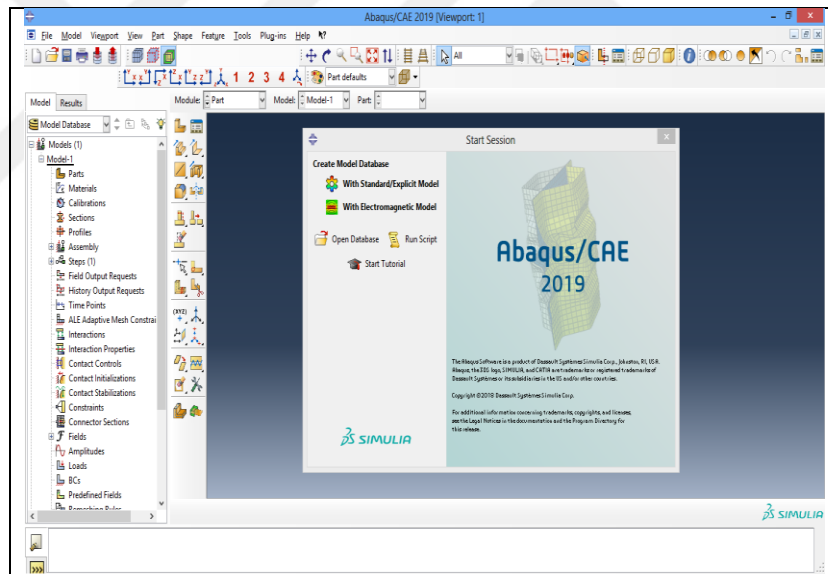


Figure 4.1 : The general view of the Abaqus/CAE 2019

4.2.1 Parts of the voided slab

The first step is creating the parts of the model. Voided slab is consist of concrete, bar, four bigger voids in the center and eight smaller voids besides them. Thus, in part section all the parts should be created. In this simulation, voids and concrete are simulated with solid shape and bar is created by wire shape. The general shape and the size of the components of voided slab is modeled ideally to make the analysis process faster but it is obvious that there are a little differences between the simulated model and the real one because of the human faults. The size of the slab and the length of the bars are the varied values of the two voided slabs. Figure 4.2 shows the summery of part creation.

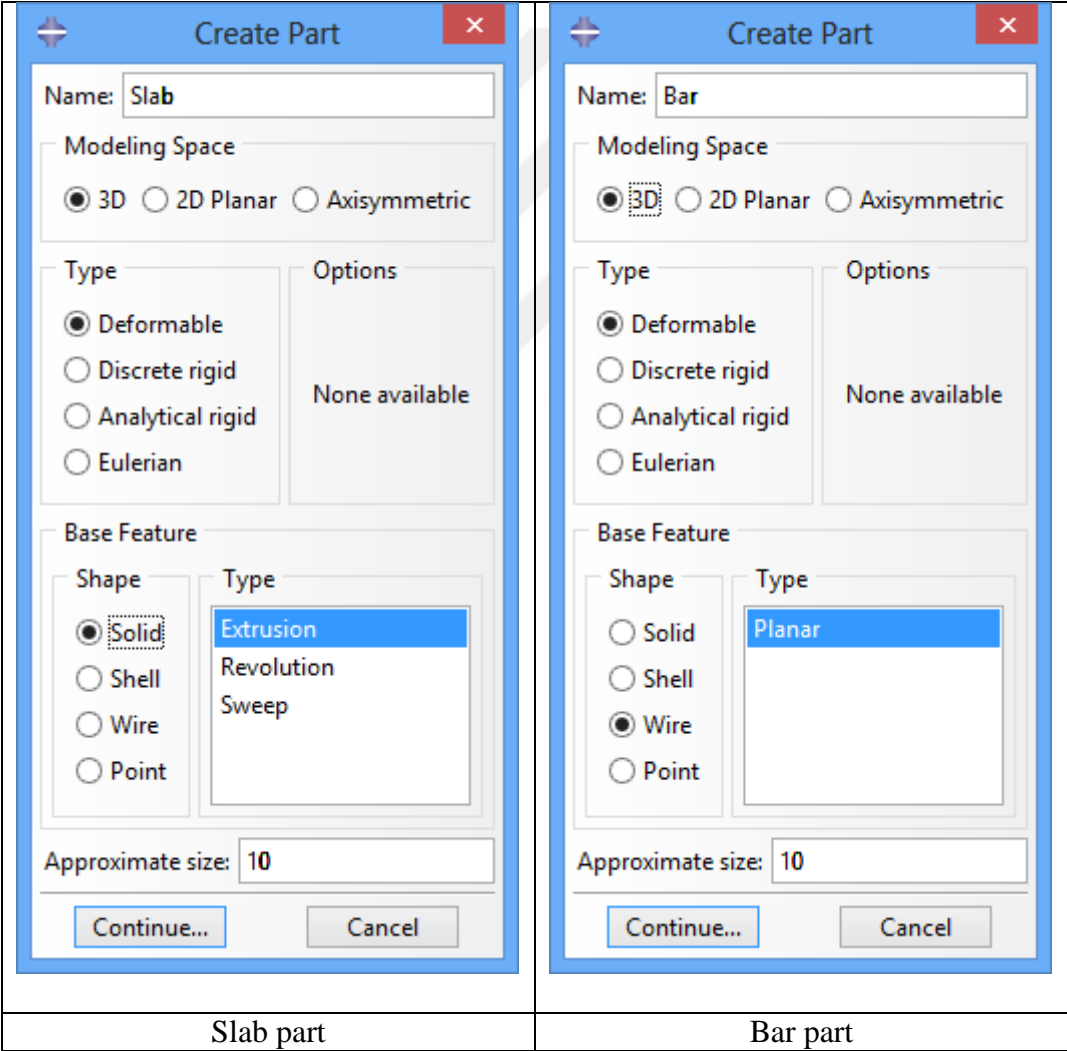


Figure 4.2 : The summery of the part section.

4.2.2 Materials of the voided slab

In the material section, the properties of the steel and concrete should be defined. The density, Young's modulus and Poisson's ratio of the steel are assigned as 7800 Kg/m³, 2.00E+11 N/m² and 0.3, respectively. The plastic behavior of the steel should be considered to observe the nonlinear part of the analysis. Figure 4.3 illustrates the properties of the steel in the program.

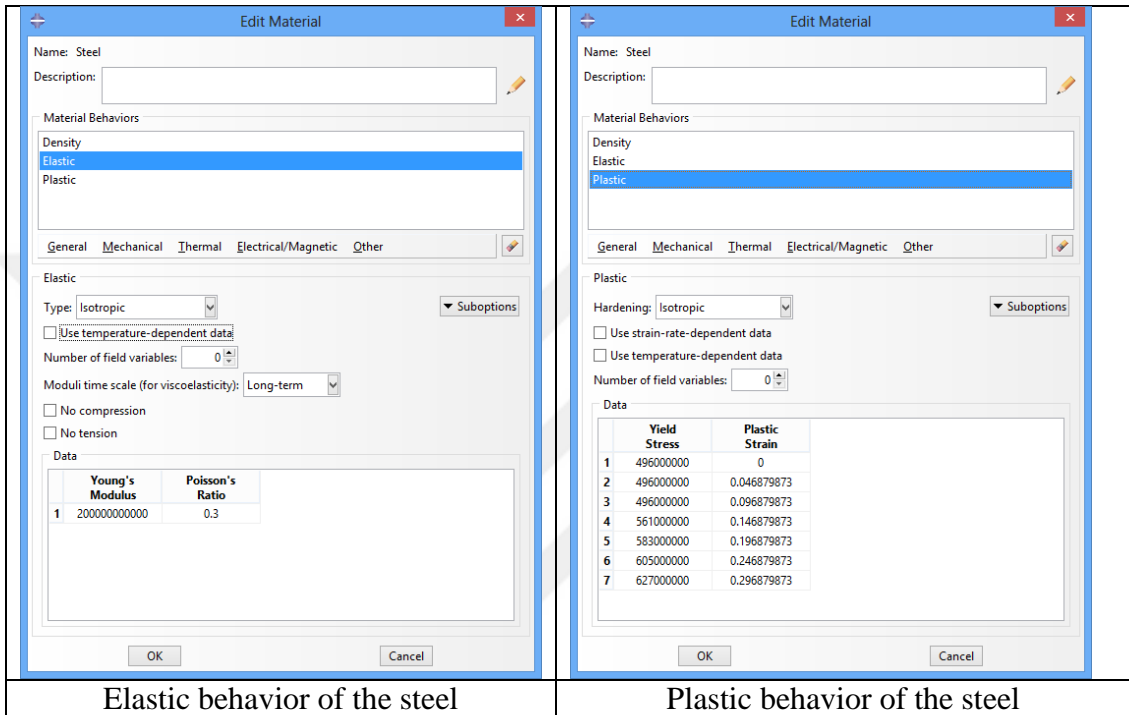


Figure 4.3 : The properties of the steel.

The properties of the concrete is more complex than steel's. The mass density and the Poisson's ratio of the concrete are considered as 2400 Kg/ m³ and 0.2, respectively and the Young's modulus of it is calculated by using the Equation (4.1) which is from TS 500.

$$3250\sqrt{f'_c} + 14000 \quad (4.1)$$

Where, f'_c is the compressive strength of concrete which is obtained from the average value of the taken samples from the voided slabs.

As mentioned in chapter two, the Popovics model is used to calculate the compressive behavior of the concrete and after that the tension behavior of it can be found based on the equations from the chapter two (Figure 4.4).

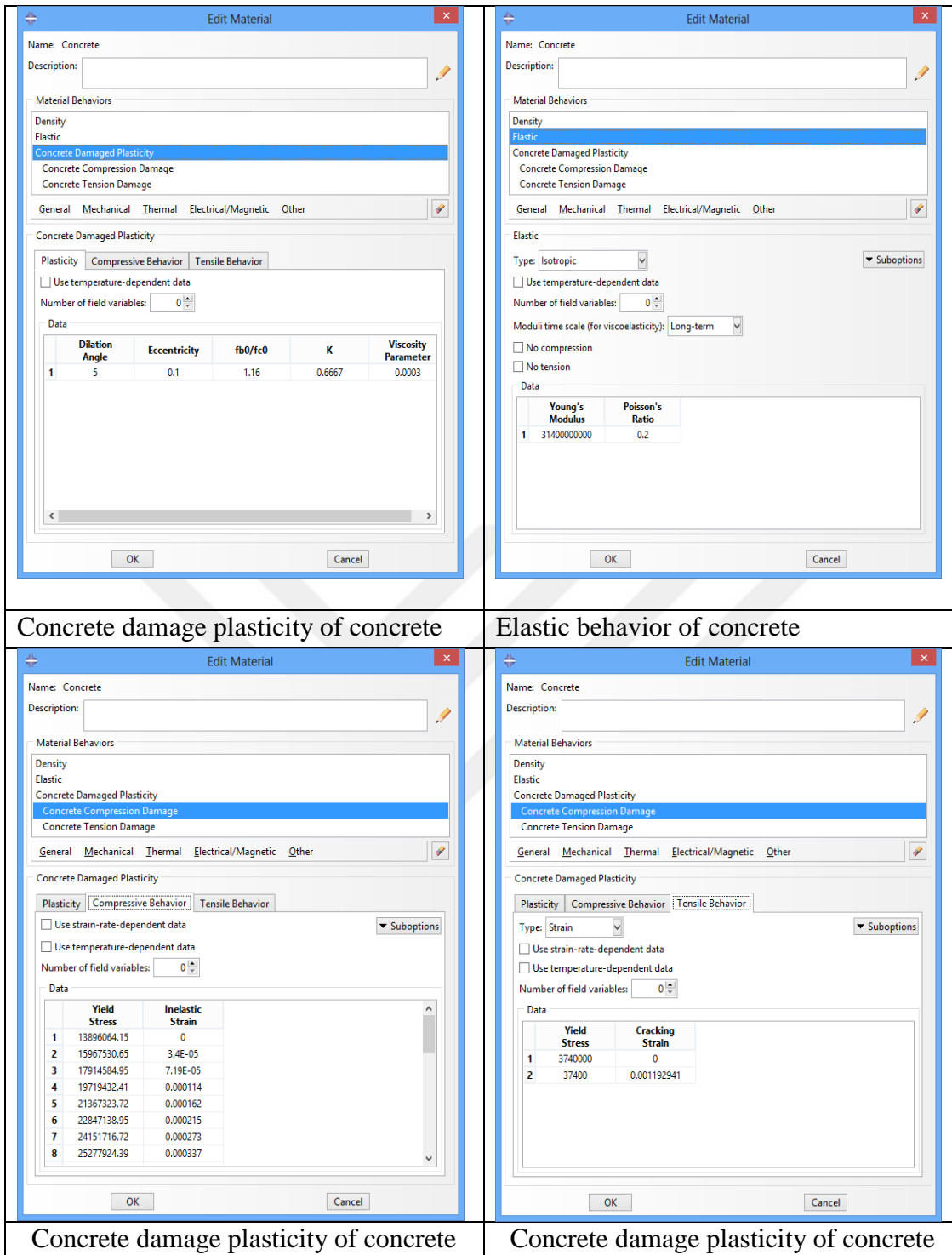


Figure 4.4 : The properties of the concrete.

Finally, in sub option part of the both behavior, the damage parameter and inelastic strain can be assigned as shown in Figure 4.5.

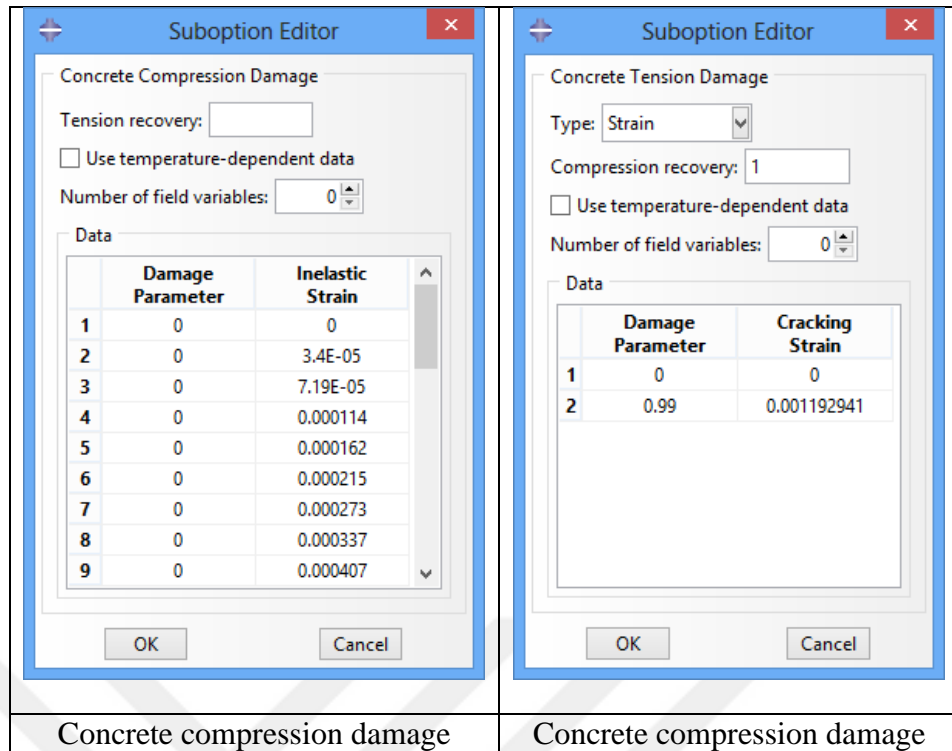


Figure 4.5 : The properties of the concrete.

4.2.3 Assembly of the voided slab

The voided slab can be modeled as is shown in Figure 4.6 by merging all the parts of it. The bars are assembled in the specified condition (Figure 4.7) and they are assembled in the top and bottom of the voided slab. It is obvious that this final assembled model is the ideal form of the investigated voided slab and the unnecessary details are not considered. Also, Figure 4.8 shows a view cut of the voided slab from the y axis which gives a chance to see the inner part of the voided slab.

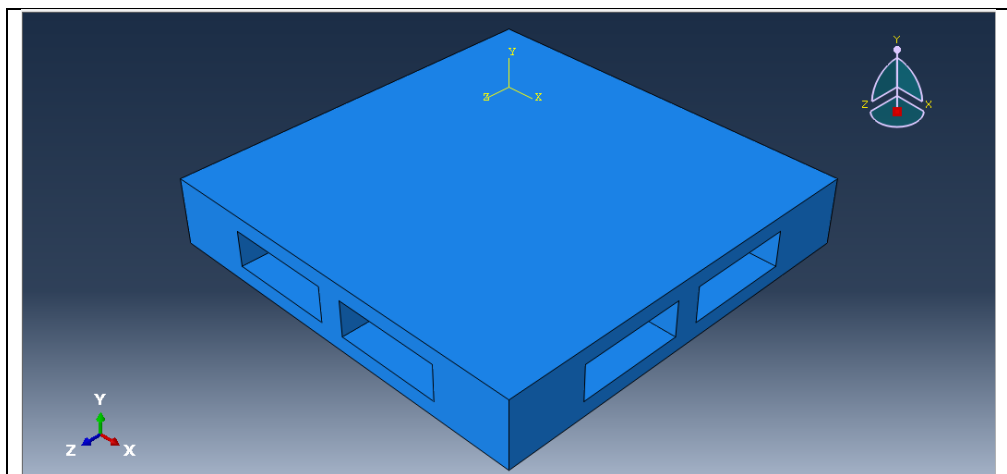


Figure 4.6 : The assembled form of voided slab.

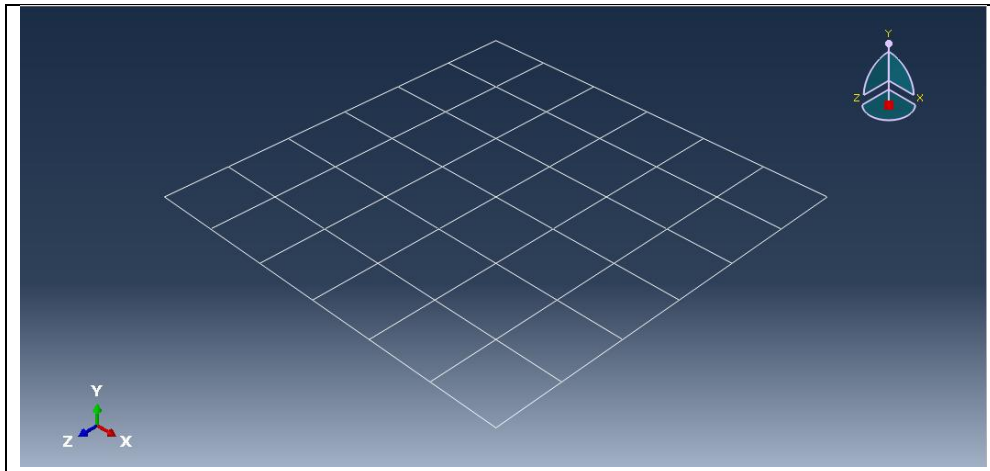


Figure 4.7 : The bars of the voided slab.

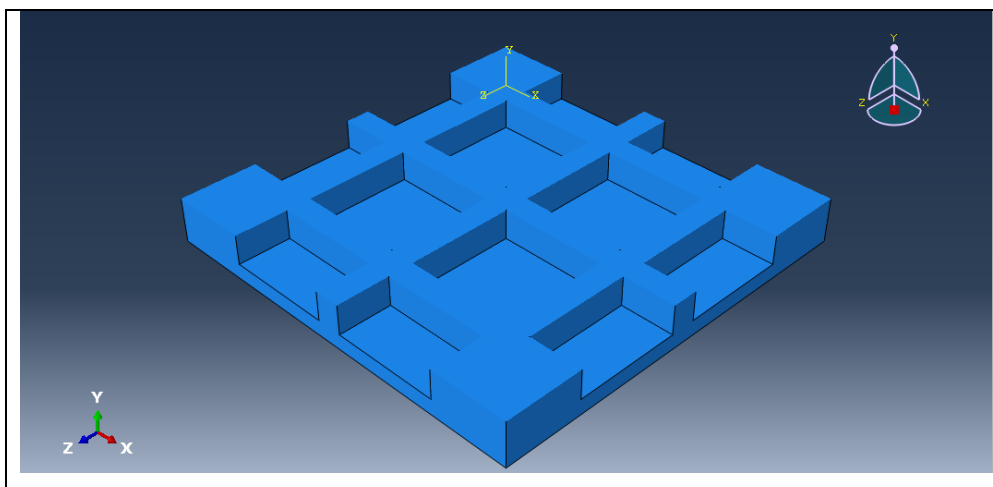


Figure 4.8 : The view cut of the voided slab from y axis.

4.2.4 Step of the voided slab

In this investigation there is a need to one step to get the results of the analysis in that step. So a step is created and the considered results, such as displacement, force and shear stress are determined to this step to get in the result part.

4.2.5 Interaction of the voided slab

Interaction of the voided slab and bars are considered in this part. Because the bars are within the voided slab, a constraint should be created to show the Abaqus that these two parts are interact with each other. The type of the constraint of the bars and voided slab is embedded which means that the bars are embedded in the voided slab (Figure 4.9).

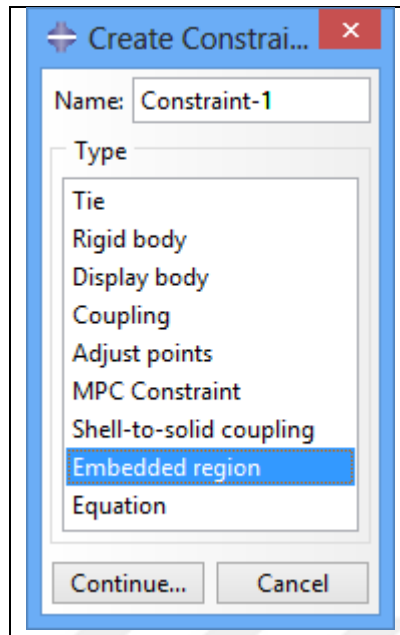


Figure 4.9 : The constraint of the voided slab and bars.

4.2.6 Boundary condition of the voided slab

Boundary conditions should be the same as the condition of the voided slab in the laboratory to get the accurate results. The supports are not necessary to be modeled. Instead, the simulated model is divided to some partitions to assign the boundary conditions to the corners in the same size of the supports. So, the fixed corner is assigned to be fixed like the experimented voided slab and the opposite corner should be fixed in the all direction except the loading direction which is assigned 0.03 m to be displaced. Figure 4.10 shows the options of the assigning the conditions and Figure 4.11 is the situation of the voided slab with boundary conditions.

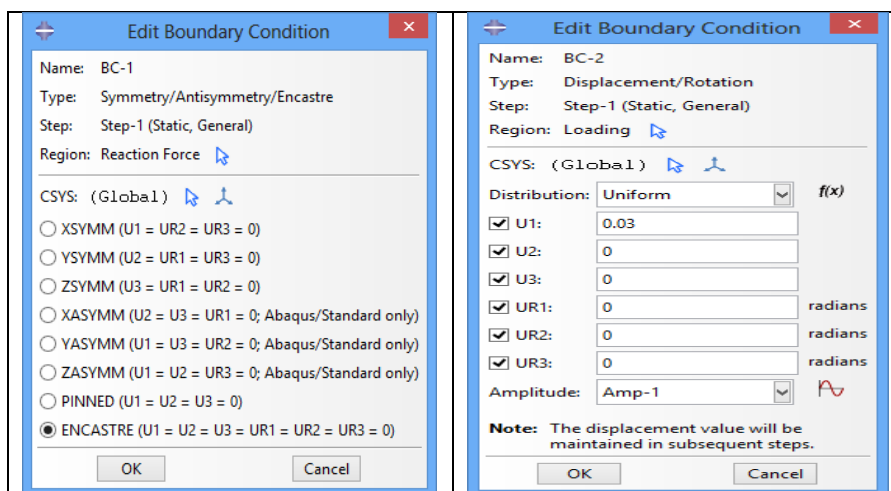


Figure 4.10 : The boundary condition option.

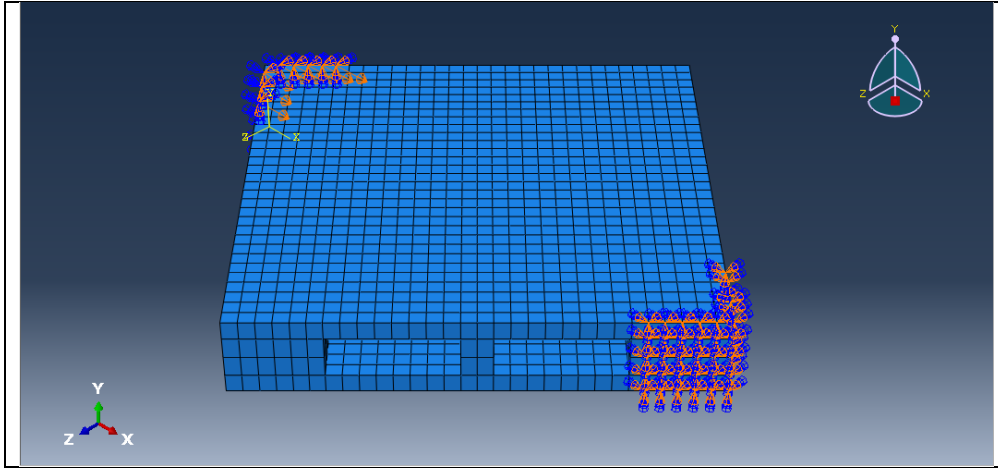


Figure 4.11 : The situation of the voided slab with boundary condition.

4.2.7 Mesh of the voided slab

Meshing is the important option in Abaqus. As it is mentioned, Abaqus analyzes a model with using the finite element methods, so the model should be divided to the tiny elements to have the true results. In addition, the size of the meshing should be realistic. Making the model to the extremely tiny elements increases the speed of the analysis dramatically and also it has some other calculating problems. The big elements, in the other hand, may causes to lose the realistic results and mislead all the investigation. Thus, the size of the mesh should be in the realistic range. In this investigation the family and size of the mesh of the bars are truss and 0.05 m, respectively. The voided slab is meshed with 3D stress family and the size of it is 0.05 m, and the parts of the voided slab which the bars are embedded there are divided to two parts manually to get more realistic results. Figure 4.12 is the last condition of the voided slab which is ready to determine a job to be analyzed.

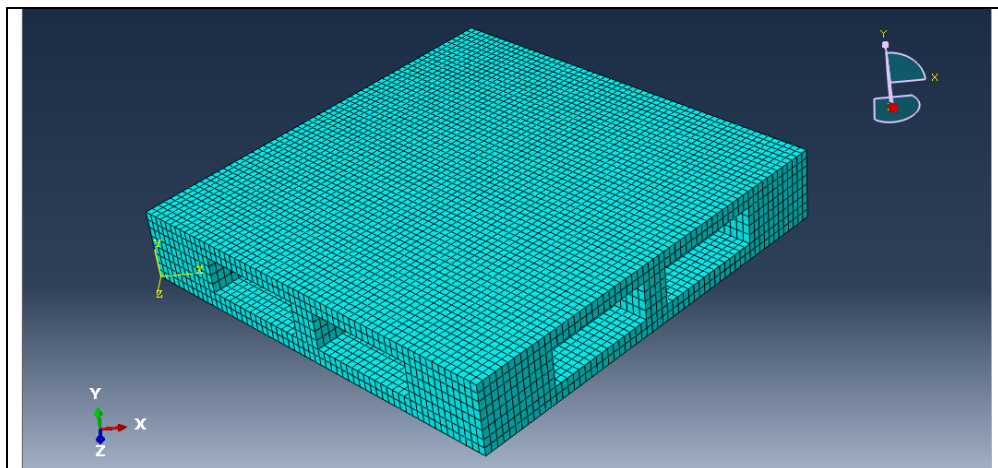


Figure 4.12 : The last condition of the voided slab before analysis.

4.3 The results of analysis

The complete analysis of the voided slab takes too much time but the results of the important parts can be obtained in an acceptable time. Thus, the results of the simulation of the two voided slabs are gathered and illustrated in this chapter.

Figure 4.13 and 4.14 show the first important graph, which is force-displacement, of the first and second voided slabs, respectively in the ultimate amount of force and displacement.

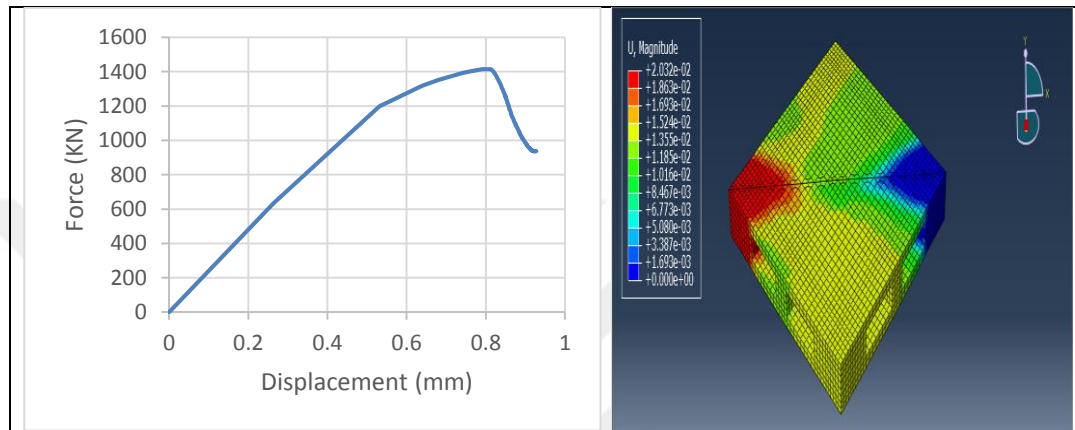


Figure 4.13 : The force-displacement graph of the first voided slab.

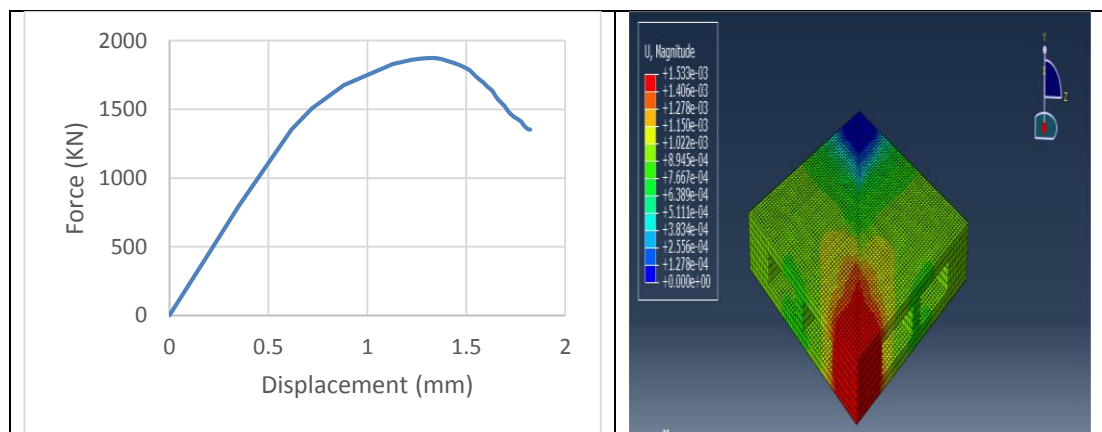


Figure 4.14 : The force-displacement graph of the second voided slab.

The obtained force-displacement graphs of the simulation are compared with the graphs of the experimental samples. Figure 4.15 and 4.16 shows this comparison and as it is obvious, the ultimate force and displacement are almost same.

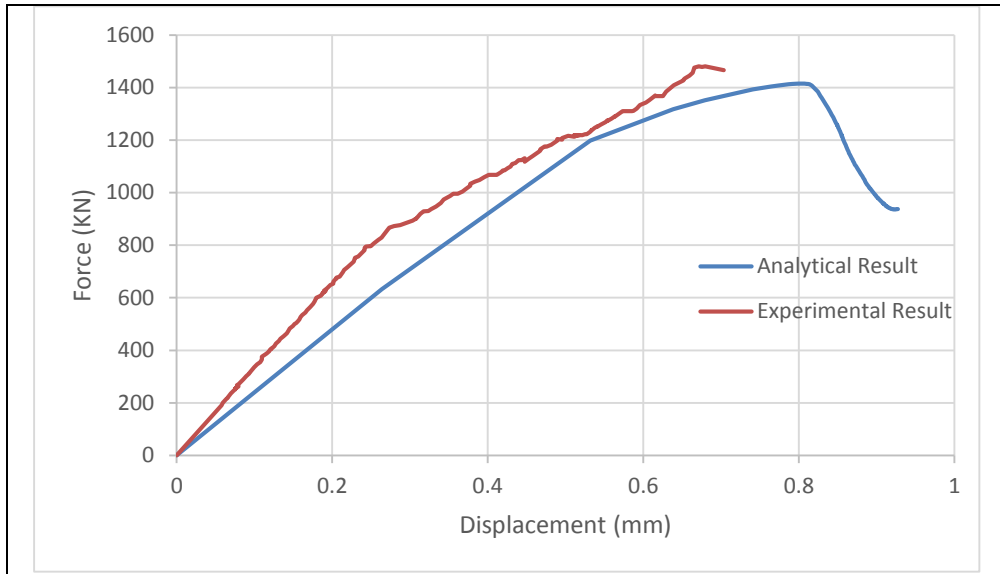


Figure 4.15 : Comparison of the force-displacement of the results for first sample.

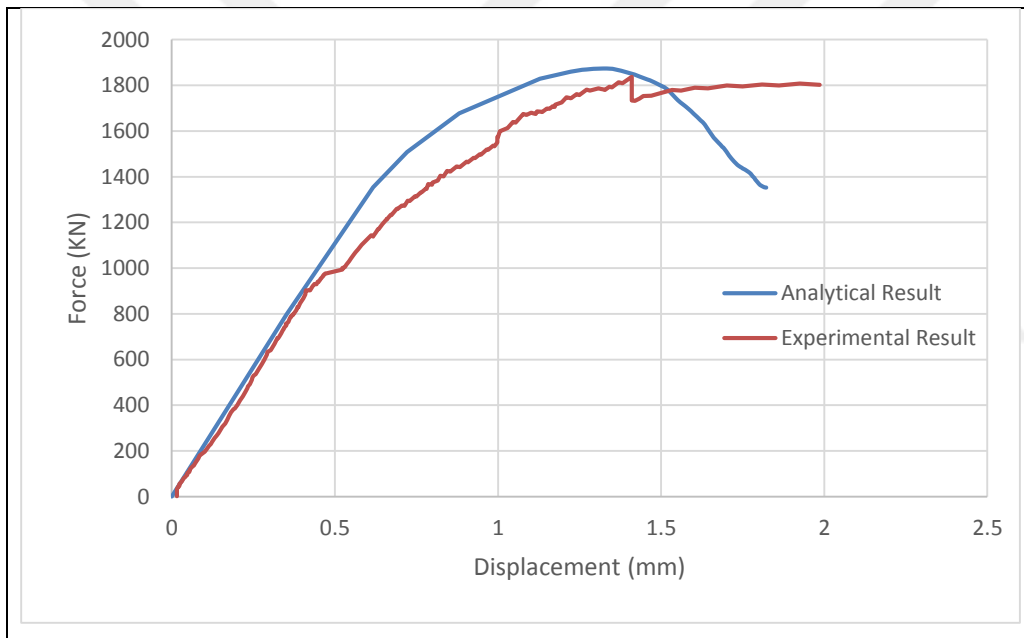


Figure 4.16 : Comparison of the force-displacement of the results for second sample.

The shear stress-shear angle graph also can be get from this simulation but because of the fact that Abaqus analyzes the sample by using the finite element method, there are plenty numbers of elements and the shear stress graph of the each element differs from the others. As it is obvious in Figure 4.17 and 4.18, which show the shear stress graphs of the samples, obtaining the accurate graph is so complicated but it can be seen that the range of the shear stress is similar to the experimental graphs.

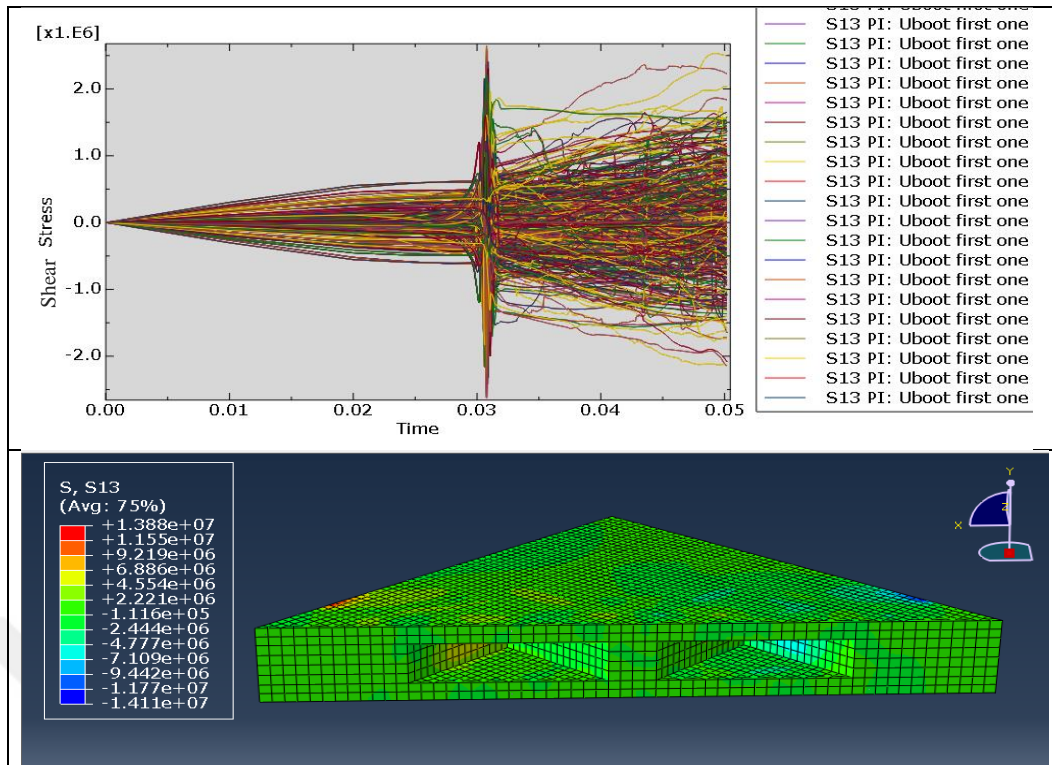


Figure 4.17 : The shear stress graph of the first voided slab.

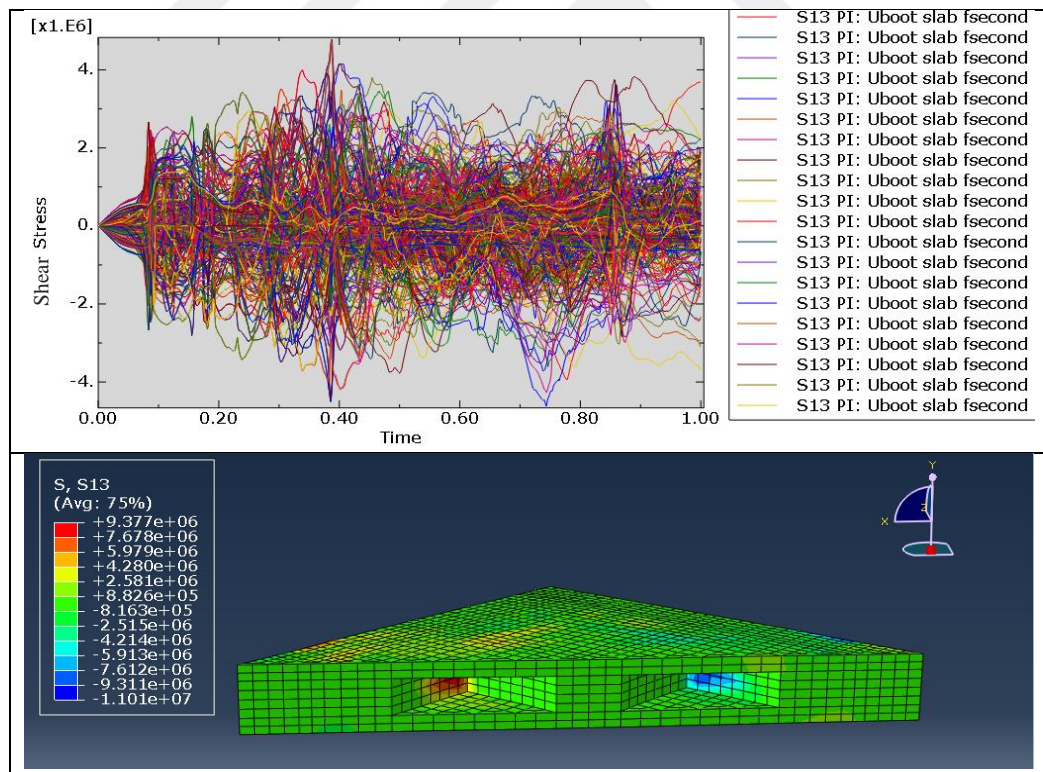


Figure 4.18 : The shear stress graph of the second voided slab.

Because of the fact that Abaqus software uses finite element method for analyzing, the shear stress of some elements can be more than the average value that we obtained

from the experimental results, but as it is obvious in Figure 4.18 the average value of most elements, which is about 2, is very similar to the experimental results.

After this simulation, two conventional slabs with the same material and dimensions are simulated to compare the voided slabs and conventional slabs. Therefore, the simulation and analysis process is the same (Figure 4.19).

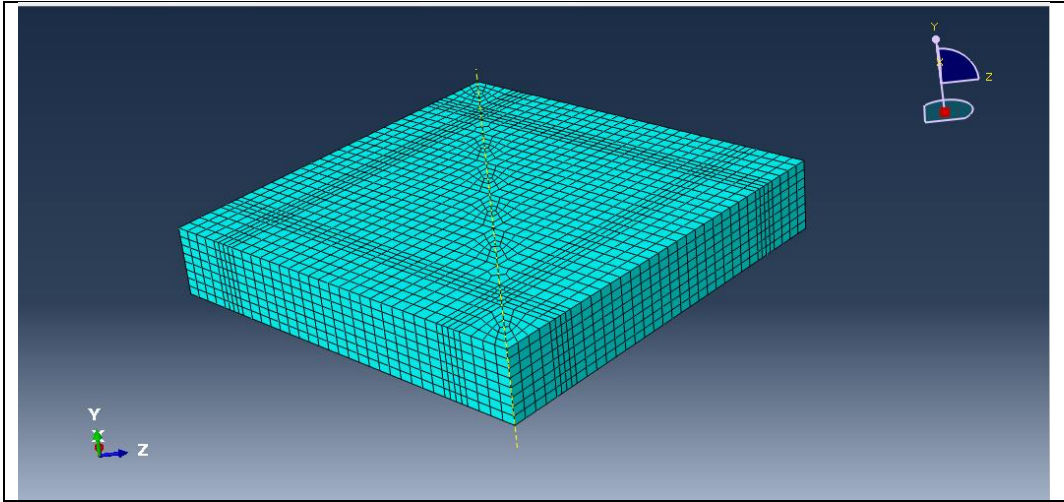


Figure 4.19 : The simulation of the conventional slab.

The force-displacement graphs of the conventional slabs for the first and second samples are shown in Figure 4.20 and 4.21, respectively. Also, they are compared with the simulated voided slabs.

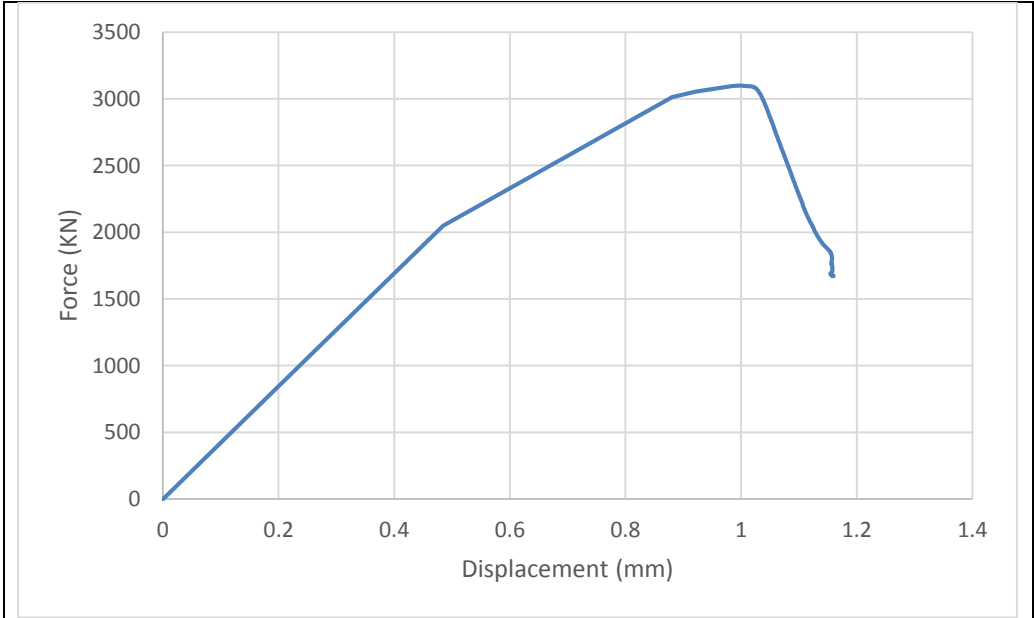


Figure 4.20 : The force-displacement of the first conventional slab.

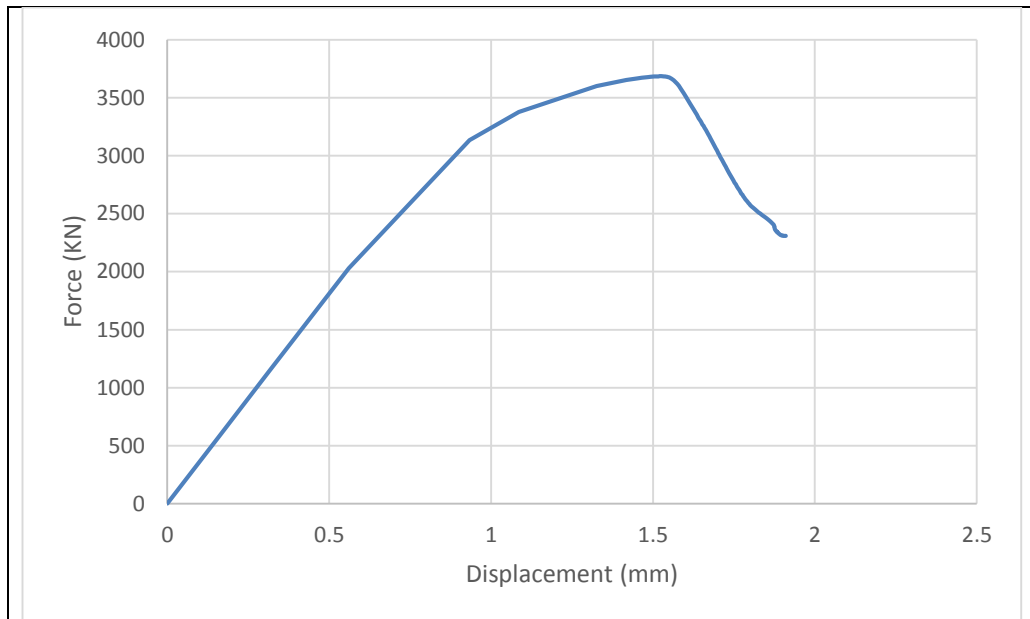


Figure 4.21 : The force-displacement of the second conventional slab.

As it is obvious the conventional slab with the same dimensions, the first one get 3000 KN force and the second one get 3572 KN.



5. CONCLUSIONS AND RECOMMENDATIONS

In this chapter there are the conclusions of the experimental and analytical investigations and there are some recommendations for the next investigations on voided slabs. .

5.1 Conclusions

The experimental and analytical researches are considered for each samples individually.

5.1.1 1-a Voided slab

1. The ultimate force on the experimental investigation was about 1480 KN that was similar to the result got from the analytical data.
2. The displacement of the ultimate force was 0.86 mm.
3. The bars reached to the yield strain when the first crack was occurred (795 KN).
4. Shear stress on the elastic behavior of the concrete was 1.44 MPa.

5.1.2 1-b Voided slab

1. Because of the bigger dimension of the second voided slab in comparison with the first one, the ultimate force was more than first one, which was 1837 KN with 5.21 mm of a displacement and the force-displacement graphs of the experimental and analytical were almost same. .
2. Shear stress of this voided slab was 1.38 for the elastic part of the voided slab.
3. The bars of this sample reached to their yield strain later than first one (1739 KN)
4. Shear modules of this voided slab was smaller than first one at the elastic part.
5. The ductility of the second one was almost two times of the first one, because of the more concrete used on the second one.

5.2 Recommendations

1. Because of the importance of the punching, it is recommended to investigate voided slabs by considering the columns to observe the shear behavior of voided slabs on the critical zones.
2. Since the vertical loads and lateral loads are applied to the structures at the same time, so it would be better to consider voided slabs subjected to the both type of loads at the same time to observe the moment and shear behavior of voided slabs.



REFERENCES

- David A. Fanella, Mustafa Mahamid and Michael Mota. (2017).** Flat Plate–Voided Concrete Slab Systems: Design, Serviceability, Fire Resistance, and Construction.
- Arati Shetkar and Nagesh Hanche. (2015).** An experimental study on bubble deck slab system with elliptical balls.
- Coronelli, D., Martinelli, L., Foti, F. (2016).** Reinforced Concrete Voided Slabs subjected to gravity and seismic action, Daliform Group, Italy.
- M. Bindea, Claudia Maria Chezan, A. Puskas. (2015).** Numerical analysis of flat slabs with spherical voids subjected to shear force.
- Saifee Bhagat, Dr. K. B. Parikh. (2014).** Parametric Study of R.C.C Voided and Solid Flat Plate Slab using SAP 2000.
- Jerry Paul Varghese and Manju George. (2018).** Parametric Investigation on the Seismic Response of Voided and Solid Flat Slab Systems.
- Joo-Hong Chung, Seung-Chang Lee, Hyun-Ki Choi, Chang-Sik Choi. (2015).** One-way shear strength of circular voided reinforced concrete floor slabs.
- Joo-Hong Chung, Hyun-Ki Choi, Chang-Sik Choi, Hyung-Suk Jung. (2017).** Punching shear design of voided slabs.
- Juozas Valivonis, Tomas Skuturna, Mykolas Daugevičius, Arnoldas Šneideris. (2017).** Punching shear strength of reinforced concrete slabs with plastic void formers.
- CRSI (2014).** Design Guide for Voided Concrete Slabs, Concrete Reinforcing Steel Institute, U.S.A.
- Aslani, F., Jowkarmeimandi, R. (2012).** Stress-strain model for concrete under cyclic loading, Magazine of Concrete Research, 64(8), 673-685.
- Bhagat, S., Parikh, K.B. (2014).** Parametric Study of R.C.C Voided and Solid Flat Plate Slab using SAP 2000, IOSR Journal of Mechanical and Civil Engineering (IOSR-JMCE).
- Marais, C. C. (2009).** Design adjustment factors and the economical application of concrete flat-slabs with internal spherical voids in South Africa. MEng Dissertation, University of Pretoria.
- Taskın, K., Peker, K. (2014).** Design factors and the economical application of spherical type voids in RC slabs, In conference proceedings of People, Buildings and Environment 2014, an international scientific conference, Kroměříž, Czech Republic, pp. 448-458, ISSN:1805-6784.
- Chung, J.H., Park, J.H., Choi, H.K., LEE, S.C., Choi, C.S. (2010).** An analytical study on the impact of hollow shapes in bi-axial hollow slabs, Korea Concrete Institute, ISBN 978-89-5708-182-2.
- Mehmet Gezer. (2018).** Analytical and experimental examination of reinforced concrete voided slabs.

Johan Blaauwendraad. (2010). Plates and FEM, solid mechanics and its applications.

Charles R. Steele and chad D. Balch. (2018). Introduction to the Theory of Plates.

Ishu Kumar. Lecture1: Introduction to plate bending problems.

Popo. Ego Paul. Mechanics of materials.

Metin Aydođan. Mehmet H, Omurtag. Finite element method lecture notes.

Abaqus CAE. Abaqus documentation.



CURRICULUM VITAE



Name Surname : Ali ATTARIYAN

Place and Date of Birth : IRAN 30.11.1993

E-Mail : ali.att72@gmail.com

EDUCATION :

- **B.Sc.** : 2017, Bonab University, Civil Engineering Faculty, Civil Engineering
- **M.Sc.** : 2019, Istanbul Technical University, Institute of science and technology, Structural Engineering